2007

Performance Characteristics of an Innovative Wind Power System

David James Kerze
Cleveland State University

PERFORMANCE CHARACTERISTICS OF

AN INNOVATIVE WIND POWER SYSTEM

DAVID J. KERZE

BACHELOR OF MECHANICAL ENGINEERING

CLEVELAND STATE UNIVERSITY

SPRING 2005

Submitted in partial fulfillment of requirements for the degree

MASTER OF SCIENCE IN MECHANCIAL ENGINEERING

CLEVELAND STATE UNIVERSITY

FALL 2007

This thesis has been approved

for the Department of Mechanical Engineering

and the College of Graduate Studies by

_____

Thesis Committee Chairperson,

_____

Department/Date

_____

Committee Member's Name

_____

Department/Date

_____

Committee Member's Name

_____

Department/Date

_____

Committee Member's Name

_____

Department/Date

ACKNOWLEDGEMENT

First and foremost, I would like to thank God for his continued support over the last couple of years. I am truly blessed to be given such a loving and caring family. He has kept me safe and healthy, while giving me the strength to fight through countless 18+ hour days. I am honored to be given the opportunity to positively contribute to the betterment of his world.

Secondly, I would like to thank Jim & Carolyn Kerze for their unyielding encouragement to be the best that I can be. They have dedicated their life to their children and have instilled nothing short of strong values, a hard work ethic, and a sense of self pride that can never be taken away.

This thesis could not have been completed without the help of Dr. Majid Rashidi who not only served as my advisor but has encouraged and challenged me throughout my academic career. In spite of his strong credentials, knowledge, and comprehensive experience in the field of engineering design he has always given his students the opportunity to implement their ideas into practice. It is a pleasure working under him in any project or research application as he has the ability to generate unique ideas and accurately delegate work.

I am thankful to all individuals that have supported my additional efforts, but it is imperative that I pay special thanks to the people that have been involved in this research project and my life on a daily basis. With that being said, I would like to specifically thank Mircea Rosca, Julien Brousseau, and Jennifer Sanchez for their collaborative effort in the various design stages of the Spiral Wind Tower System. I consider each of these individuals to have the

aptitude, knowledge, and analytical skills to excel at the art of engineering. Additionally, I would like to extend my gratitude to Gorman-Lavelle Corporation, specifically Gregg Gresko & Timothy Lavelle, for their continued support to achieve a higher level of education, while working full-time co-managing the Cleveland Clinic Heart Center and Glickman Urological institute (#1 Heart Center in America).

It is my belief that practical engineering research projects that blend state-of-the-art fields of study, software, and innovative design concepts/ideas will continue to pioneer the future of this global economy. It is for this reason that I would like to give special thanks to Cleveland State University's Fenn College of Engineering for its commitment to continuing education through its research oriented Grant Program.

PERFORMANCE CHARACTERISTICS OF AN

INNOVATIVE WIND POWER SYSTEM

DAVID J. KERZE

ABSTRACT

This project entails a study of a wind energy recovery system that utilizes a unique three-dimensional spiral structure to amplify wind speed and direct it toward pluralities of turbines. The system is comprised of an outer spiral shell, internal support structure, turbines, and mechanisms for positioning the turbines to face the prevailing wind. Computational Fluid Dynamics (CFD) analyses were conducted to determine the wind speed amplification factors as a result of a simulated wind flow around the spiral structure. To ensure accuracy of the results, state of the art CFD techniques were applied using Gambit 2.2.30 and Fluent 6.2.16. Specifically, wind speed amplification factors were determined for 25ft and 30ft radius spiral shells. The velocity profiles of the wind flow around both spiral structures were obtained under a postulated 10mph wind speed. This resulted in a turbulent flow with a Reynolds number of 5,596,819. All analyses were run using "standard k-ε" turbulence model with the "near wall treatment" option "standard wall function". A "y^+" value of 50 was held constant in all

simulations.   The affect of the grid size on the accuracy of the results was examined. Convergence criterion was satisfied in each case.

The 25ft radius spiral structure yielded an average velocity amplification factor of 1.524; while the 30ft radius resulted in an average amplification factor of 1.539. This particular information can help the designer of the system to select an appropriate overall shell size based not only on the mechanical efficiency, but also considering the cost and economical factors.

TABLE OF CONTENTS

LIST OF TABLES

LIST OF FIGURES

CHAPTER I

INTRODUCTION

1.1 BACKGROUND

"Worldwide, electricity generation in 2030 is projected to total 30,364 billion kilowatthours, nearly double the 2004 total of 16,424 billion kilowatthours. Higher fossil fuel prices, energy security concerns, and environmental considerations are expected to improve the prospects for nuclear power capacity in many parts of the world." [1] In non-OECD[2] countries, largely within Asia and South America, large growth is seen in hydroelectric power and is projected to increase through 2030. In OECD countries, such as the United States, hydropower is not expected to

---

[1] See References, (Energy Information Administration, Official Energy Statistics From the U.S. Government, 2007, p. 1)
[2] See Appendices, section *3 Abbreviations*

grow substantially because most of the available resources have already been developed. "Instead, most of the increase in OECD reliable energy is expected to be in the form of non-hydroelectric resources such as wind, solar, geothermal, municipal solid waste, and biomass." [3] As the energy statistics show, wind energy has proven to be a viable energy alternative for many of the industrialized nations. In fact, many studies prove that wind energy is one of the most dependable sources of electricity worldwide.

According to *Distributed Energy*, "The Green Energy industry is forecast to be one of the fastest growing industries over the next decade. According to the market research firm *Clean Edge* the Fuel Cell, Solar, Wind, and BioFuels (Ethanol and BioDiesel) markets will grow to more than $167 billion worldwide by 2015" (Senall, 2007). **Table 1** lists the revenue projections for each Sub-sector.

	2005	2015
Fuel Cells	$1.2 billion	$15.1 billion
Solar Equipment	$11.2 billion	$51.1 billion
Wind Power	$11.8 billion	$48.5 billion
BioFuels	$15.7 billion	$52.5 billion
Total:	$39.9 billion	$167.2 billion

Table 1 - Industry Sub-sector 2005 revenues 2015 forecast, (Senall, 2007)

---

[3] **See References**, (Energy Information Administration, Official Energy Statistics From the U.S. Government, 2007, p. 1).

Many studies have shown that wind energy is valued as one of the most dependable sources of electricity worldwide. In order to maintain this status, continued efforts to refine design and production techniques are necessary. It is imperative that the rust belt states lead the research initiative as "wind and solar energy is likely to furnish one of the largest sources of manufacturing jobs worldwide." [4] If this industry is further pursued, there is strong promise that the existing factories in the region could be retooled cost effectively. This could possibly replace the thousands of jobs that have been lost as a result of outsourcing and corporate downsizings in the textile, steel, oil, and automobile industries. To date, twenty two states have already put Renewable Energy Standards in place. In an effort to contribute to this cause, Dr. Majid Rashidi and a team of graduate students have undertaken several research projects, each with the goal of developing system optimizations that will contribute to more competitive energy costs.

There are two common methods that are used to recover wind power (this determination is a result of the known formula $P = \frac{1}{2} * \rho * S * v_1^3$, where S (area) and v_1 (velocity) are the only two parameters that directly influence power generation). The first, most commonly used, method is to increase the blade swept diameter. The second technique is to try to amplify the natural wind speed. As a starting point for the first approach, it is important to understand Betz law, which provides theoretical calculations proving the coefficient of maximum performance for a wind turbine. The calculations presented in Albert Betz's publication *Introduction to the Theory of Flow Machines* define the maximum theoretical efficiency of a rotor.

---

[4] See References, (Senall, 2007)

Please review and analyze the formulations deriving the Betz law in the attached footnote: [5]

[5] "In order to calculate the maximum theoretical efficiency of a rotor (of, for example, a wind mill) one imagines it to be replaced by a disc that withdraws energy from a fluid passing through it. At a certain distance behind the disc, the fluid, that has passed through, flows with a reduced velocity. Let v1 be the speed of the fluid in front of the rotor and v2 that of the fluid downstream of it. The mean flow velocity through the disc representing the rotor is vavg, where

$$v_{avg} = \frac{1}{2} * (v_1 + v_2)$$

With the area of the disc equal to S, and r equals the fluid density, the mass flow rate (the mass of fluid per unit time) is given by:

$$\dot{m} = \rho * S * v_{avg} = \frac{\rho * S * (v_1 + v_2)}{2}$$

The power delivered is the difference between the kinetic energies of the flows approaching and leaving the rotor in unit time:

$$\dot{E} = \frac{1}{2} * m * (v_1{}^2 - v_2{}^2)$$
$$= \frac{1}{4} * \rho * S * (v_1 + v_2) * (v_1{}^2 - v_2{}^2)$$
$$= \frac{1}{4} * \rho * S * v_1{}^3 * \left(1 - \left(\frac{v_2}{v_1}\right)^2 + \left(\frac{v_2}{v_1}\right) - \left(\frac{v_2}{v_1}\right)^3\right)$$

By differentiating $\dot{E}$ with respect to $\frac{v_2}{v_1}$ for a given fluid speed v1 and a given area S one finds the maximum or minimum value for $\dot{E}$. The result is that $\dot{E}$ reaches maximum value when $\frac{v_2}{v_1} = \frac{1}{3}$.
Substituting this value results in:

$$P_{max} = \frac{16}{27} * \frac{1}{2} * \rho * S * v_1{}^3$$

The work rate obtainable from a cylinder of fluid with area S and velocity v1 is:

$$P = \frac{1}{2} * \rho * S * v_1{}^3$$

The coefficient of performance $C_p (= \frac{P_{max}}{P})$ has a maximum value of: $C_{p,max} = \frac{16}{27} = 0.593$ (or 59.3%; however, coefficients of performance are usually expressed as a decimal, not as a percentage). Rotor losses are the most significant energy losses in, for example, a wind mill. It is, therefore, important to reduce these as much as possible. Modern rotors achieve values for Cp in the range of 0.4 to 0.5, which is 70 to 80% of the theoretically possible". (Betz, 1966)

4

There have been several attempts at amplifying the natural wind speed. An example of this would be the Web Concentrator, designed by BDSP Partnership (Serbia) and was optimized using CFD modeling techniques by Imperial College, London (UK). A conceptual image can be viewed in Figure 1. (Dutton, Halliday, & Blanch, 2005)
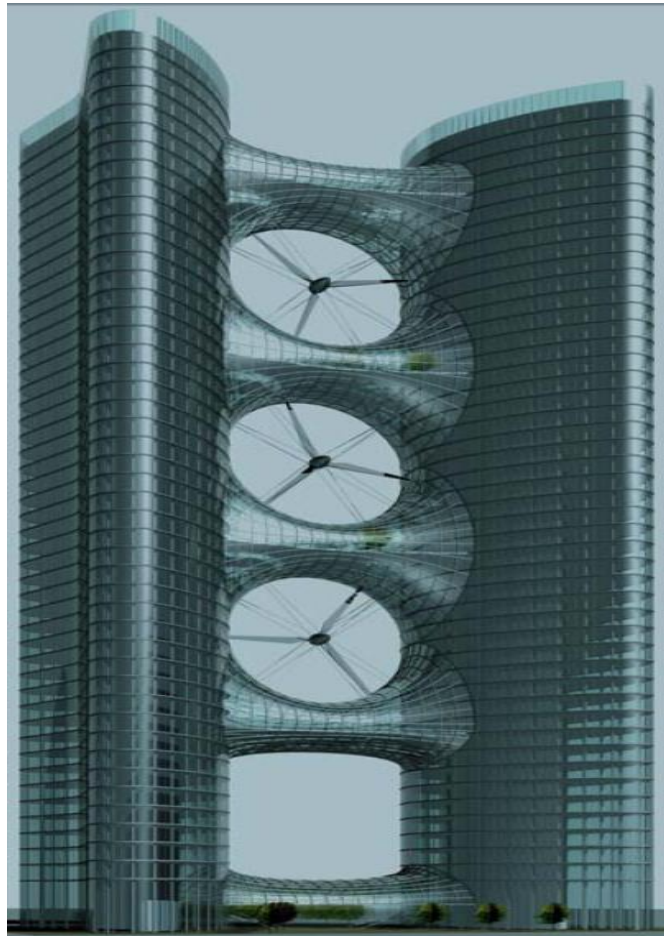
Figure 1 - Web Concentrator, (Dutton, Halliday, & Blanch, 2005)

This design achieved a power improvement ratio of roughly 0.8 when tested with winds flowing orthogonal to the tower. Because this is implemented into the structure of a commercial building the cost of such a structure would be relatively high. The status of the production of this structure is currently pending due to a lack of funding sources. An alternative design that is adaptable to many flat and pitched roof structures would be the Altechnica's patented Aeolian

planar concentrator wind/solar system, which can be seen below in **Figure 2**. This structure does not use standard turbines, but instead uses a specially designed cross flow turbine. This wind energy system is very unique and economical, but it does not deliver high wind amplification factors of that of several other designs.
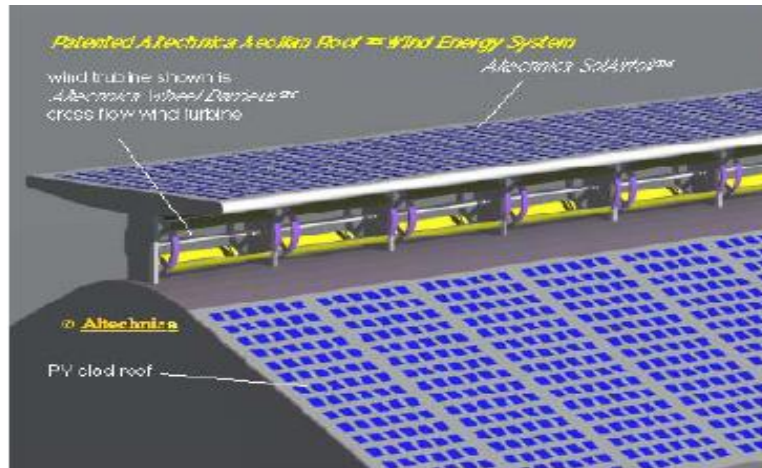
Figure 2 - Altechnica's Patented Aeolian Planar Concentrator Wind/Solar System

The WARP Tower Configuration, **Figure 3**, is a standalone electrical generation tower that contains a series of individually rotating modules for turbine positioning. To date this tower has not been produced due to the high cost of its movement system as well as its high patent price.
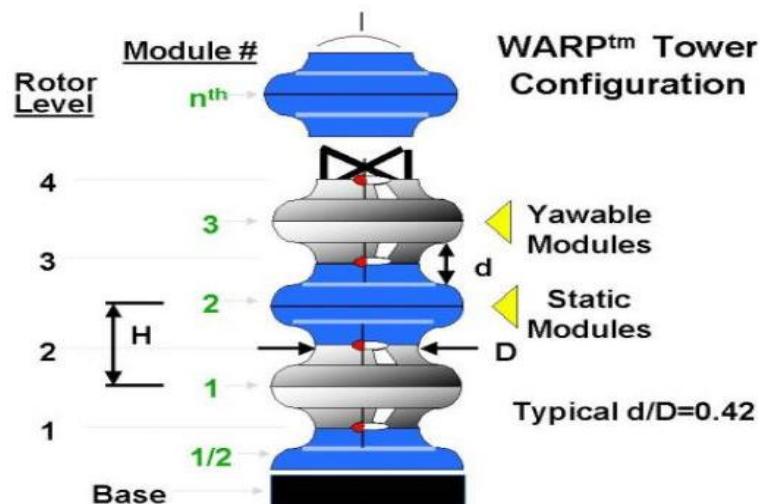
Figure 3 - WARP Tower Configuration

The shortfall of many of these designs is either the feasibility or the cost associated with the structures. With this being said there is still a need for improvements and new innovations in wind amplification, structural integrity, and cost effectiveness.

1.2 IDENTIFY PROBLEM/NEED

The wind power industry has grown exponentially over the past decade, particularly in the research and development of large scale wind turbines. Advances in the ability to generate large quantities of electricity from giant offshore wind turbines, described in Popular Science Magazine's October 2004 Issue and made the front cover of WindTech International's February 2007 Issue. There have also been additional proposals for flying electric generators by Sky WindPower Corporation, explained in further detail in Popular Science Magazine's July 2006 Issue. Although many of these techniques look good on paper, engineers alike have found that most of these wind power systems need extensive amounts of additional research and testing to perfect these designs. Millions of dollars are being poured into research to identify and fix the critical components that are linked to wind power system failures. It is important to realize that every minor improvement that can help to prolong the working lifespan of modern wind power systems will be implemented into thousands of production models, thus often leading to savings in the millions of dollars for companies as failures usually have costs associated with machine downtime, associated service labor, and replacement material costs to name a few. In fact, a

short article presented on November 3rd, 2005 named "The Gearbox: Wind Power's Achilles Heel" globally illustrates how these issues can impact a once prospering company. [6]

Additional information can be found in "Wind Power Monthly News Magazine", Volume 21 - Number 11, from November 2005. The cover, shown in **Figure 4** below, gives a clear illustration of the size a magnitude of what could be considered to be a standard wind power system gearbox.

---

[6] "Gearboxes have been failing in wind turbines since the early 1990s. Barely a turbine make has escaped. Six years ago the problem reached epidemic proportions, culminating in a massive series failure of gearboxes in NEG Micon machines. At the time, the NEG Micon brand was the most sold wind turbine in the world. The disaster brought the company to its knees as it struggled to retrofit well over one thousand machines. It has since been taken over by Vestas, the world's largest wind turbine manufacturer. Vestas is still grappling with the aftermath of the gearbox catastrophe.

The wind power industry and its component suppliers now believe that such major series failure of gearboxes is a thing of the past. Today's far larger and more sophisticated turbines, they say, are safe from mistakes encountered in early phases of technology development.

Bigger turbines, however, are proving to be far from immune to gearbox failure, as Windpower Monthly reports in its November issue. ...

The wind industry's gearbox problem has for years been shrouded in secrecy. While blame for the failures has been spread far and wide, questions outnumber the answers by far. At Windpower Monthly we set ourselves the task of finding out the true scale of the problem. Why is it that gearboxes in wind turbines have so massively failed? What is the solution? ...

The good news is that understanding of the highly complex loads that gearboxes -- and particularly their bearings -- are subject to is being helped by a new industry willingness to co-operate and face up to the challenges of wind power's rapid technological evolution. But only time will tell whether a definitive solution has been found -- and whether it will stay the course as wind turbines get ever bigger and more demanding of engineering ingenuity." (Kirby Mountain, 2005)
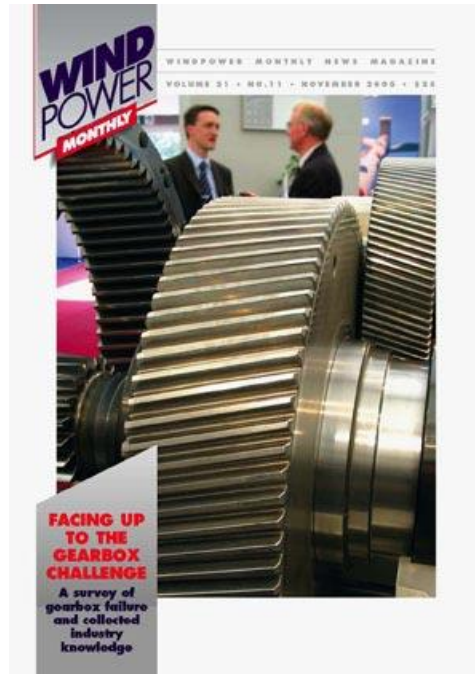
Figure 4 - Wind Power Monthly Vol. 21, Num. 11 (11/05)

The structural issues of large scale turbines continue to act as a bottleneck to the wind industry. Although engineers do not want to "reinvent the wheel", thus minimizing high startup costs associated with research, testing, and implementation of an unproven system, it is still important to "think outside of the box" when attempting solve challenging problems. The system presented and studied in this thesis implements a series of smaller turbines into a controlled system, which would eliminate the high number of failures associated with large scale turbine gearboxes. The aspect of this design that separates it from existing designs is that this is the first wind structure that has been designed to use an outer spiral shell to amplify wind natural wind speed toward an attached system of small turbines. A number of *smart* technologies were used to optimize the towers rotational movement method, weight/rigidity, and aerodynamics. The result is a tower with a significantly lower start-up cost and cost/energy ratio keeping the tower competitively priced in the energy market.

1.3 STRUCTURAL BENEFITS OF HELICAL SPOILERS

The spiral shape possesses inherent properties that can't be found in most other shapes such as its ability to amplify flow and maintain structural rigidity by minimizing flow induced vibrations. For example, "For tall chimneys, helical spoilers or strakes can be provided around the chimney shown below in **Figure 5**. The helical spoilers break down the vortex pattern so that no well defined excitation is applied to the chimney wall."[7]
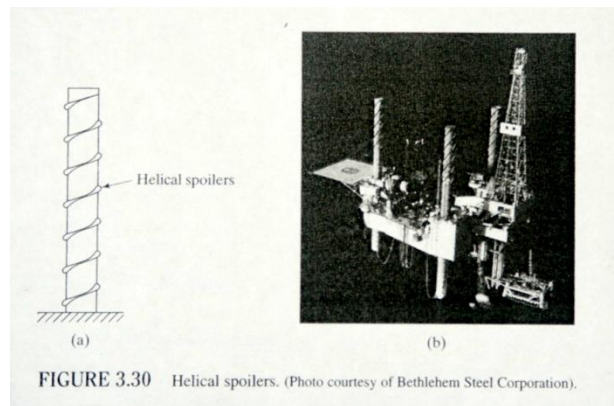
FIGURE 3.30   Helical spoilers. (Photo courtesy of Bethlehem Steel Corporation).

Figure 5 - Reduction of Flow Induced Vibrations [Photo courtesy of Bethlehem Steel Corporation], (Inman, 2001)

Further evidence of the benefits of the spiral shape can be seen in the Chicago Spire project, or the Fordham Spire, which was proposed by a Spanish architect in July of 2005. The structure is designed to exceed heights of 2000ft and will accommodate roughly 115 floors. **Figure 6 & Figure 7** depict artistic renderings of the finished tower amongst the Chicago landscape.

---

[7] (Inman, 2001, p. 264)
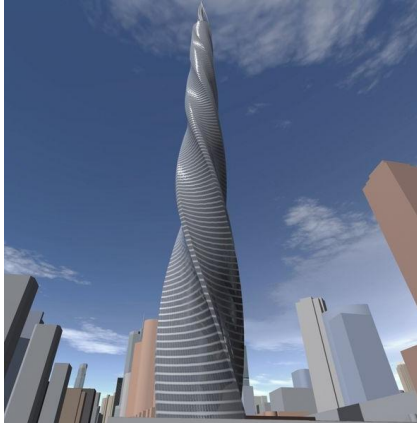
Figure 6 - Santiago Calatrava Structures – Pic#1, (Wikipedia, 2007)

Figure 7 - Santiago Calatrava Structures – Pic#2, (Wikipedia, 2007)

As noted by Wikipedia's web article <u>Chicago Spire</u>, "the architectural design of this structure poses several benefits. The two primary benefits are described to be the added structural strength to the structure as well as the minimization of wind forces. As scientific theory will prove, this will by no means eliminate all wind forces so a tapering concrete core and shear walls will be used to counteract these forces." [8]

---

[8] (Wikipedia, 2007)

Figure 8 - Burj Dubai, Spiral Structure w/Triple Lobed Footprint, (Wikipedia, 2007)
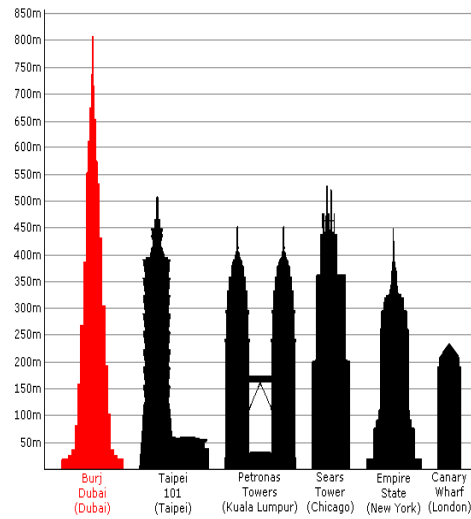
Figure 9 - Projected Heights of World's Largest Skyscrapers, (Wikipedia, 2007)

The Burj Dubai, Figure 8 & Figure 9, has an expected completion date of June 30th 2009, will be throwned the tallest building in the world with rumored heights of roughly 3,005ft. The towers central core is comprised of three elements, which include the flat desert base, setbacks that occur in an upward spiraling pattern, and at the top the central core emerges and is shaped to form a finishing spire. As shown the spiral shape is being implemented into the designs of some of today's most renowned architecture. The shape has been proven and is here to stay.

Although there are many studies that deem the spiral shape and helical spoilers to be a positive attribute to structures of varying heights, industry has yet to implement this into its designs. The benefits of this structure are such as reduction in wind induced vibrations as well as inherent wind amplification properties need to outweigh the added material, manufacturing, and installation costs. Through research, it was determined state of the art automation processes were implemented this shape could be produced at feasible costs.

13

CHAPTER II

INTEGRATION OF OUTER SPIRAL SHELL, SUPPORT STRUCTURE AND MECHANICAL COMPONENTS

2.1   RESTRICTIONS & DESIGN CONSTRAINTS

A compilation of guidelines/requirements must be followed throughout the design process. To simplify this process the requirements were broken down into three categories:

1. Top Level Requirements
2. Local Level Requirements
3. Scope of Work

Top & local level requirements are general requirements that serve as a guide for the design. These requirements are often established due to driving factors such as manufacturing facility size/tooling, build site restrictions, material transportation, and most often funding. Several of

the requirements listed below are self imposed restrictions that were determined by consensus following extensive research on shortfalls of the prior art. The top & local level requirements that were established are as follows:

2.1.1 <u>Top Level Requirements:</u>

1. Electricity must be generated at a minimum of 5 mph wind speeds instead of 11 mph, which will greatly improve the market potential of wind energy.

2. Noises made by the rotor blades must be minimized.

3. "Off the shelf" impellers having a tip-to-tip dimension of 15ft in diameter should be implemented. The tower must proportionally accommodate the aforementioned impellers, while maintaining the requirement that the outer diameter of the spiral structure must not exceed 60 feet. Each turbine is expected to provide a nominal 10-15KW of energy as a result of recent technological developments. In most cases an expected power output of the final system is expected to be between 100KW-500KW.

4. The tower must be aesthetically pleasing for any given surroundings. In addition to being visually pleasing, the tower must accommodate the use in large farms, urban areas or onto rooftops of residential districts.

5. The spiral tower must have the capability to be equipped with antennas to allow for self-sustaining communications and with solar panels in order to improve power generation.

2.1.2   <u>Local Level Requirements:</u>

1. The structure's shape must amplify the wind velocity over the plane collinear to the windmill in order to maximize efficiency. [9]

2. Each windmill blade has the capability to travel a maximum rotation of $\pm 180°$.

3. Tower design is to be modular for ease of assembly. This shape allows various tower sizes depending on the applications.

4. Windmills must be orthogonal to the wind to obtain the highest energy recovery.

5. Easy access and maintenance must be assured.

6. The design of the tower has to be capable to handle a minimum of category 4 (Saffir-Simpson Scale) winds that can range anywhere between 131-155mph.

7. The tower design has to be capable of upgrading old towers with ease.

The Scope of Work is different from the top and local level requirements in that it specifically states exact requirements. This removes any form of uncertainties and allows the engineer to focus on the R&D optimization.

---

[9] High priority requirement

2.2 DEFINITION OF SCOPE OF WORK

1. **Exterior Shell**

Design an exterior shell for a wind energy system that meets all of the previously stated design constrains, while integrating the "spiral shape". The design is to be modular to accommodate low cost tooling, transportation, and assembly. Provide a minimum of one drawing(s) of the "building block" (modular shape that is to be replicated).

2. **Load Carrying Cage**

Drawing(s) for a load carrying cage structure to which the spiral shell is rigidly attached.

3. **Building blocks (1 Rev.)**

Drawing(s) of a system of "building blocks" that when assembled complete one turn (360 degrees) of the spiral shell for a typical 300KW tower system.

4. **Connecting Elements**

Drawing of the connecting elements that rigidly link the spiral shell to the cage.

5. **Assembly**

Drawings of load carrying cage and one turn of spiral shell, which includes two electric generators on its diametrically opposite concave sides.

6. **Hydrostatic Thrust Bearing**

Schematic drawing(s) of a thrust bearing(s). [10] This bearing is to support the CAGE in the vertical direction, and should allow rotation of the spiral system about its longitudinal axis.

7. **Hydrostatic Radial Bearing**

Schematic drawing(s) of radial bearing(s). [11] These bearings are to support the cage in the radial directions, and prevent tilting of the spiral system from its vertical standing. These bearing(s) must still allow rotation of the system on the thrust bearings.

8. **Design Analysis – FEA Simulated Snow Test**

FEA testing of fiberglass shell structure. This takes into consideration a load that is equivalent to the weight resulting from a volume of three cubic feet of snow as an additional load bearing weight on the structure.

---

[10] Designed by Dr. Majid Rashidi (Cleveland State University); Note: Actual sizing and design parameters are classified not disclosed as they are property of Dr. Majid Rashidi (Cleveland State University).
[11] Designed by Dr. Majid Rashidi (Cleveland State University); Note: Actual sizing and design parameters are classified not disclosed as they are property of Dr. Majid Rashidi (Cleveland State University).

2.3 CONCEPTUAL DESIGN

The illustration of the spiral tower structure, Figure 10, was artistically rendered in SolidWorks and PhotoWorks.   This conceptual design served as the basis for all future design changes/modifications.   Also shown is an array of small wind turbines mounted on the structure. The conceptual design does not take into consideration:

1. Bill of Materials (Type of Material, Properties, Weight, Cost, Quantity, etc.)

2. Structural Integrity (Support Members, FEA Testing, Wind Force Testing)

3. Spiral Structure Mobility (Rotation)

4. Size Optimization (CFD Analyses)

5. Method of Assembly (Modularity & Actual Connection Points)

6. Manufacturability
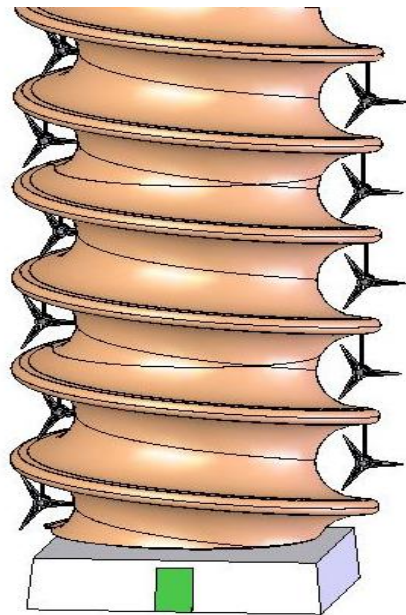
Figure 10 - Spiral Tower Structure Concept w/Turbines

Initial design ideas included a variety of different parameters. The spiral module concept illustrated in Figure 11 was designed with the idea that the external shell membrane would be a very flexible skin that is similar to that of saran wrap. The skin was the driving parameter in the design of the "formed" piping support system that is comprised of twelve unique bend combinations per module. Additional I-Beam truss elements were used to structurally support the I-Beam track and trolley system that would be used as a guide rail. A pulley system was designed to invoke the movement required to position the turbines orthogonal to the wind at any moment of time in any type of weather condition.
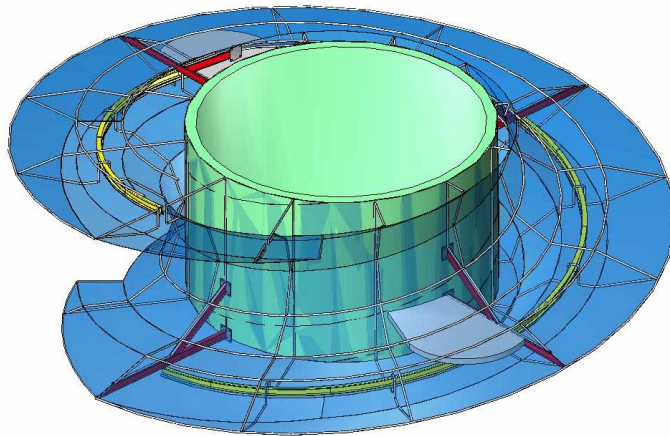
Figure 11 - Spiral Module Concept w/Supporting Elements

2.4 MODEL/PROTOTYPE

These conceptual models were taken further by producing small "plaster" based 3D prototypes on Cleveland State Universities Z-Corporation 3D printer. This printer provides a means of producing early stage concept models quickly and efficiently from CAD data. Other benefits include the ability to:

1. Perform Iterative Design

2. Communicate With Clients

3. Identify Problems Early

4. Achieve a Consensus on a Design

5. Perform Ergonomic Testing

Figure 12 shows actual models that were used in the design process of the spiral tower structure.

Figure 12 - Z-Corporation 3D Model

2.5   DESIGN EVOLUTION

The figures below show the evolution of the external shell structure from inception to completion. The WARP Tower, Figure 3, which is comprised of donut shaped modules was proposed by Alfred L. Weisbrich in 1996. The idea was to have individually rotating tower sections that would be able to alter the positions of wind turbines by way of angular ball bearings. This idea was good in concept, but proved to be cost ineffective. The original shape did not provide the benefits of a spiral structure such as structural stability or wind amplification. By consensus the spiral structure also proved to be more aesthetically pleasing to the human eye.
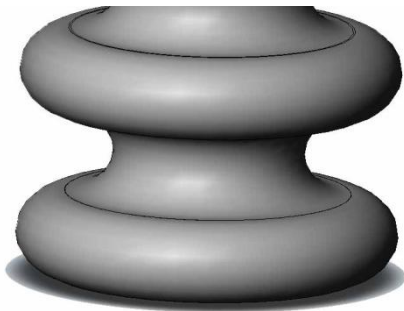
Figure 13 - Prior Art - Proposed Shell Design Concept [Weisbrich, 1996]
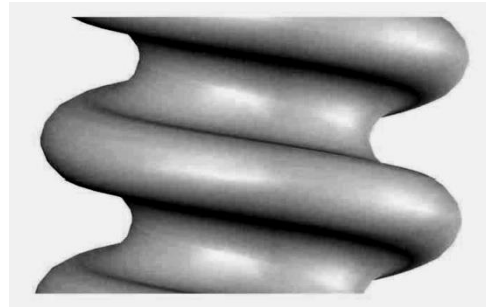
Figure 14 - Original Spire Tower System Shell Design [CSU, 2005]
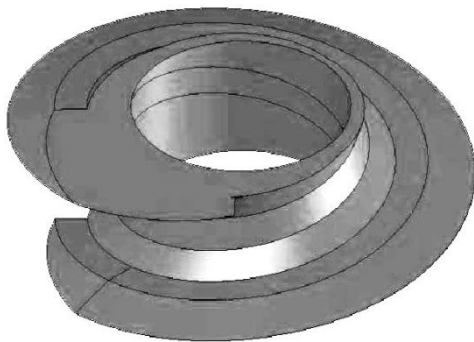
Figure 15 - Deca Tower System Shell
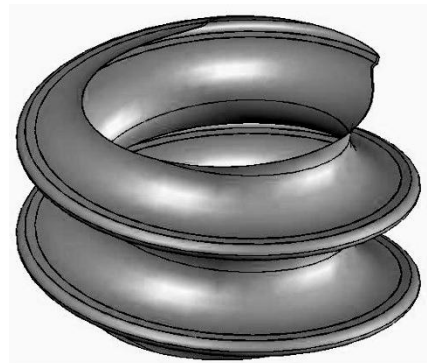
Figure 16 - Final Tower System Shell

Several design iterations were needed before achieving the final product. As previously stated, the turbines original positioning system was based on a track/trolley/pulley system, which later was modified to a more efficient system that used hydrostatic thrust bearings and hydrostatic radial bearings to stabilize and position the tower so that the turbines could always operate orthogonal to the wind. The new system reduced the amount of material, labor, and time to assemble each tower system. The primary reason for the change in positioning systems was due to new composite materials and material fabrication technologies that became more readily available. The new shell material provided a more rigid external shell, while allowing for the elimination of several previously required supports (thus indirectly resulting in a structure with a significantly lower weight).

The aerodynamics of the tower has also changed significantly since its inception. Each stage in the shells evolution from its inception through it present shape can be viewed in **Figure 13** - **Figure 16**. A few variables needed to be considered in the shape optimization process include:

1. ease of production,
2. reduction in surface area,
3. reduction of wind induced vibrations,
4. & amplification of wind to the turbine blades.

To do this the shapes had to be created in a 3D modeling software, in this case SolidWorks, and then imported into a preprocessing program such as Gambit 2.2.30. Once in Gambit 2.2.30, the objects need to be meshed and assigned boundary conditions before moving to the primary processor. The engineering analysis was performed using Fluent, which is a CFD (Computational Fluid Dynamics) code that is used to model flow and heat transfer. To simplify

the process, the software takes unsolvable PDE's and approximates them as FDE's, which then can be solved using numerical methods and known CFD equations. (Note: By applying CFD to run this analysis versus conventional methods of trial and error by experimentation, no major costs were incurred).

2.6   DESIGN RESULTS

2.6.1   Exterior Shell

This idea changed significantly to the construction of what is now classified as the "building block". The term "building block" signifies the section of the outer shell that will be made out of fiberglass and then interconnected onsite in single revolution assemblies, which when combined total 16 pieces per revolution. The "building block" piece as illustrated in Figure 17 weighs approximately 143lbs for the 25ft-R building block and 188lbs for the 30ft-R building block.
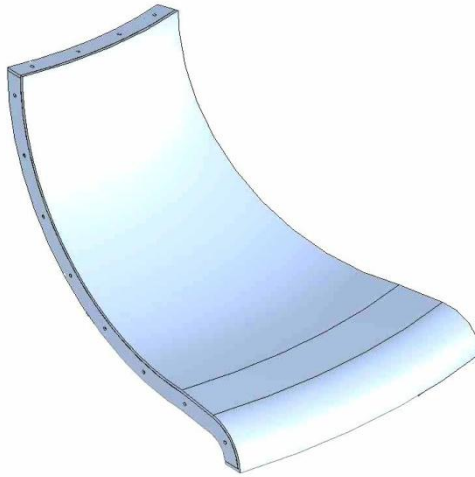
Figure 17 - Building block (1/16th of One Revolution)

2.6.2   Load Carrying Cage

The internal cage of the spiral tower structure was also designed in SolidWorks. This structure was built with the sole purpose of providing a support method for the wind turbines as well as structural base that the hydrostatic thrust bearing will be able to lift. Exact details of material selection and individual connections must be done by a structural analyst in order to make sure that the overall structure complies with the building and zoning codes of the particular site in which the tower is erected.
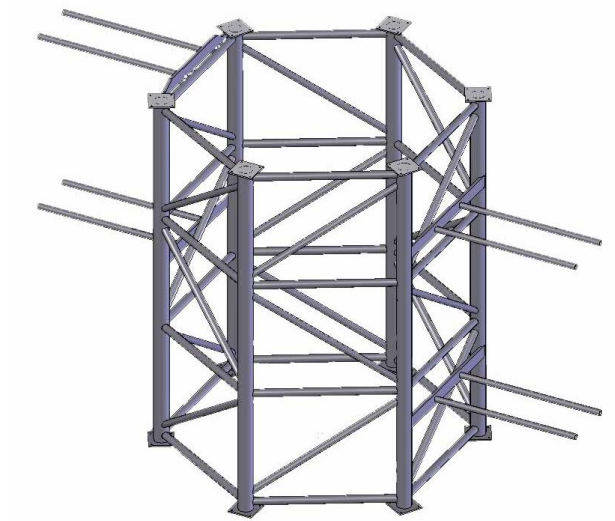
Figure 18 - Load Carrying Cage

2.6.3   Building Blocks - (1) Revolution

One full revolution of "building block" pieces assembled together, which is comprised of 16 fiberglass constructed building blocks and weighs 2288lbs for the 25ft-R tower and 3008lbs for the 30ft-R tower. Two revolutions of the building block are categorized by the term "module". Figure 19 is a representation of an assembly of one full revolution of building block pieces.
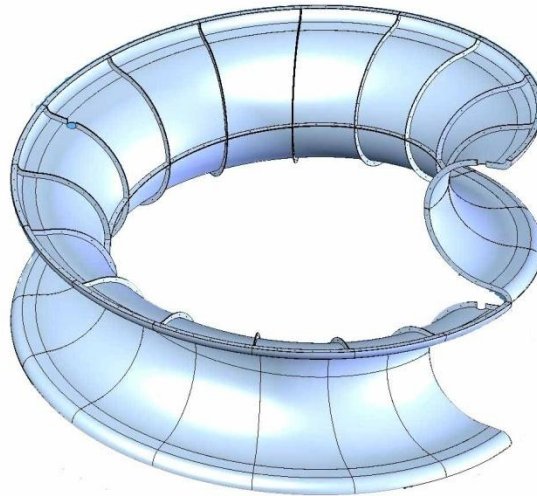
Figure 19 - Building block - One Full Revolution

Each piece occupies exactly 22.5° of a full 360° revolution, thus resulting in a total of 16 fiberglass pieces. These pieces are joined using a specially designed gaskets, nuts, and bolts.

2.6.4   Connecting Elements

In most applications a high safety factor can be achieved by solely using structural steel members as the primary support method.   In areas of extreme conditions such as high wind velocities or snowy conditions the spiral structure can be additionally supported with a cable/turnbuckle support as illustrated by Figure 20.
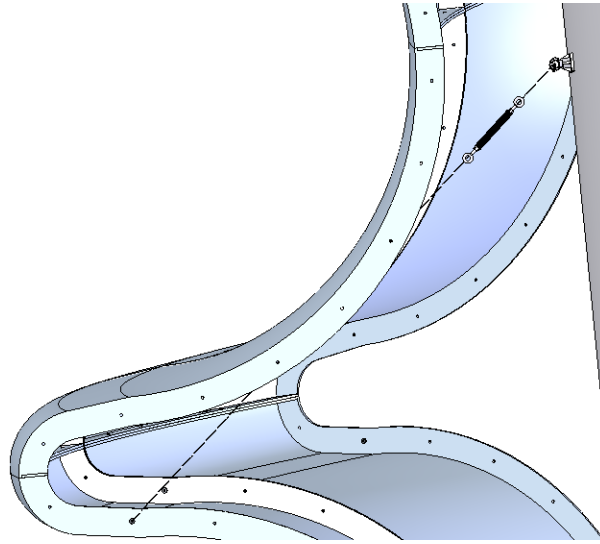
Figure 20 - Cable/Turnbuckle Support Configuration

2.6.5   <u>Assembly</u>

The assembly below provides a clearer representation of how each of the previous components assemble together to form a short version of a spiral tower. Smaller versions of the spiral tower have been proposed to be used as cost efficient rooftop models. The wind turbines, 15ft tip-to-tip, have also been included in this assembly to illustrate the fit. As shown in on left side of Figure 21, an access door (typical for all turbines) will accommodate maintenance access to the wind turbines.
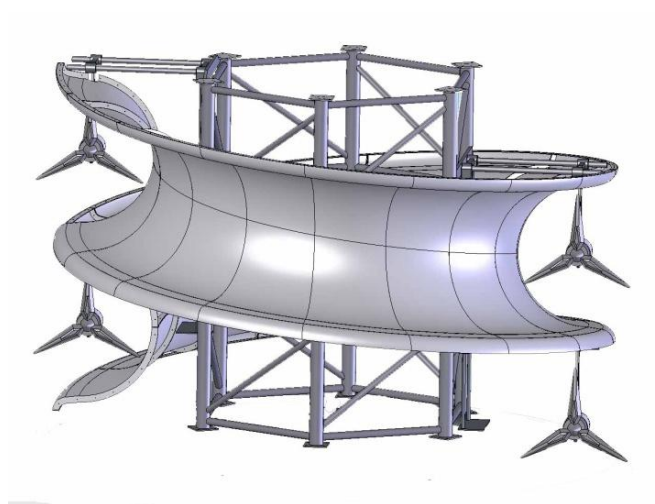
Figure 21 - Assembly of Components

2.6.6   Design Analysis (FEA) – Snow Test

To verify structural integrity a pressure test was simulated on one building block component. The simulated test case is designated as "static stress" and the material that is being used is assumed to be fiberglass material that is provided in the CosmosWorks material library. The purpose of this test is to prove that this fiberglass building block component is more than capable of supporting this type of loading. The figure below shows the specific locations of the load/restraints.

2.6.6.1   Load/Restraints
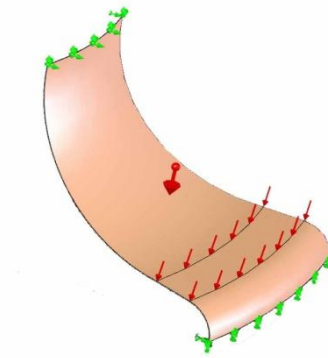
Figure 22 - Load/Restraints Placement

The loading/restraints were applied in the following manner:

- The top & bottom connection points were designated using the "fixed" boundary condition. The side connection flanges are neglected in this test, but will be present in the production model. The flange connections will provide supplemental load handling capability and structural rigidity.

- A force having a magnitude equivalent to that of the weight of three cubic feet of dense snow was equally applied over the flat shelf surface area.

- A gravitational force was applied to the entire domain of the model.

The material type that was used was defined as a "Linear Elastic Isotropic" by the fabricator. Table 2 shows the values that were used to define the material.
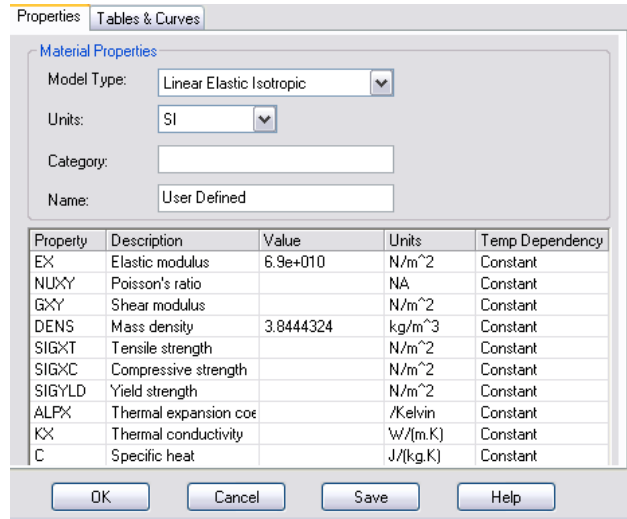
Table 2 - Material Properties (FEA Testing)

2.6.6.2   Stress

The three stress plots shown below were generated to illustrate points of the building block that experience the highest levels of stress. The scale uses a coloring scheme that shows values of lower stress in blue and areas of higher stress in red. By no means does the red coloring mean that the model will fail as the legends scale is designed to exaggerate the magnitude of the color for visual purposes.

31
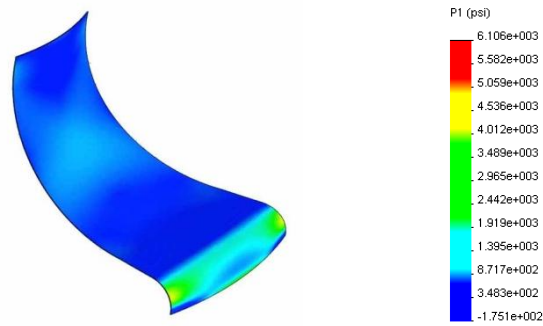
Figure 23 - First Principle Stress

The First Principle Stress is defined as the point at which shear stress is equivalent to zero and the normal stress is maximum (the direction of the velocity component determines whether it is a tensile/compressive stress). The maximum principle stress value was determined to be 6,106psi, which below the specified material strength.
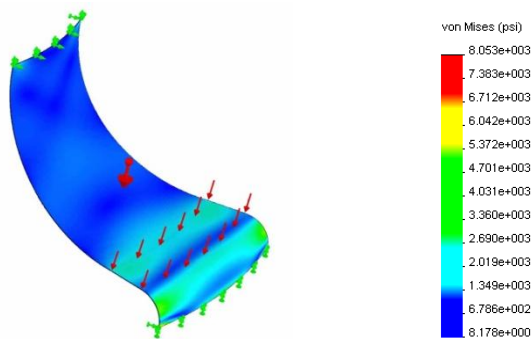
Figure 24 - Von Mises Stress

The Von Mises Stress or equivalent stress is a stress quantity that is independent of any direction that is used to assess the safety of a design for many ductile materials. The maximum principle stress value was 8,053psi, which is also within the limits of the material.
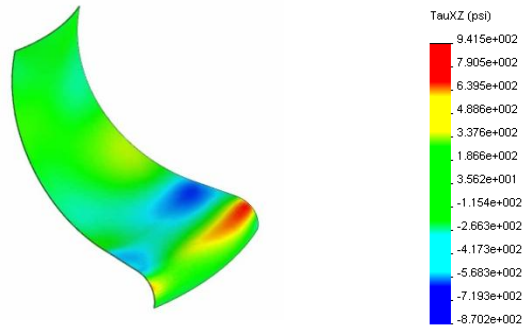
Figure 25 - Shear Stress

The Shear Stress is defined as the stress that is tangential to the face of the object. The maximum principle stress value was that was determined was 941.5psi, which is the lowest of all forms of stresses. Thus, shear stress poses the lowest risk of material failure for the current analysis.

2.6.6.3 Displacement
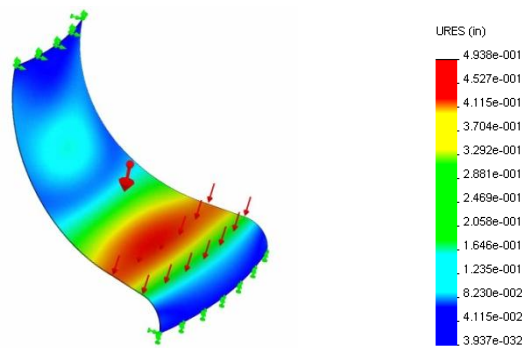
Figure 26 - Resultant Displacement

By definition, displacement is the position or point of a particle in relation to a datum or original point. The figure above shows the maximum point of displacement, having a magnitude of roughly 0.5 inches, to occur in the region where the load was applied. Because the material is proprietary the yield, tensile,

and compressive strengths can't be disclosed. As stated earlier, support flanges will

be added and used for the purpose of providing fastening points as well as adding

structural rigidity.

2.6.6.4   Strain
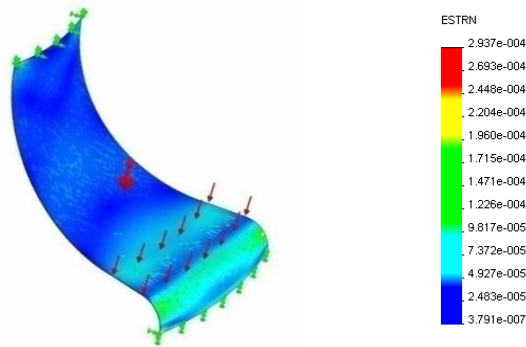
Figure 27 - Equivalent Strain

This figure above shows the strain distribution of the building block component.

Engineers usually design their components so that they fall within an acceptable

strain level. The definition of strain is the ratio of change in length "dL" to the

original length "L". Because this ratio is determined using similar measurement

qualities, strain is considered to be a dimensionless quantity.

2.6.6.5 Deformation

Study name Snow Test
Plot type Deformed shape Deformation
Deformation scale 50
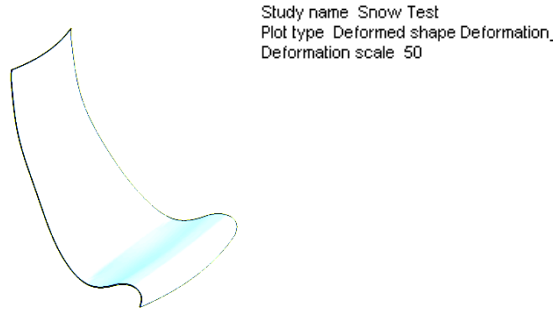
Figure 28 - Deformation (Amplified X50)

The deformation of the shape is nearly invisible to the human eye with an amplification factor of 1. It is for this reason that an amplification factor of X50 was applied to the model to show how the model would deform if a large enough load was applied.

With access to the proper software, additional testing can be performed on the building block shell structure. For example, new software technologies allow the user to run test cases that mimic the material properties of some of the newest materials on the market. Today's fiberglass composites (fiberglass or plastic polymers) are often composed of over 30 layers of material.

2.7 FINAL DESIGN

The final spiral design will resemble the image shown in Figure 29. The quantity of wind turbines that are used will be dependent on the specific application. For a "roof top" application as few as a quantity of two turbines can be used. For applications that require larger quantities of energy, the structure (and supporting elements) can be modified to accommodate additional wind turbines and the wind positioning system.
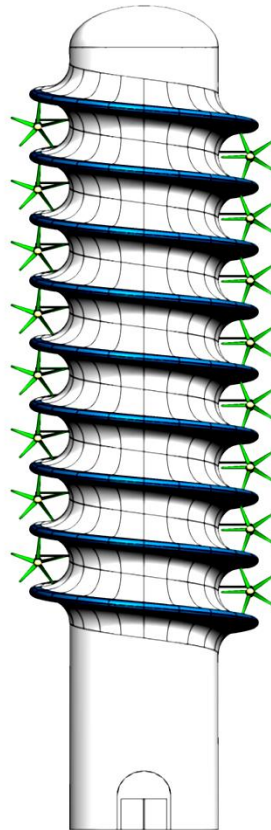
Figure 29 - Spiral Tower (Illustrated using Eight Revolutions)

In addition to the benefits of wind power, the outer shell can accommodate various types of solar panels. This may be beneficial in regions where days are longer.

The spiral tower is especially beneficial in rural areas as it has the capability to be equipped with several forms of wireless telecommunication mediums. Note: In areas where large quantities of spiral structures are present, only one tower is required to be equipped with the telecommunications medium.

CHAPTER III

SIZE OPTIMIZATION OF SPIRAL SHELL USING ADVANCED CFD TECHNIQUES

3.1   INTRODUCTION TO COMPUTATIONAL FLUID DYNAMICS

The words *computational fluid dynamics* (CFD) can be defined as a computational technology that provides a means to model and study the flow mechanics of nearly any type of physical problem. Although a strong education in the field of fluid mechanics is required to accurately understand the subject matter, this exciting technology of CFD is pioneering the way engineers solve complex fluid flow problems. For example, CFD software provides the means to simulate the flow of gases and liquids, heat and mass transfer, moving bodies, multiphase physics, chemical reaction, fluid-structure interaction, and acoustics through computer modeling.

A common question that is asked is "Why would I use CFD techniques to solve a fluid flow problem over the conventional method of experimentation?" The answer is because while experimentation, such as in a wind tunnel test, provides accurate results this is often very time consuming and costly to perform. CFD minimizes these drawbacks and provides additional benefits such as insight, foresight, and efficiency. The term insight is used to emphasize the user's ability to analyze system designs that are difficult to prototype or test through experimentation. Foresight can be defined as the user's ability to predict how a design will perform as well as test several configurations until an optimal result is achieved. The history from the various test configurations that is documented allows for more efficient future designs and testing (better, faster, and cheaper designs).

The CFD process can be broken down into three subcomponents pre-processing, solving, and post-processing. The pre-processing stage entails the CAD design, mesh generation, and application of boundary conditions. For the purpose of this thesis a combination of SolidWorks (CAD) and Gambit (pre-processing tool/meshing software) were used in the setup of all models. The solving portion is the stage where the actual calculations are performed and data results are compiled. This step was performed using the Fluent's CFD code and solver. The final step in an analysis involves the post-processing stage, which is also available in Fluent. Fluent's post-processing software provides a number of tools that can be used to manipulate data and produce color based CFD images and animations.

3.2 FLUID FLOW ANALYSIS SOLUTION METHODS

There are three fundamental means that are used when approaching fluid flow problems. The control volume, infinitesimal system, and experimental approaches. The *control volume* approach is often classified as an integral analysis. This analysis is accurate for any flow distribution, but is often based on one dimensional or average values at the boundaries. An encompassing description of the *control volume* approach would be "a method that is used to seek an estimate of gross effects (mass flow, induced force, energy change) over a finite region". These effects are generated as a result of four basic laws:

1. Conservation of mass

2. The linear momentum relation

3. The angular momentum relation

4. The energy equation

In addition to that a state relation may also be required in order to complete an analysis.

Another approach that is often used is the *Infinitesimal System* (differential analysis). This method involves seeking a point-by-point detail of a flow pattern by analyzing an infinitesimal region of flow. To date there is very little that is known about the general properties of the differential equations. This approach is not prominently used in problems of a very complex nature.

The third and final approach is performed through experimentation. Experimentation is often used to verify new FDE's to confirm that they accurately model the real life phenomenon. The benefits of experimentation are that exact results can be obtained based on the surrounding environment. The disadvantage is the initial setup costs, setup time, and feasibility. There is no

need to perform the same exact experiment that has already been performed several years or decades earlier when a FDE's has already been determined to be able to accurately represent the specific case (this would also result in unnecessary costs). Experimentation will always be needed, but should be kept to a minimum wherever possible.

The fluid flow analysis for flow around a 2D cylinder, 3D cylinder, 25ft (radius) spiral structure, & 30ft (radius) spiral structure will be performed using the control volume approach in the CFD program *Fluent*. To begin any problem, the first step that needs to be taken is to create the specific geometry. Note: The geometry should be created to scale within the respected computer aided design software. This is important as the size of the geometry plays an important role in determination of several variables within the respected problem.

The size of the two spiral structures are driving variables for the two cylinder cases. The size of the cylinder will be modeled in similar sizes, respectively 25ft and 30ft radii. This will allow for an accurate comparison between the results of all analyses later in the document. This fixed variable allows us to create a spatial domain for the analysis of this problem. The size of the spatial domain is sometimes calculated using formulae that are determined following years of testing and experimentation. Initially the domain was kept relatively small due to computational demands and time efficiency. Through several iterations the domain had to be gradually enlarged in order to minimize wall effects on solution results. This, in return, required much more memory and computational time. It is often the goal to achieve near perfect results in any analysis, but with CFD a compromise needs to be made between:

1. Accuracy/Error
2. Time Restraints

3. Hardware Availability

Following this testing, a document "Flow Over a Cylinder" (Kulkarni & Moeykens, 2005) was found, which accurately denotes the domain size for external flow around a cylindrical shaped object. The spatial domain is dimensioned as shown in **Figure 30**:
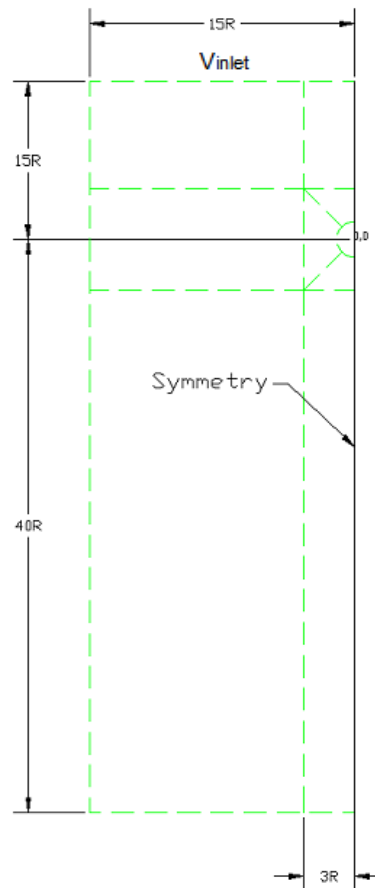
Figure 30 - Domain Sizing; (Kulkarni & Moeykens, 2005)

Note: For three dimensional flows the vertical dimension (domain height), is equal to 28.125ft tall or 1.5 revolutions. The parameters that are applied to the domain, such as the cylinder size, are required to initiate the fluid flow analysis and determine the parameters that most accurately represent the problem. A basic starting point is illustrated in **Figure 31**:

42
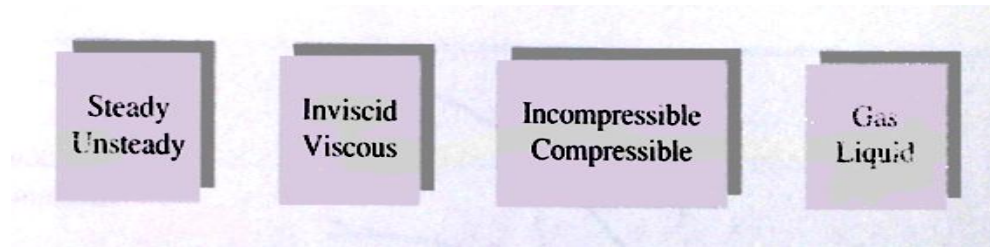
Figure 31 - Fluid Flow Analysis - General Assumptions (White, 2003, p. 39)

Extensive definitions of all of the above terms can be found in the glossary appended to the end of the document. For a very simplistic fluid flow problem steady state flow is chosen (independent of time). The second assumption was inviscid flow (μ is approximately zero) meaning that friction forces in the fluid are negligible when compared to inertial forces. The assumption of inviscid flow essentially eliminates the friction variable in the fluid and along the free surface being studied. The next two varying assumptions need to be solved simultaneously since the type of fluid is often used as a variable in the determination of Incompressible or Compressible flow regimes. Research has proven that the Mach number, a dimensionless parameter, is accurate at determining the flow regime. Aerodynamicists use the dimensionless numbers shown in Table 3 to describe flow behaviors between various ranges of numerical values.

Ma<0.3	*Incompressible flow*, where density effects are negligible
0.3<Ma<0.8	*Subsonic flow*, where density effects are important but no shockwaves appear.
0.8<Ma<1.2	*Transonic flow*, where shockwaves first appear, dividing subsonic and supersonic regions of the flow. Powered flight in the transonic is different because of the mixed character of the flow field.
1.2<Ma<3.0	*Supersonic flow*, where shockwaves are present but there are no subsonic regions
3.0<Ma	*Hypersonic flow*, where shockwaves and other flow changes are especially strong.

Table 3 - Mach Number - Flow Regime Classifications

The Mach number that is specific to the spiral structures can be viewed in **Table 4**:

Air				
Input	Conversion Factor		Result	
60 ft	0.3048	m	18.288	m
10 mph	0.44704	m/s	4.4704	m/s
MACH # (M<=0.3 then flow is incompressible)				
M=	0.013136644	Unitless	Compressible	
			Incompressible	
a	Speed of Sound	340.3 m/s		
u	Velocity	4.4704 m/s		
Air	Compressible			
	OR			
	Incompressible			
	Re=	5,596,819 unitless		
D	Diameter	18.288 m		
u	Velocity	4.4704 m/s		
ρ	Density	1.225 kg/m^3		
μ	Viscosity	1.79E-05 kg/(m*s)		
ν	Viscosity	1.46073E-05 m^2/s		

Table 4 - Mach Number & Reynolds Number Calculations

Table 4 proves that if air (flow medium) is approaching a tower of 60ft in diameter at a constant velocity of 10mph, it will have Reynolds number $(Re = \frac{\rho V D}{\mu})$ of 5,596,819 and thus be classified as turbulent flow. Additionally, these parameters can be used to determine the Mach number, which in this case is equivalent to 0.0131366. Based on the predefined criteria in **Table 3**, the flow is can be classified as incompressible since the calculated value is less than 0.3.

3.3 FUTURE PROSPECTS OF TURBULENCE MODELING

The understanding of the phenomenon *turbulent motion of fluids* has been sought after for centuries. This continued to puzzle even the greatest minds until a breakthrough derivation, known as the Navier-Stokes equation, was made. The basis of the Navier-Stokes equation is the three fundamental equations in fluid dynamics, which are the continuity equation (conservation of mass), momentum equation (Newton's second law), and the energy equation (Newton's first law).

To allow for a better understanding, the generic Navier-Stokes equation is presented below:

$$\rho \frac{DV}{Dt} = \rho \boldsymbol{f} - \nabla p + \frac{\partial}{\partial x_j}\left[\mu\left(\frac{\partial u_i}{\partial x_j} + \frac{\partial u_j}{\partial x_i}\right) - \frac{2}{3}\delta_{i,j}\mu\frac{\partial u_k}{\partial x_k}\right]$$

The general equation can be further broken down into three scalar Navier-Stokes equations:

$$\rho \frac{Du}{Dt} = \rho f_x - \frac{\partial p}{\partial x} + \frac{\partial}{\partial x}\left[\frac{2}{3}\mu\left(2\frac{\partial u}{\partial x} - \frac{\partial v}{\partial y} - \frac{\partial w}{\partial z}\right)\right] + \frac{\partial}{\partial y}\left[\mu\left(\frac{\partial u}{\partial y} + \frac{\partial v}{\partial x}\right)\right] + \frac{\partial}{\partial z}\left[\mu\left(\frac{\partial w}{\partial x} + \frac{\partial u}{\partial z}\right)\right]$$

$$\rho \frac{Dv}{Dt} = \rho f_y - \frac{\partial p}{\partial y} + \frac{\partial}{\partial x}\left[\mu\left(\frac{\partial v}{\partial x} + \frac{\partial u}{\partial y}\right)\right] + \frac{\partial}{\partial y}\left[\frac{2}{3}\mu\left(2\frac{\partial v}{\partial y} - \frac{\partial u}{\partial x} - \frac{\partial w}{\partial z}\right)\right] + \frac{\partial}{\partial z}\left[\mu\left(\frac{\partial v}{\partial z} + \frac{\partial w}{\partial y}\right)\right]$$

$$\rho \frac{Dw}{Dt} = \rho f_z - \frac{\partial p}{\partial z} + \frac{\partial}{\partial x}\left[\mu\left(2\frac{\partial w}{\partial x} + \frac{\partial u}{\partial z}\right)\right] + \frac{\partial}{\partial y}\left[\mu\left(\frac{\partial v}{\partial z} + \frac{\partial w}{\partial y}\right)\right] + \frac{\partial}{\partial z}\left[\frac{2}{3}\mu\left(2\frac{\partial w}{\partial z} - \frac{\partial u}{\partial x} - \frac{\partial v}{\partial y}\right)\right]$$

Additionally, if the flow is deemed to be incompressible these equations can be simplified further because the viscosity is held constant. The resultant equation is:

$$\rho \frac{DV}{Dt} = \rho \boldsymbol{f} - \nabla p + \mu\nabla^2 V$$

It is important to note that although this equation is used to accurately represent the variables that define the phenomenon of turbulent flow, the exact solution has never been obtained. Because of the complexity of the Navier-Stokes PDE (partial differential equation), engineers have vested large amounts of research into the development of approximation methods or FDE's (finite difference equations). With the proper computational resources, these equations can then be analyzed in CFD packages such as Fluent using either DNS (direct numerical simulation) or LES (large eddy simulation) methods. One of the main difficulties in solving a problem using direct numerical simulation is that it requires that all of the relevant *length scales*[12] be resolved, which range from smallest eddies all the way up to scales that are nearly equivalent of the physical dimensions of the problem domain.

---

[12] "Sometimes it is easier to think in terms of turbulence length scale instead of turbulent viscosity ratio. The turbulence length scale, l, is a physical quantity which represents the size of the large eddies in turbulent flows. Empirical relationship between the physical size of the obstruction (or characteristic length), L, and the size of the eddy, l, can be used to get an approximate length scale.

l = 0.07L

For external flows, it is often not possible to determine a good characteristic length. In using the formulas below, pick a value of β and a value of u' and use the formulas on the left, the ones not involving the length scale. In the case of external aerodynamic flows, choose smaller values of β (0.1 to 1), whereas in the case of wind-tunnel external flows, choose larger values of β (1 to 10).
NOTE: For external flows it is very important to specify appropriate turbulent quantities at the freestream boundaries. If the values are unphysical it can cause the solution to be unrealistic and can lead to divergence or non-convergence." (ESI Group, 2007)

3.4 CFD CODE VALIDATION – FLOW OVER A CYLINDER

3.4.1 Flow Over a Cylinder - Superposition of a Doublet and Uniform Flow

Assumptions:

1. Two dimensional

2. Incompressible

3. Irrotational flow (formed from superposition of a doublet and a uniform flow)

3.4.1.1 Stream function and velocity potential

$$\psi = \psi_d + \psi_{uf} = -\frac{\Lambda * \sin(\theta)}{r} + U * r * \sin(\theta)$$

$$\phi = \phi_d + \phi_{uf} = -\frac{\Lambda * \cos(\theta)}{r} - U * r * \cos(\theta)$$

$$V_r = -\frac{\partial \phi}{\partial r} = -\frac{\Lambda * \cos(\theta)}{r^2} + U * \cos(\theta)$$

$$V_\theta = -\frac{1}{r} * \frac{\partial \phi}{\partial r} = -\frac{\Lambda * \sin(\theta)}{r^2} + U * \sin(\theta)$$

3.4.1.2 Velocity field

$$\vec{V} = V_r * \hat{e}_r + V_\theta * \hat{e}_\theta = \left(-\frac{\Lambda * \cos(\theta)}{r^2} + U * \cos(\theta) \right) * \hat{e}_r + \left(-\frac{\Lambda * \sin(\theta)}{r^2} - U * \sin(\theta) \right) * \hat{e}_\theta$$

3.4.1.3 Stagnation points

$$V_r = 0 = -\frac{\Lambda * \cos(\theta)}{r^2} + U * \cos(\theta) = \cos(\theta) * \left(U - \frac{\Lambda}{r^2}\right)$$

$$V_\theta = 0 = -\frac{\Lambda * \sin(\theta)}{r^2} - U * \sin(\theta) = -\sin(\theta) * \left(U + \frac{\Lambda}{r^2}\right)$$

3.4.1.4 Cylindrical surface

$$\frac{p_\infty}{\rho} + \frac{U^2}{2} + g * z = \frac{p}{\rho} + \frac{V^2}{2} + gz$$

$$p - p_\infty = \frac{1}{2} * \rho * (U^2 - V^2)$$

3.4.1.5 Surface pressure distribution

$$V^2 = V^2{}_\theta = \left(-\frac{\Lambda}{a^2} - U\right)^2 * \sin^2\theta = 4 * U^2 \sin^2\theta$$

$$p - p_\infty = \frac{1}{2}\rho * (U^2 - 4 * U^2 \sin^2\theta) = \frac{1}{2}\rho * U^2(1 - 4 * \sin^2\theta)$$

$$\frac{p - p_\infty}{\frac{1}{2}\rho * U^2} = 1 - 4 * \sin^2\theta$$

3.4.2　Flow Over a Cylinder - Application of Formulae

For the case shown in **Figure 32**,
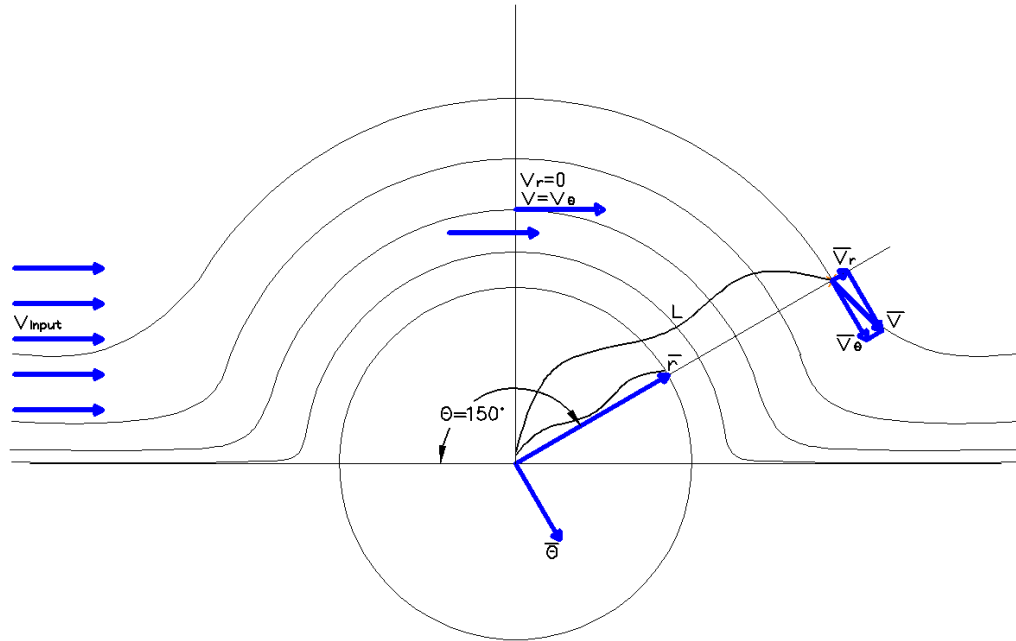
Figure 32 - 2D Cyl. - Velocity Stagnation Points

We see that for,

$$\theta = 150 \rightarrow \vec{v} = v_r * \hat{r} + v_\theta * \hat{\theta}$$

The velocity components are defined as,

$$\vec{v}_r = \cos(\theta) * \left(U - \frac{\Lambda}{r^2} \right) = \frac{-\Lambda * \cos(\theta)}{r^2} + U * \cos(\theta)$$

$$\vec{v}_\theta = -\sin(\theta) * \left(U + \frac{\Lambda}{r^2} \right) = \frac{-\Lambda * \sin(\theta)}{r^2} - U * \sin(\theta)$$

where Λ & U are defined as

$$\Lambda = U * a^2$$

U=free stream velocity

Then apply the formula below to obtain the velocity magnitude,

$$\vec{\bar{v}} = \sqrt{v_r^2 + v_\theta^2}$$

For $\theta = 90°$ (Note: $\cos(90) = 0$ & $\sin(90) = 1$),

$$\vec{v}_r = 0$$

$$\vec{v}_\theta = \frac{-\Lambda}{r^2} - U$$

By substituting the variable Λ and evaluating the expression of $\vec{v}_\theta$ where r=a,

$$\vec{v}_\theta = \frac{-U * a^2}{a^2} - U = -2U$$

Thus, if the free stream velocity is defined to be 10mph the tangential velocity at r=a will be equal to 2.0E+01 or 20mph. Note: This assumption assumes inviscid flow with a no slip boundary condition applied at the cylinder wall. This example provides a basis to compare the numerical results against.
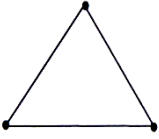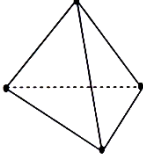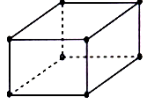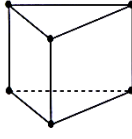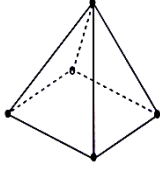
3.4.3   Numerical Verification (CFD) – 2D Cyl

The domain, mesh, and B.C.'s were developed by implementing research of prior arts. A series of tests were then performed to verify that what had previously been done. The purpose of these tests was to improve the accuracy of the solution in any way possible, while reducing the user's setup time and computational time. Driving parameters that were applied in these tests include:

1. Domain size & aspect ratio

2. Mesh type (map, submap, pave)

3. Mesh quality (transition between regions of importance)

4. Mesh size (element size)

5. Boundary layer

6. Boundary conditions

As mentioned earlier, each parameter can have an effect on the accuracy of the solution.

Before proceeding, it is imperative that the user understands the solution process as well as the capabilities of Fluent's code. The beginning of the grid generation process takes place in Gambit, Fluent's pre-preprocessor. Gambit provides the user with a three-dimensional environment and a GUI that allows the user to position the test model(s) within the respected domain. Upon finishing the model, the appropriate 2D/3D mesh elements, shown in **Table 5**, can then be applied to the model.

2D Elements		3D Elements	
Unstructured	Structured	Unstructured	Structured
Triangle	**Quadrilateral**	**Tetrahedron**	**Hexahedron**
		Unstructured	Unstructured
		Prism/Wedge	**Pyramid**

Table 5 - Mesh Element Types

This structured/unstructured mesh can then be exported to a file format that is compatible with Fluent. Since Fluent is inherently an unstructured solver, it uses internal data structures to assign an order to cells, faces, and grid points in a mesh, thus relieving any restrictions that would be present with the i,j,k indexing method. This flexibility provides a huge time and cost savings for problems that are simple in nature and creates additional opportunity for those problems that were once deemed unsolvable due to the computational restrictions of the past. It is important to remember that this code was not created overnight, but rather has been developed by some of the greatest minds in academia, government, and private industry over several decades.

The choice of mesh is highly dependent upon the specific application. In general, CFD discretization schemes result in a problem set that is computationally demanding. As a result these additional factors must be considered:

1. Setup time

2. Computational expense (CPU(s), memory, storage capacity, time)

3. Numerical Diffusion

Setup time will vary with every new problem. Users will often need to develop a grid based on a series of trial and errors in order to achieve the optimum mesh for their specific problem and computer system. In most cases structured grids should be used due to better result accuracy, memory savings, and computational time savings. Experienced users will be able to notice how to distribute their often finite number of elements, usually giving added emphasis (refinement) to the areas of interest. Because many engineering problems involve complex geometries, structured grids may not always be a viable option. For these complex cases unstructured grids often prove to be beneficial. The time savings in mesh generation in most cases is worth the added computational time and the sacrifice of accuracy. In the case of the spiral shape, a combination of unstructured and structured elements was combined in order to achieve optimum results. **Table 6 & Table 7** denote some initial parameters and guidelines that have been proven to produce consistent results. Note: If the geometry is relatively simple there may be no clear savings in setup time with either approach as the added setup of elements will take very little time using either method and there will be a very small discrepancy in computational time.

Mesh Density	Refinement Factor
Fine	1
Medium	1.3
Coarse	1.69

Note: Reynolds Number is used to determine Yplus. Yplus values for turbulent flow conditions can be viewed in the table below:

Reynolds Number	Flow Regime	Yplus/First Cell Height
Re < 1000	Laminar	First Cell Height
1000 <= Re <= 20000	Turbulent, Enhanced Wall Treatment	First Cell Height = Cylinder Radius/24
Re > 20000	Turbulent, Standard Wall Functions	Yplus > 30

$$First\_Cell\_Height = Re\_finement\_Factor * \left[\frac{Yplus * (Characteristic\_Length^{0.125} * T_u \cos i_0{}^{0.875})}{(0.199 * Velocity^{0.875} * Density^{0.875})}\right]$$

Fine

First Cell Height	0.003435467	m
Refinement Factor	1	unitless
Yplus	30	non dimensional
Characteristic Length	18.288	m
Viscosity	1.79E-05	kg/(m*s)
Velocity	4.4704	m/s
Density	1.225	kg/m^3

Medium

First Cell Height	0.004466107	m
Refinement Factor	1.3	unitless
Yplus	30	non dimensional
Characteristic Length	18.288	m
Viscosity	1.79E-05	kg/(m*s)
Velocity	4.4704	m/s
Density	1.225	kg/m^3

Coarse

First Cell Height	0.005805939	m
Refinement Factor	1.69	non dimensional
Yplus	30	non dimensional
Characteristic Length	18.288	m
Viscosity	1.79E-05	kg/(m*s)
Velocity	4.4704	m/s
Density	1.225	kg/m^3

$$Intervals = INT\left[\frac{Log\left(\frac{Edge\_Length * Growth\_Ratio}{First\_Cell\_Height} - 1\right)}{Log(Growth\_Ratio)} + 1.0\right]$$

Note:
* A boundary layer with 10 rows is placed at the cylinder wall using the calculated value of the first cell height
* The entire domain is meshed using map scheme

Physical Models

Re < 1000	Laminar
1000 <= Re <= 10000	Low Reynolds number k-e model
Re > 10000	k-e model

Boundary Conditions
* Inlet Velocity
* Wall roughness | (To be specified only when the flow is modeled as turbulent)

In Fluent,

Boundary	Assigned As
Cylinder	Wall
Inlet	Velocity Inlet
Side Boundaries	Periodic/Outflow
Outlet	Pressure Outlet

Table 6 - Model/Mesh/&B.C. Guidelines (25ft Spire)

Mesh Density	Refinement Factor
Fine	1
Medium	1.3
Coarse	1.69

Note: Reynolds Number is used to determine Yplus. Yplus values for turbulent flow conditions can be viewed in the table below:

Reynolds Number	Flow Regime	Yplus/First Cell Height
Re < 1000	Laminar	First Cell Height = Cylinder Radius/24
1000 <= Re <= 20000	Turbulent, Enhanced Wall Treatment	Yplus < 10
Re > 20000	Turbulent, Standard Wall Functions	Yplus > 30

$$First\_Cell\_Height = Re\_finement\_Factor * \left[\frac{Yplus * (Characteristic\_Length^{0.125} * Viscosity^{0.875})}{(0.199 * Velocity^{0.875} * Density^{0.875})} \right]$$

Fine

First Cell Height	0.003356058 m
Refinement Factor	1 unitless
Yplus	30 non dimensional
Characteristic Length	15.24 m
Viscosity	1.79E-05 kg/(m*s)
Velocity	4.4704 m/s
Density	1.225 kg/m^3

Medium

First Cell Height	0.004365475 m
Refinement Factor	1.3 unitless
Yplus	30 non dimensional
Characteristic Length	15.24 m
Viscosity	1.79E-05 kg/(m*s)
Velocity	4.4704 m/s
Density	1.225 kg/m^3

Coarse

First Cell Height	0.005675117 m
Refinement Factor	1.69 unitless
Yplus	30 non dimensional
Characteristic Length	15.24 m
Viscosity	1.79E-05 kg/(m*s)
Velocity	4.4704 m/s
Density	1.225 kg/m^3

$$Intervals = INT \left[\frac{Log(Edge\_Length * Growth\_Ratio - 1)}{Log(Growth\_Ratio)} \right] + 1.0$$

over $First\_Cell\_Height$

Note:
* A boundary layer with 10 rows is placed at the cylinder wall using the calculated value of the first cell height
* The entire domain is meshed using map scheme

Physical Models

Re < 1000	Laminar
1000 <= Re <= 10000	Low Reynolds number k-e model
Re > 10000	k-e model

Boundary Conditions

* Inlet Velocity
* Wall roughness (To be specified only when the flow is modeled as turbulent)

In Fluent,

Boundary	Assigned As
Cylinder	Wall
Inlet	Velocity Inlet
Side Boundaries	Periodic/Outflow
Outlet	Pressure Outlet

Table 7 - Model/Mesh/&B.C. Guidelines (30ft Spire)

Computational expense is affected by a number of parameters. In general, the ideal aspect ratio of an element has a magnitude of (1). This will provide the most accurate results with the shortest time for residual convergence. When geometries are more complex or the range of length scales of the flow is large an unstructured mesh can often be created with far fewer cells than an equivalent structured mesh. This is a result of structured cells (having high aspect ratios) being forced into undesired areas. Additional cells contribute to added computation time, the requirement for more memory, and possibly the addition of multiple CPU's (parallel processing). The computational expense needs to be assessed for each unique problem.

Numerical diffusion, a form of truncation error, is an error made by numerical algorithms that arises from taking a finite number of steps in a computation. Use of arbitrarily small steps is prevented in numerical calculations due to computational limitations (inherent to the FDE's), thus resulting in what is known as round-off error. The Fluent User's guide provides an exact explanation of this, denoted below (Fluent Inc., 2007):

1. "Numerical diffusion is most noticeable when the real diffusion is small, that is, when the situation is convection dominated.
2. All practical numerical schemes for solving fluid flow contain a finite amount of numerical diffusion. This is because numerical diffusion arises from truncation errors that are a consequence of representing the fluid flow equations in discrete form.
3. The second-order discretization scheme used in FLUENT can help reduce the effects of numerical diffusion on the solution.
4. The amount of numerical diffusion is adversely related to the resolution of the mesh. Therefore, one way of dealing with numerical diffusion is to refine the mesh.
5. Numerical diffusion is minimized when the flow is aligned with the mesh."

The mesh generation of the 2D cylinder was generated using a 100% structured grid. When generating this grid it is important to optimize the aspect ratio of the quadrilateral elements as this will result in a quicker convergence and more accurate solution result. It is important to note the mesh refinement in areas of interest.
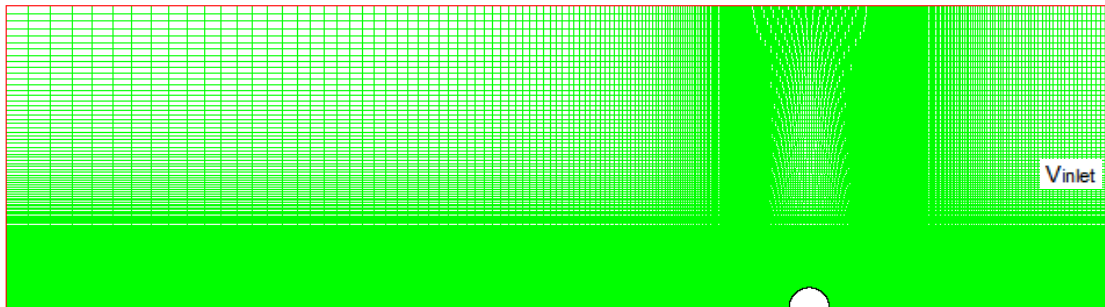
Figure 33 - 2D Cyl. - Structured Grid, Entire Domain

Notice how the localized square region that is located around the cylinder is broken into three zones. Because of this separation, the same numbers of elements per unit of area were used in each region. This was done, while maintaining similar aspect ratios amongst each of the quadrilateral elements.
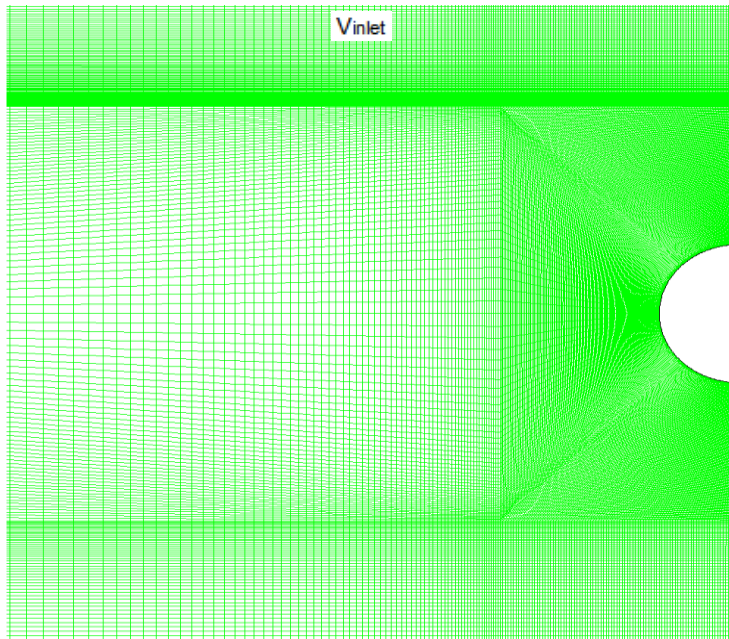
Figure 34 - 2D Cyl. – Structured Grid, Zoom

Figure 34 shows the emphasis on the boundary layer around the exterior of the cylinder. In this case, (10) layers were created using values similar to the "first row height" values provided in the preceding tables.
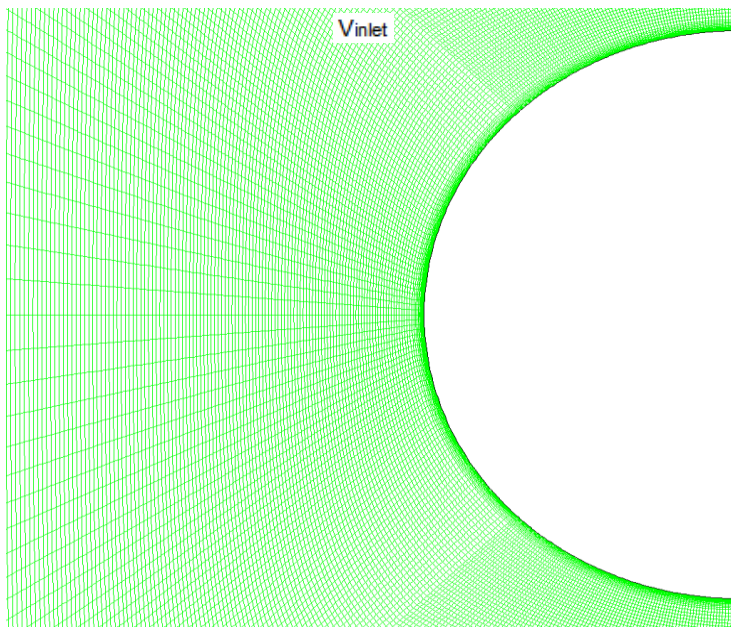
Figure 35 - 2D Cyl. – Structured Grid, Boundary Layer

3.4.3.1 Case I - 2D Cyl.

The boundary conditions that were applied to case I are as follows:

1. Velocity Inlet - fluid inlet

2. Pressure Outlet - fluid exit

3. Symmetry - Side Where cylinder is cut

4. Symmetry – Side opposite of the cylinder

5. Wall – Cylinder

The flow model that was used for this case using inviscid flow (meaning $\mu=0$).

The input velocity was equally distributed about the velocity inlet having a velocity of 10mph. The results of this analysis should provide the closest solution match to the theoretical model.[13] The residual criterion was set to a convergence criterion of 10^-6 for each parameter.
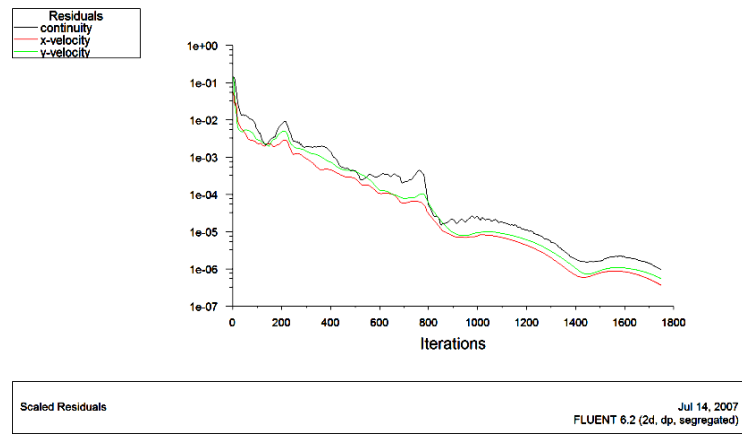
Figure 36 - 2D Cyl. – Scaled Residuals (Inviscid Flow)

---

[13] Note: This analysis will be used for a comparison against the theoretical model only.

The scaled residual plot shows that the continuity, x-velocity, and y-velocity all converged just shy of 1800 iterations, which further instills a level of confidence in the grid and solution results that are based on the specified conditions.
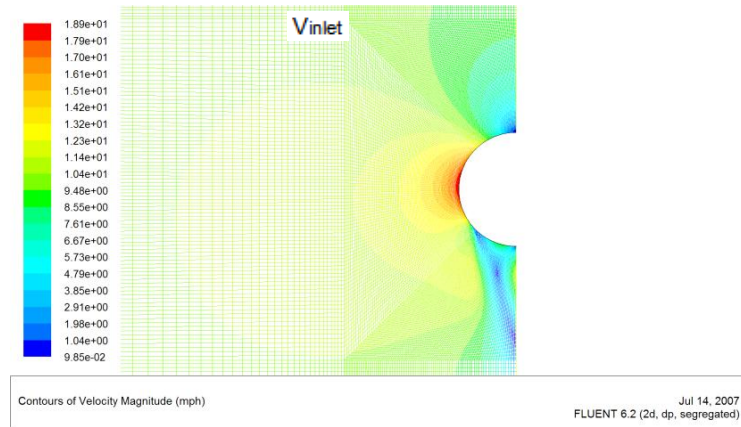
Figure 37 - 2D Cyl. – Vel. Magnitude Contours (Inviscid Flow)

The velocity magnitude results for inviscid flow around a 2D cylinder show a region of negative pressure (with possible reversed flow) in front of and behind the cylinder. The region of maximum velocity is shown in the middle left portion of the cylinder having an amplification factor of roughly 1.9.[14]
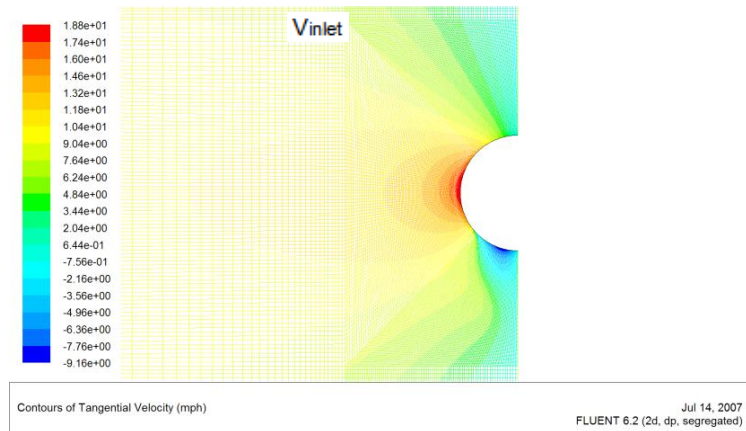
Figure 38 - 2D Cyl. – Tangential Vel. Contours (Inviscid Flow)

---

[14] No slip wall conditions are inherently present.

The tangential velocity results for inviscous flow around a 2D cylinder show similar regions of negative pressure as shown in the Velocity Magnitude Contour figure. The tangential velocity inlet profile is linear in nature, while the region beyond the cylinder has a slight curve.
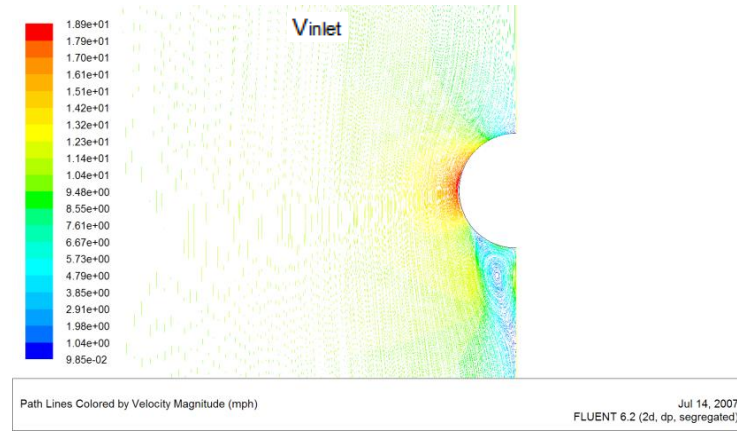
Figure 39 - 2D Cyl. - Vel. Magnitude Pathlines (Inviscid Flow)

The velocity magnitude pathlines can be rendered with extensive detail, which gives the user a very clear representation of the magnitude and path of the velocity vectors within the designated plane. For this specific case, which involves inviscid flow, there is a small region of reversed flow after the cylinder. It is important to note that because Re=∞ (when μ=0) vortices do not exist.

3.4.3.2   Case II - 2D Cyl.

The boundary conditions that were applied to case II were as follows:

1. Velocity Inlet - fluid inlet

2. Pressure Outlet - fluid exit

3. Symmetry - side where cylinder is cut

4. Symmetry – side opposite of the cylinder

5. Wall – cylinder

The flow model that was used for this case was k-ε turbulence model (Re>20,000).[15] The input velocity was equally distributed about the velocity inlet having a velocity of 10mph. The results of this analysis will be contrasted against a 3D cylinder model to confirm that the mesh maintains its accuracy when being transformed into the 3D domain. The residual criterion was set to a convergence criterion of 10^-6 for each parameter.
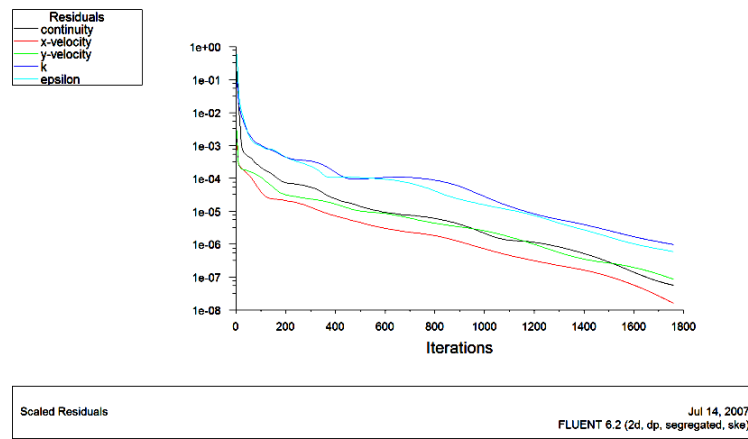
Figure 40 - 2D Cyl. - Scaled Residuals (k-ε turbulence model)

The scaled residual plot, **Figure 40**, for a 2D cylinder and the k-ε model shows that the

1. continuity,

2. x-velocity,

3. y-velocity,

4. k,

5. and epsilon (ε)

---

[15] (Kulkarni & Moeykens, 2005)

all variables converged just shy of 1800 iterations, which further instills a level of confidence in the grid and solution results that are based on the specified conditions.
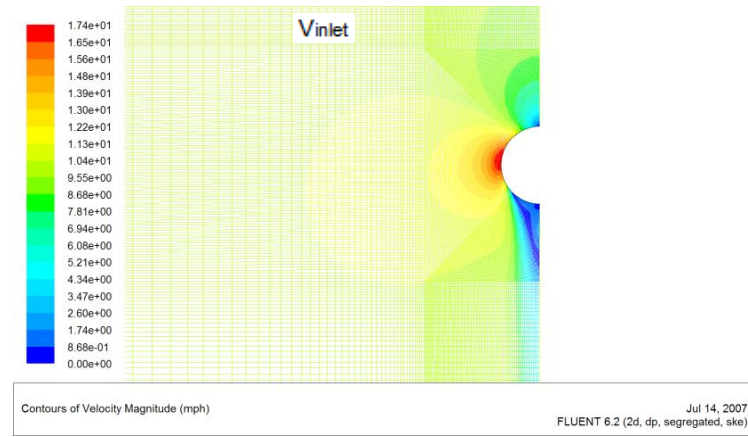
Figure 41 - 2D Cyl. – Vel. Magnitude Contours (k-ε turbulence model)

The velocity magnitude results for turbulent flow around a 2D cylinder shows a small region of negative pressure in front of the cylinder and a large region (with possible reversed flow) behind the cylinder. The region of maximum velocity when applying the turbulent model is shown in the middle left portion of the cylinder having an amplification factor of roughly 1.74.
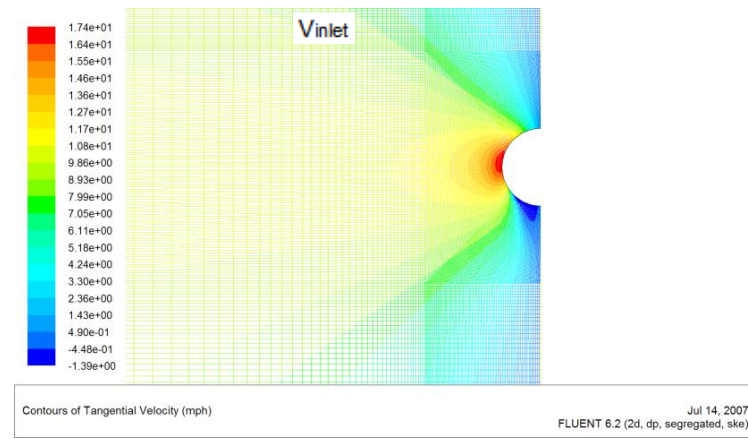
Figure 42 - 2D Cyl. - Tangential Vel. Contours (k-ε turbulence model)

The tangential velocity results for turbulent flow around a 2D cylinder show similar regions of negative pressure as shown in the velocity magnitude contour figure. The tangential velocity near the front of the cylinder has a relatively uniform profile, while the region beyond the cylinder is slightly more drastic curve.
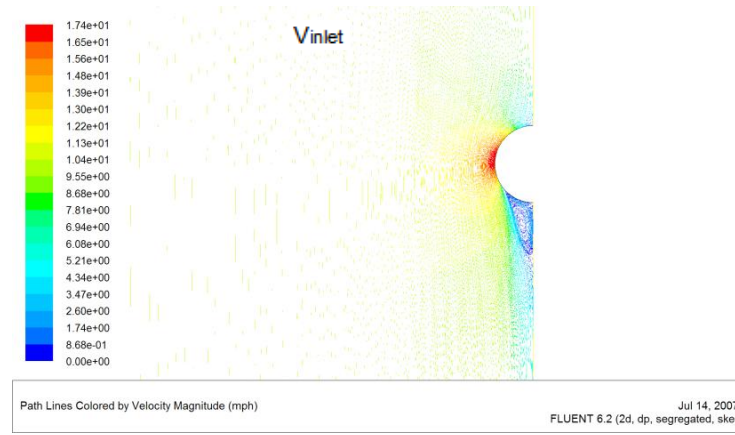
Figure 43 - 2D Cyl. – Vel. Magnitude Pathlines (k-ε turbulence model)

The velocity magnitude pathlines can be rendered with extensive detail, which gives the user a very clear representation of the magnitude and direction of the velocity vectors on the designated plane. This is extremely useful for more complex models such as the k-ε model in that the regions of reversed flow and vortices are clearly represented.

3.4.4   <u>Numerical Verification w/Grid Independence Verification – 3D Cyl.</u>

The domain, mesh, and B.C.'s that were developed in the 2D cylinder model produced accurate results in a relatively short number of iterations. Computational requirements such as memory and the number of CPU's were minimized due to the implementation of a structured mesh within the domain. Although this was relatively simple to setup in a two dimensional environment, there is an additional level of difficulty that is added when designing a mesh for a three dimensional environment.

Three dimensional domains are often resource intensive, thus alternatives such as symmetry boundary conditions or short flow inlets can significantly save the users time. For example **Figure** 44, courtesy of Gambit Users Manual, displays an efficient way of positioning the test object within the three-dimensional domain. The reason the sedan is merged with the wall of the domain is to utilize the benefit of symmetric boundary conditions.
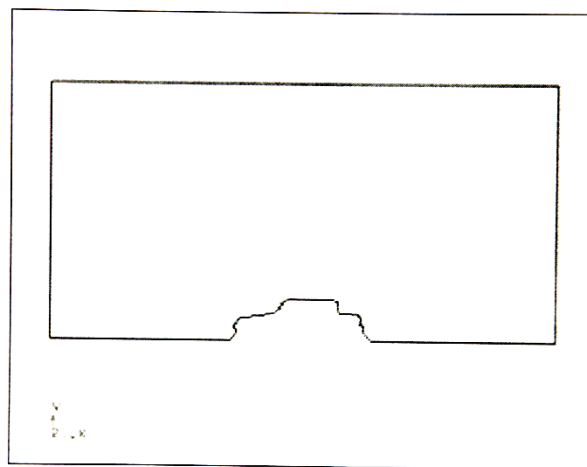
Figure 44 - Edges used to create face at top of sedan; (Fluent Inc., 2001)

All sides of the domain in **Figure 45** have the boundary type set to "symmetry" except for the major flow inlet/outlet. Further research will specify that for this type of problem a pressure outlet is required at the flow exit, thus relieving the user of additional calculations that would be required if it were to be specified as a velocity outlet. The flow inlet can be specified as either a velocity inlet or a pressure inlet. This boundary type is problem specific and will not alter the problems results.
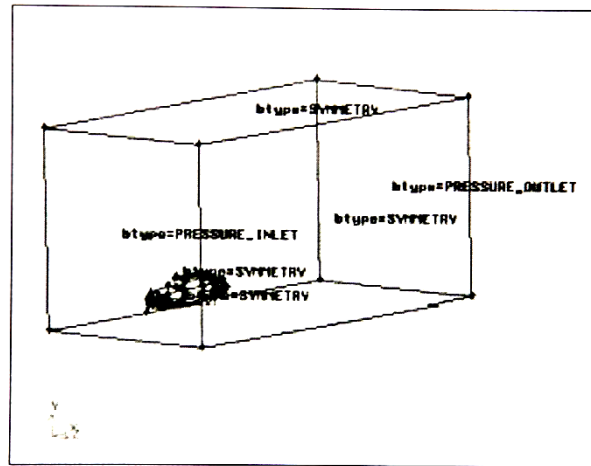
Figure 45 - Boundary types for sedan geometry; (Fluent Inc., 2001)

The same parameters that are used in **Figure 45** will be applied to the 3D cylinder analyses. The 3D cylinder tests will compare the flow results of two unique grid types with the goal of verifying that both meshes produce consistent results. The two meshes will be denoted by the following nomenclature "Case I" (structured grid) and "Case II" (unstructured grid). Note: The unstructured grid must yield equivalent results of the structured mesh because the complex shapes present in the analysis of the spiral structure make the use of a structured grid inefficient and nearly impossible.

66

3.4.4.1 Case I - 3D Cyl. (Turbulent Flow w/Structured Grid)

The first case applies a 3D structured grid, which is a product of a linear pattern of a 2D structured grid. All top faces in the domain were meshed using a quadrilateral "map" meshing scheme. All bottom faces in the domain were meshed using a quadrilateral "submap" meshing scheme. The edges that are located between the top and bottom faces were all meshed uniformly using the "Cooper" meshing scheme in Gambit.
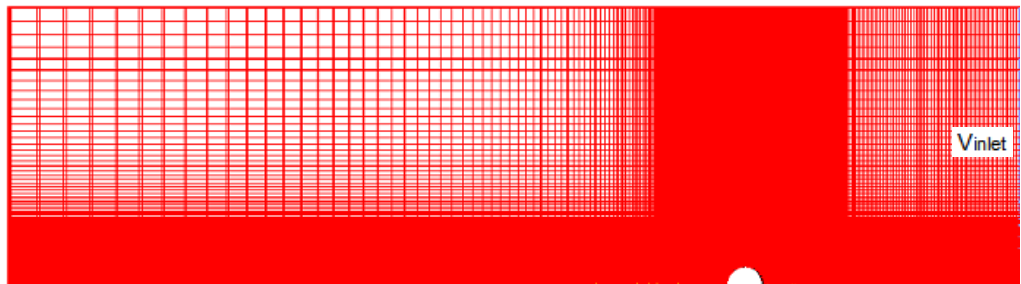
Figure 46 - 3D Cyl. - Structured Grid, Entire Domain

Figure 46 illustrates proof that the 3D grid maintained the same characteristics of the 2D cylinders structured grid (notice the local mesh refinement in areas of importance). A zoomed perspective can be viewed in Figure 47.
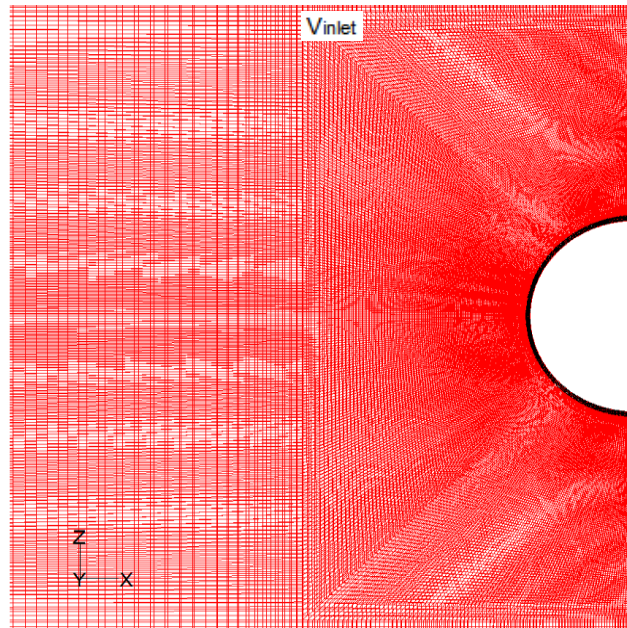
Figure 47 - 3D Cyl. – Structured Grid, Zoom

The elevation detail shows the δ between each of the linearly stacked 2D structured meshes. The grid maintains the same localized mesh in areas of importance around the perimeter of the cylinder.
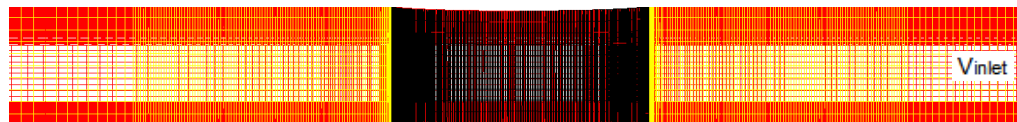
Figure 48 - 3D Cyl. - Structured Grid, Elevation Detail

Now that the mesh has been obtained, the boundary conditions that were typical to the sedan example can be applied. The only alteration that needs to be made is the change from pressure inlet to velocity inlet. To be specific, the boundary conditions that were applied to case I are as follows:

1. Velocity Inlet - fluid inlet

2. Pressure Outlet - fluid exit

3. Symmetry - side Where cylinder is cut

4. Symmetry – side opposite of the cylinder

5. Symmetry – top of domain

6. Symmetry – bottom of domain

7. Wall – cylinder

The flow model that was used for this case was k-ε turbulence model (Re>20,000).[16] The input velocity was equally distributed about the velocity inlet having a velocity of 10mph. The results of this analysis should provide the closest solution match to the theoretical model. The residual criterion was set to a convergence criterion of 10^-6 for each parameter.
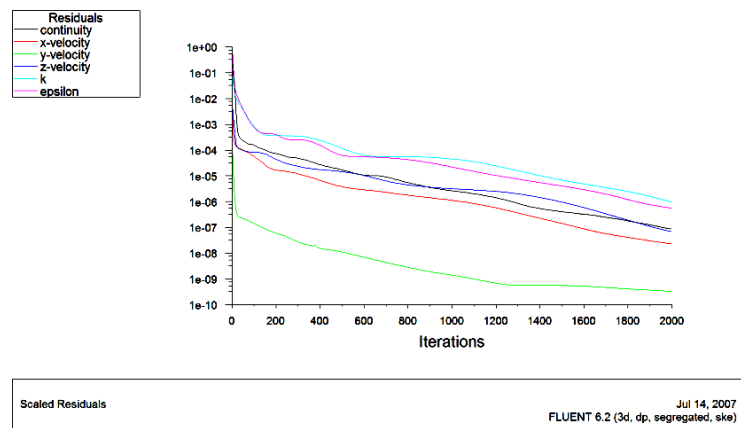
Figure 49 - 3D Cylinder – Scaled Residuals (k-ε turbulence model)

Figure 49 shows the residuals of the three velocity components, continuity, and k-ε variables. Although each variable converges at different points the convergence criterion is not satisfied until all of the residuals have converged to a value of 10^-6. This takes place at roughly 2000 iterations.

---

[16] (Kulkarni & Moeykens, 2005)
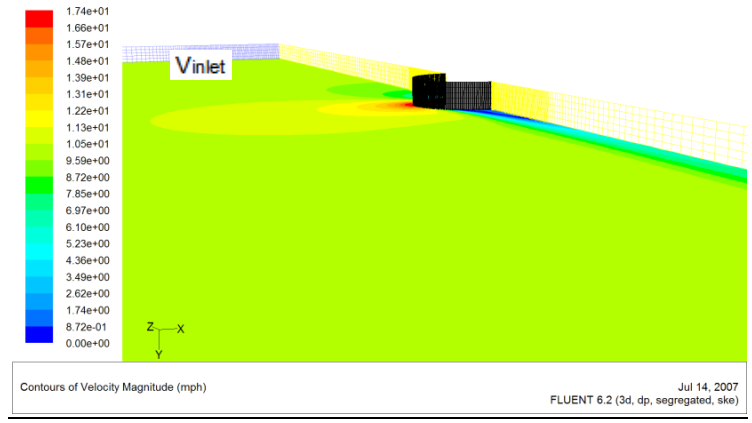
Figure 50 - 3D Cyl. – Vel. Magnitude Plane 10 Contours (k-ε turbulence model)

Figure 50 illustrates the velocity distribution over *plane 10* of the 3D cylinder grid. The velocity magnitude is computed based on all of the node points that exist within the *default interior* of the domain. The results of this 3D structured grid exactly match that of the 2D structured grid with the same velocity distribution and maximum velocity of roughly 17.4 mph.
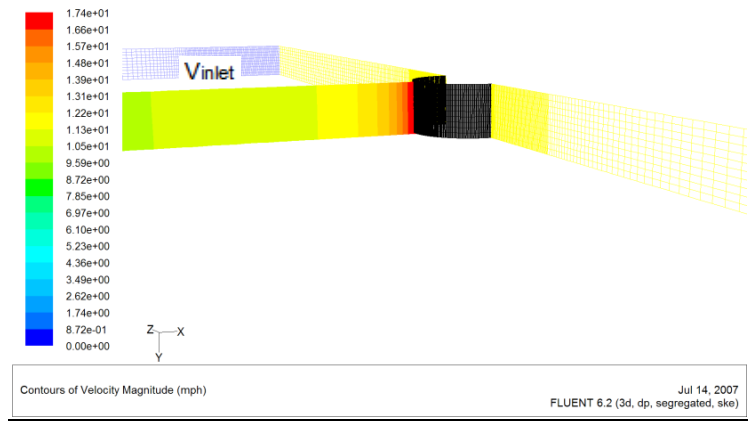
Figure 51 - 3D Cyl. – Vel. Magnitude Plane 9 Contours (k-ε turbulence model)

This cut plane, denoted as *plane 9*, displays a different perspective of the velocity magnitude distribution within the domain. The figure shows the region near the cylinder where the points of maximum velocity occur. It is important to also note

that the color uniformity, especially near the wall of the cylinder, confirms that the boundary conditions are correctly defined for this problem set.
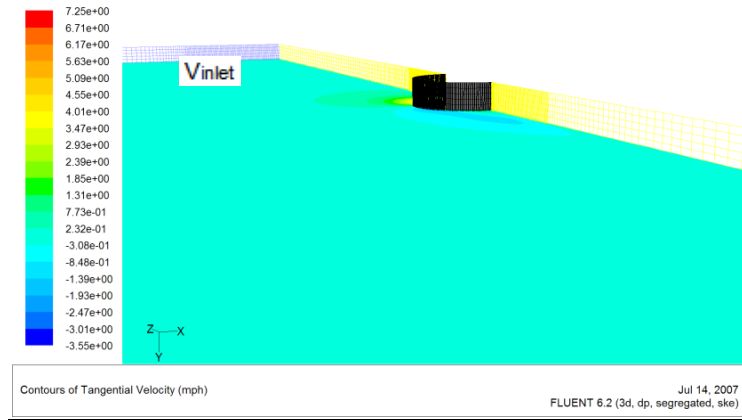
Figure 52 - 3D Cyl. - Tangential Vel. Plane 10 Contours (k-ε turbulence model)

The tangential velocity that is shown on *plane 10* has a maximum value of 7.25mph. This figure differs slightly from that of the 2D cylinder problem because the domain is three-dimensional, thus containing an additional velocity vector. As a result the region of amplified velocity vectors is much smaller than 2D cylinders grid.
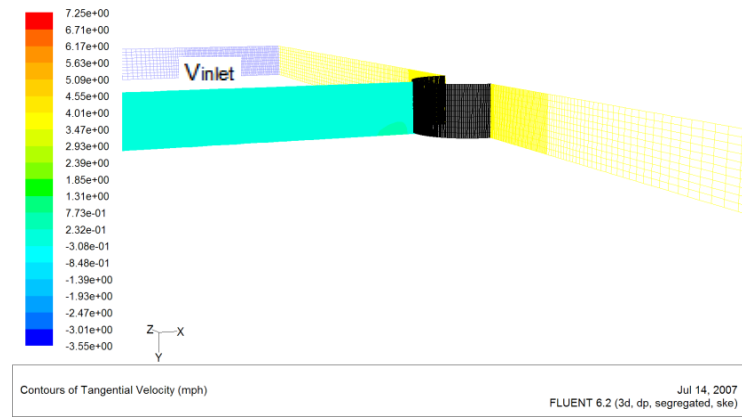
Figure 53 - Tangential Vel. Plane 9 Contours (k-ε turbulence model)

The tangential velocity that is displayed on *plane 9* is uniform throughout except for a very small δ in velocity near the cylinder.

3.4.4.2   Case II - 3D Cyl. (Turbulent Flow w/Unstructured Grid)

The boundary conditions and flow model are the same that were applied to Case I. The only change in parameters between Case I and Case II was the type of grid.
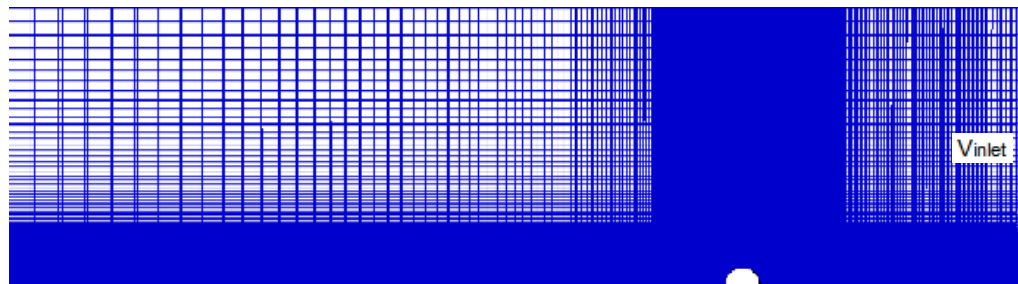
Figure 54 - 3D Cyl. - Unstructured Grid, Entire Domain

This grid maintains a zone/mesh structure that is similar to that of the previous 3D cylinders structure grid. The only difference in this mesh and the previous mesh is in the region near the cylinder. The local mesh refinement was altered from a very fine structured grid that used hex elements to an unstructured grid that used tet/hybrid elements. A zoomed view is shown in **Figure 55**.
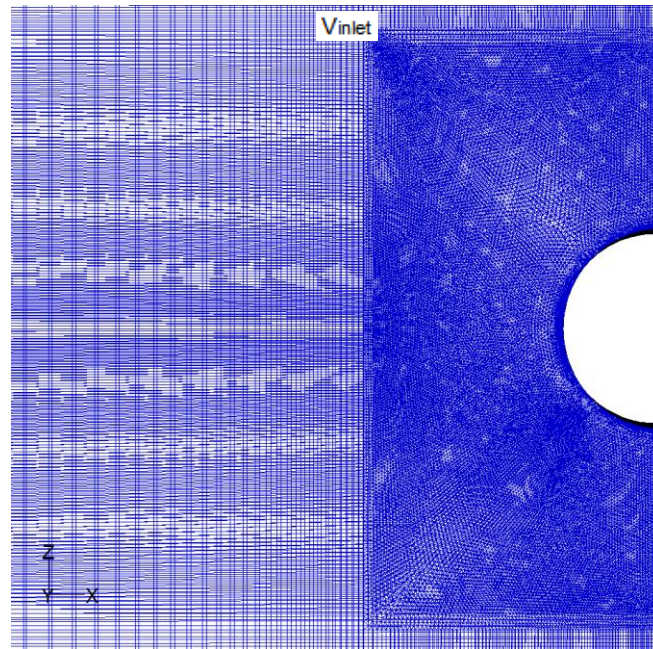
Figure 55 - 3D Cyl. – Unstructured Grid, Zoom

The elevation detail shows the δ between each of the linearly stacked 2D structured mesh elements in the global region of the mesh. The local region shows the tightly packed unstructured elements, which were created independent of any user enforced restrictions.
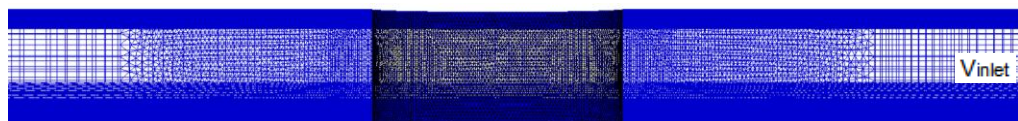
Figure 56 - 3D Cyl. - Unstructured Grid, Elevation Detail
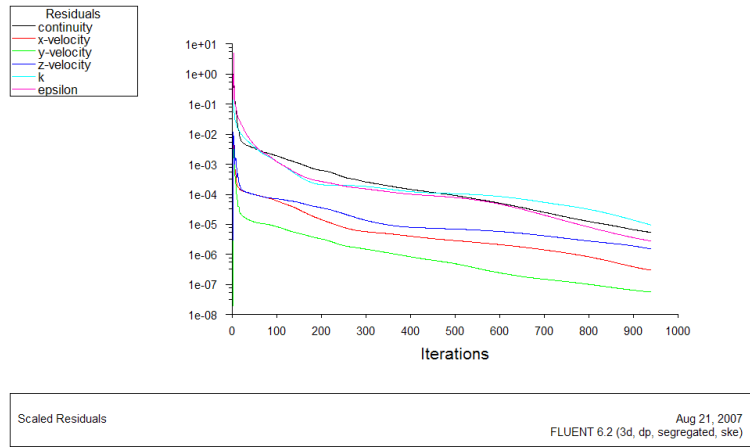
Figure 57 - 3D Cylinder – Scaled Residuals (k-ε turbulence model)

The residuals in Figure 57, unstructured grid, converge in less iterations than the structured grid because the tet/hybrid mesh type is designed to optimize the placement of additional elements into the local zone around the cylinder, thus resulting in smaller error and better accuracy. However, the disadvantage of this is that this mesh type requires a significant amount of additional memory. Although the residuals still converge at different points from one another, the residuals in the unstructured case remain much closer together. All residuals satisfy the convergence criterion of 10^-6 at roughly 950 iterations.
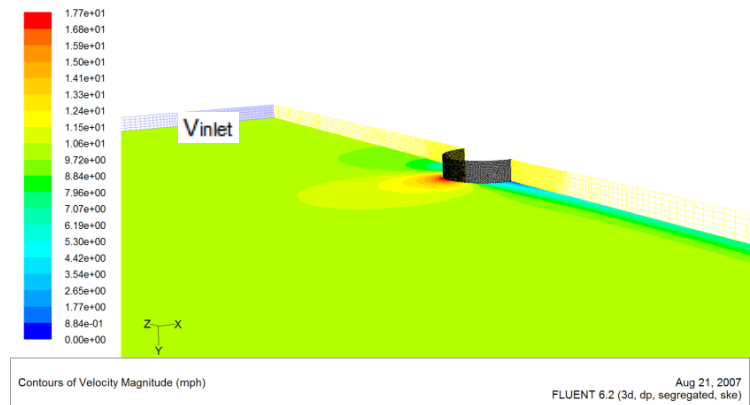
Figure 58 - 3D Cyl. – Vel. Magnitude Plane 10 Contours (k-ε turbulence model)

The velocity distribution of the unstructured mesh shows a near exact match to that of the structured mesh. The maximum velocity has a slightly larger value (max value of roughly 17.67 mph) than in the structured case.
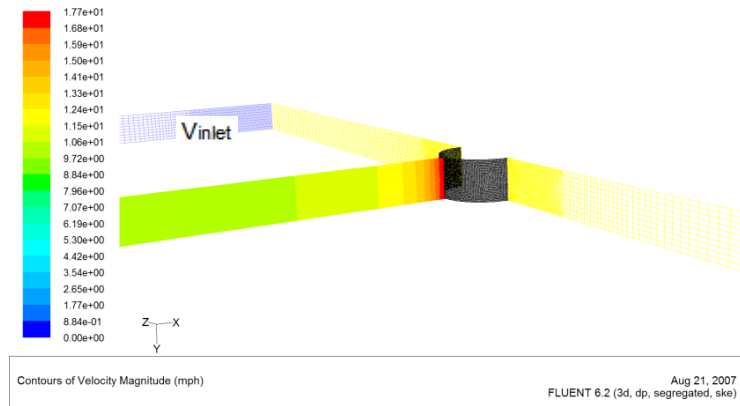
Figure 59 - 3D Cyl. – Vel. Magnitude Plane 9 Contours (k-ε turbulence model)

Note that the displayed color distribution is the same as that of the structured mesh, thus confirming that the results are consistent amongst the two problem sets.
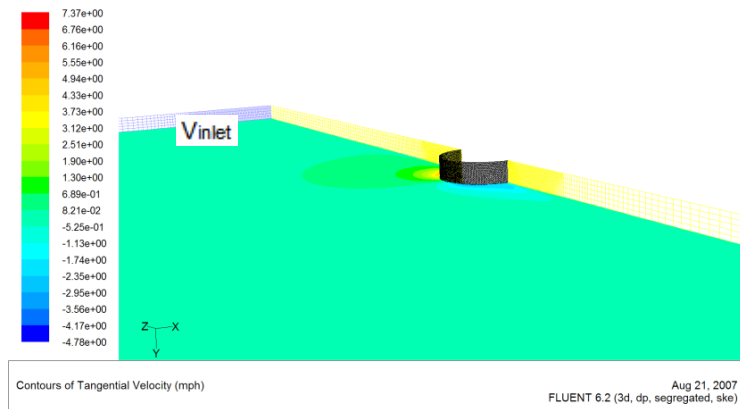
Figure 60 - 3D Cyl. - Tangential Vel. Plane 10 Contours (k-ε turbulence model)

The display of the tangential velocity over *plane 10* shows the same region of amplification on the front side of the cylinder.
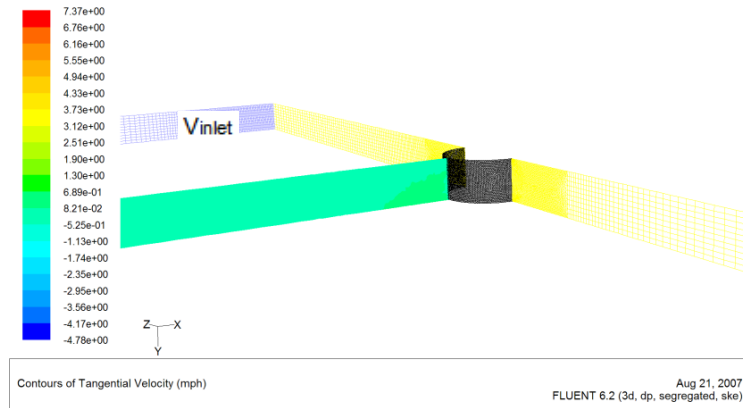
Figure 61 - Tangential Vel. Plane 9 Contours (k-ε turbulence model)

Figure 61 displays the same small semi-circle of amplification near the bottom of the cylinder. This figure provides a final confirmation that the two grids produce the same solution results.

3.4.5 <u>Comparison</u>

In order to verify that the 3D structured grid matches the results of the 3D unstructured grid, several data points were randomly selected from each problem domain and then compared. The results proved to be the same in both cases, thus proving that both the unstructured and structured grids produce similar results when meshed properly (proper proportions/grid refinement).[17]

---

[17] Note: No comparisons should be made between these 3D cylinder tests and the latter 3D spiral tests because the cylinder diameter was not kept consistent with the spiral tower diameters. To be specific, the inner radius that the wind turbine actually nearly touches in the center of the 25ft-R spiral tower is actually only a 15ft-R from the center of the structure and the inner radius of the 30ft-R spiral tower is 19ft-R. The 25ft-R and 30ft-R naming denotes the outer radius of the spiral flanges. The 3D cylinder analysis used a 30ft inner/outer radius for testing, which is much larger than the respective 15ft-R and 19ft-R radii used in the spiral tower analyses. To achieve an equivalent comparison a 15ft-R and 19ft-R cylinder would need to be independently tested and compared against the corresponding spiral towers.

3.5 WIND SHELL SIZE OPTIMIZATION

The core focus of this research is focused on the determination of the wind amplification factors for two towers differing in tower diameter, a 25ft-R (50ft diameter) and 30ft-R (60ft diameter) spiral tower. The difference in the diameter of the two towers can be observed in Figure 62.
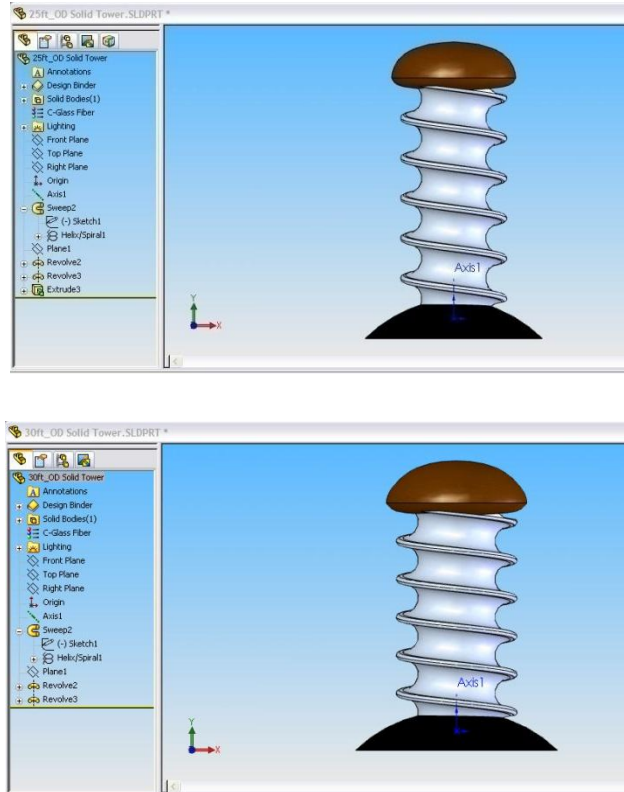
Figure 62 – 25ft Radius Spire vs. 30ft Radius Spire

The purpose of this research is to determine whether enlarging the towers structure is a cost effective approach in achieving larger wind amplification factors, and as a result an increase in productivity (power generation).

3.5.1   Initial Setup – 3D Spiral Structures

The mesh development up to this point proved to be an exhaustive process that required over 20+ different mesh cases to be run before a proper grid was deemed acceptable. Also, the proof that very similar results could be obtained by using the 3D unstructured grid as opposed to the original 3D structured grid opened up addition flexibility and time savings for problems with complex contours. This was done methodically, thus eliminating any uncertainties and instilling a high level of confidence that any objects tested in this domain will result in an accurate solution set.

It is important to analyze and understand the results of each of the tests that have been performed thus far as this information will serve as the basis for the next case. As mentioned earlier, the preparation and preliminary setup that was required to achieve the final grid for the 3D spire was complex and very time consuming to say the least. Every test that has been performed thus far was necessary. The 2D cylinder test (structured mesh, inviscid flow) gave proof that the theoretical calculations could be closely mirrored using the widely accepted CFD code that is implemented by Fluent. The second 2D cylinder test was then run using a different flow regime (structured mesh, turbulence model) for the purpose of comparing the 2D cylinder results against the 3D cylinders results (similar mesh – cooper meshing scheme). Once these results were confirmed to be similar, a second case was run that applied a very fine unstructured mesh (Elements: Tet/Hybrid & Type: TGrid) in the local region around the 3D cylinder. The purpose of this test is to verify that the unstructured mesh produces the equivalent results of the structured mesh. This presented an alternative method to accurately test the complex

curvature of nearly any object, specifically the spiral shell structure that is present in this thesis.

Three planes will used to view the velocity contours following the 3D spiral tower analysis, two of which are the same as in the 3D cylinder analysis. *Plane 9*, which is the plane that is vertically perpendicular to the 3D cylinder, was altered for the each 3D spiral tower case so that the plane would be perpendicular to the helix angle. The 25ft-R tower was rotated about its origin by 6.55° and the 30ft-R tower was rotated by 5.68°. **Figure 63** & **Figure 64** provide a confirmation of these angles and dimensions.
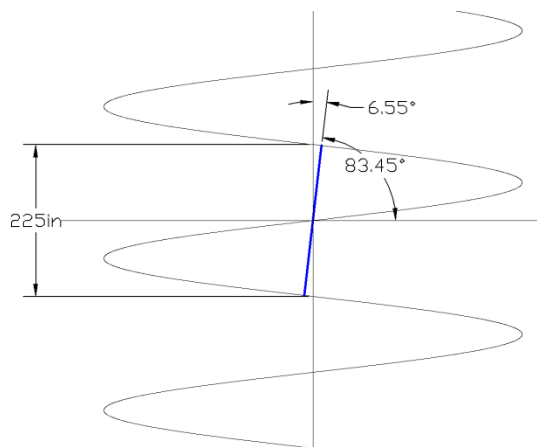
Figure 63 – 25ft Perpendicular Helix Plane   **Figure 64 – 30ft Perpendicular Helix Plane**
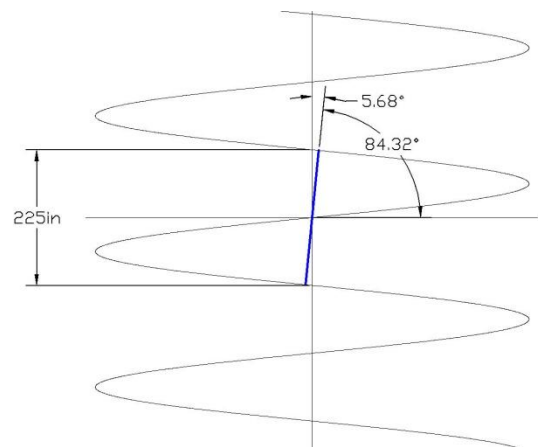
The coordinates for these two planes can be found using the intersection point of the angled line and the intersection point of the helix. This can be done through some simple geometrical calculations.
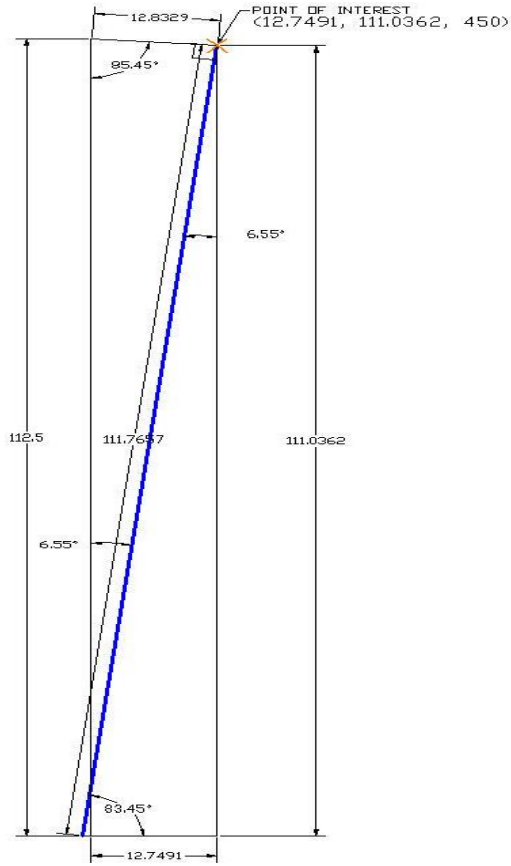
Figure 65 – 25ft Perpendicular Helix Plane   **Figure 66 – 30ft Perpendicular Helix Plane**
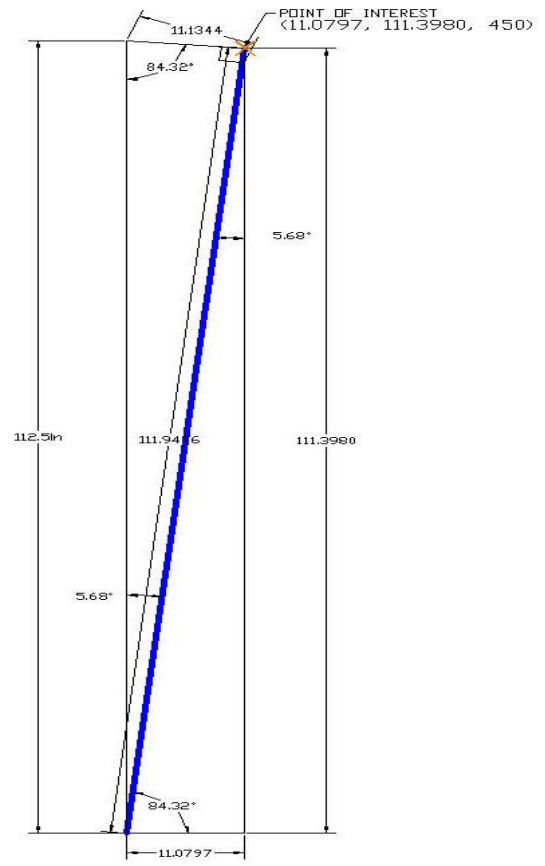
Figure 65 & Figure 66 provide all necessary information for obtaining the planes coordinates. The center point of the plane is located at the bottom left of each figure. The upper right point in the figure displays the coordinates of the intersection between the plane and the surface of the spiral tower. The other coordinates, not displayed, can be found by mirroring the geometry about the x-axis and then the y-axis, thus negating the x & y coordinates. (Note: the z coordinate will remain positive in all cases).
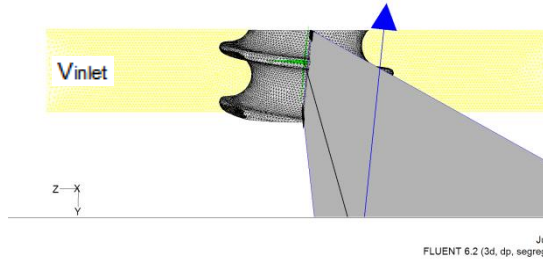
Figure 67 - Perpendicular Helix Plane (ISO#1)
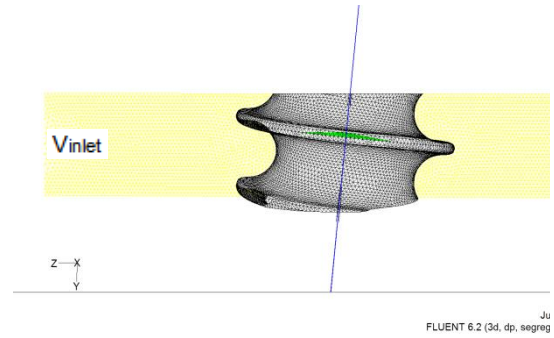
Figure 68 - Perpendicular Helix Plane (ISO#2)

For understanding purposes a 3D illustration of this plane that was created in Fluent can be viewed in **Figure 67** & **Figure 68**. The final coordinates of these two planes can be viewed in the appendix. (Note: These planes are denoted as *plane 11a* for the 25ft-R case and as *plane 11b* for the 30ft-R case).

3.5.2   Numerical Verification (CFD) – 3D Spiral Structures

The purpose of performing a CFD test on multiple spiral structures is to determine if it is cost effective and thus beneficial to build a larger structure for its additional velocity amplification. To do this the 3D spiral structure was broken down into two cases, each with a different tower diameter. Several scenarios can be analyzed, but for the purpose of this document the two cases that will be analyzed are a 25ft-R and 30ft-R tower. All other parameters were held constant. A few of these parameters would include:

1. helix angle,

2. pitch (height & revolutions)

3. flange length

4. turbine size

3.5.3 Case I – 25ft-R Spiral Structure (Turbulent Flow w/Unstructured Grid)

The same mesh parameters that were used on the unstructured 3D cylinder grid were applied to both 3D spiral tower cases. These values are provided and can be found in the appendix.
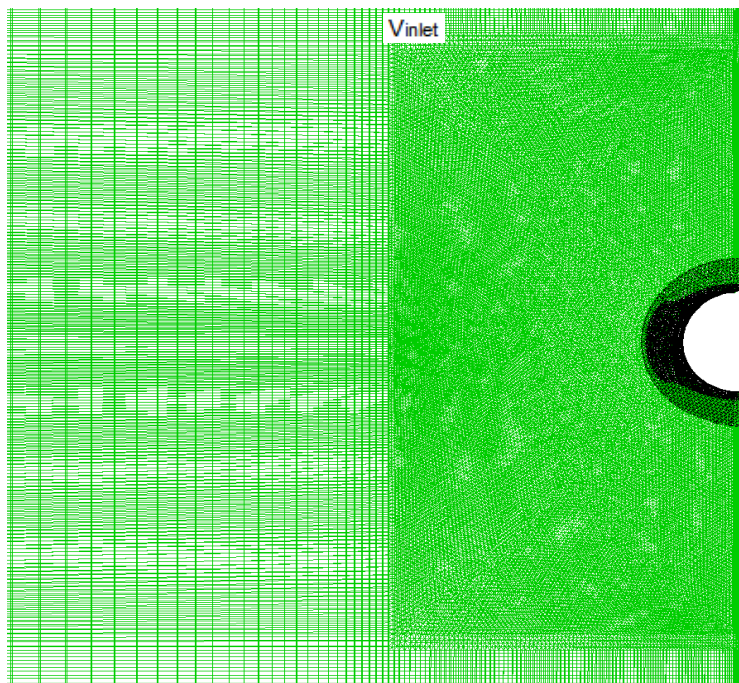
Figure 69 – 25ft-R - Structured to Unstructured Grid Transition

Figure 69 shows the transition between the global structured mesh into the local unstructured mesh. The additional refinement is evident when directly compared against one of the earlier structured grid types. A zoomed view of the unstructured region can be seen below.
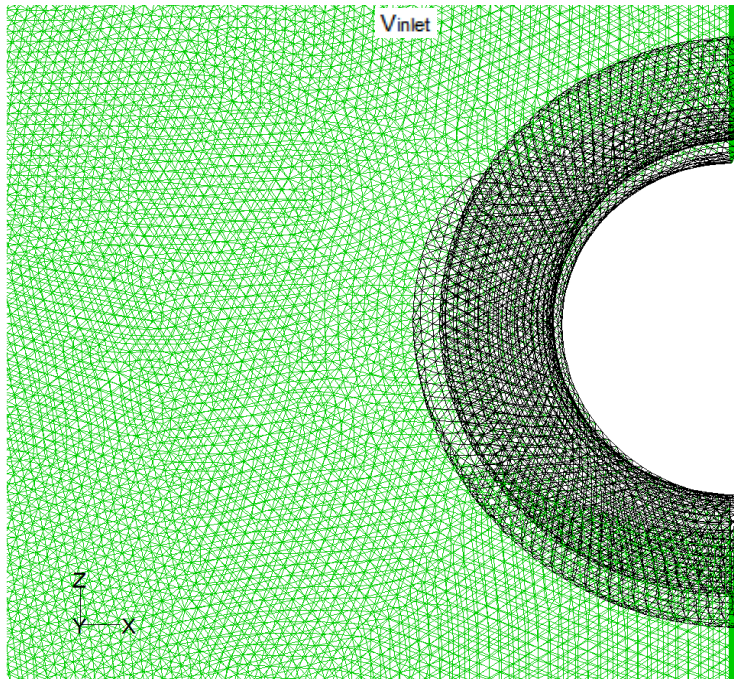
Figure 70 – 25ft-R - Unstructured Grid, Zoom

The elevation detail shows the δ between each of the linearly stacked 2D structured mesh elements in the global region of the mesh. The local region shows the tightly packed unstructured elements, which were created independent of any user enforced restrictions.
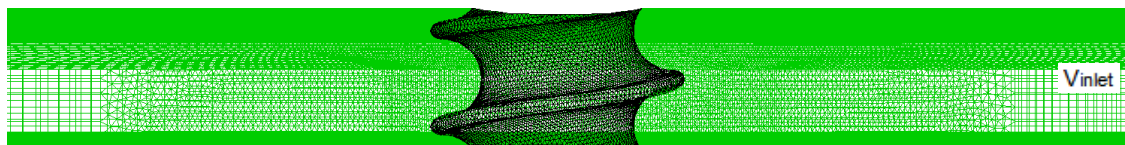
Figure 71 – 25ft-R - Unstructured Grid, Elevation Detail
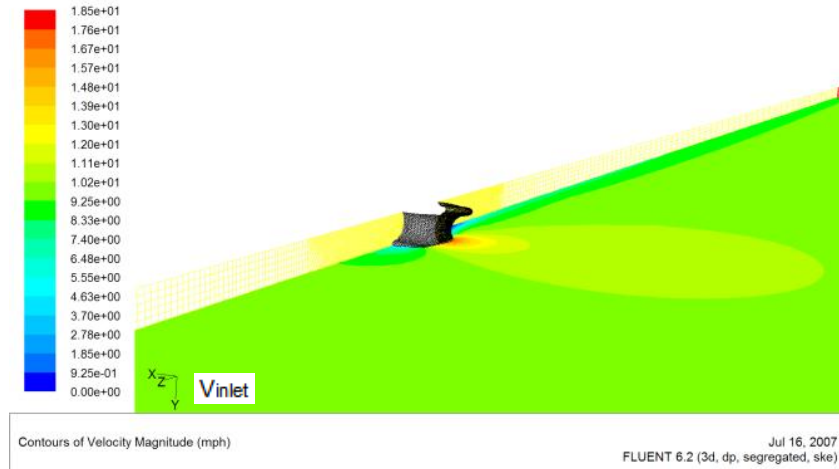
Figure 72 – 25ft-R Spire. – Vel. Magnitude Plane 10 Contours (k-ε turbulence model)

Figure 72 shows the velocity distribution over *plane 10* of the 25ft-R spiral tower. The

velocity magnitude is computed based on all of the node points that exist within the *default*

interior of the domain. The maximum velocity, which is displayed by the legend in red, is

shown to have a value around 18.5mph. This value would have a slightly larger magnitude

than a 3D cylinder analysis that compared equal internal radii because of the additional

velocity vectors that deflect off of the spiral structures flanges.
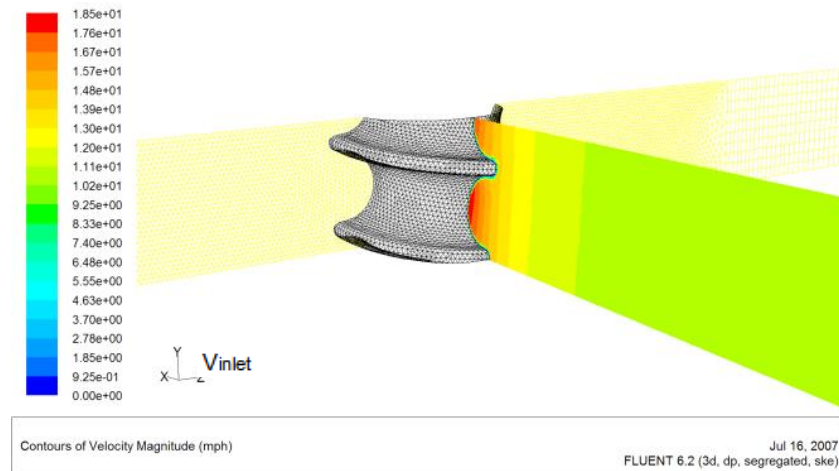
Figure 73 – 25ft-R Spire. – Vel. Magnitude Plane 11a Contours (k-ε turbulence model)

This cut plane, denoted as *plane 11a*, displays a different perspective of the velocity magnitude distribution within the domain. The figure shows the region near the cylinder where the points of maximum velocity occur. Also, it is important to notice the uniform color distribution, especially near the wall of the cylinder. This confirms that the boundary conditions were correctly defined for this problem set.

Path Lines Colored by Velocity Magnitude (mph)

Jul 16, 2007
FLUENT 6.2 (3d, dp, segregated, ske)
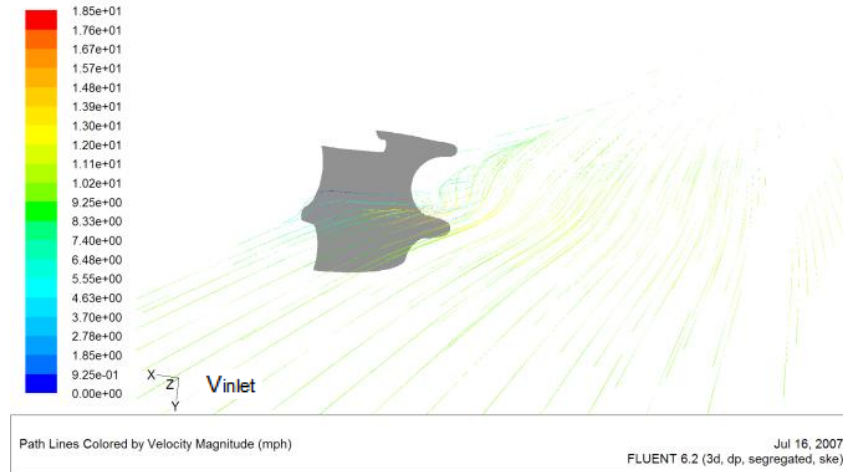
Figure 74 – 25ft-R Spire. – Vel. Magnitude Plane 10 Pathlines (k-ε turbulence model)

The velocity magnitude pathlines clearly illustrate the fluid flows path, direction, and speed around the spiral tower structure.

3.5.4 Case II – 30ft-R Spiral Structure (Turbulent Flow w/Unstructured Grid)

The mesh for the 30ft-R spiral structure is identical to that of the 25ft-R spire with the only difference being from the substitution of the structure itself.
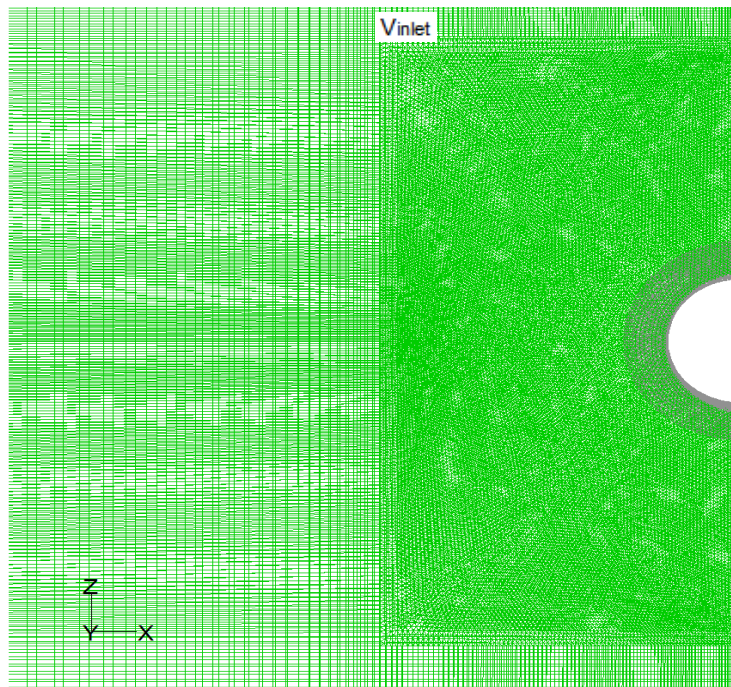
Figure 75 – 30ft-R - Structured to Unstructured Grid Transition

Figure 75 illustrates the transition between the global structured mesh into the local unstructured mesh. The additional refinement is evident when directly compared against one of the earlier structured grid types. A zoomed view of the unstructured region can be seen below.
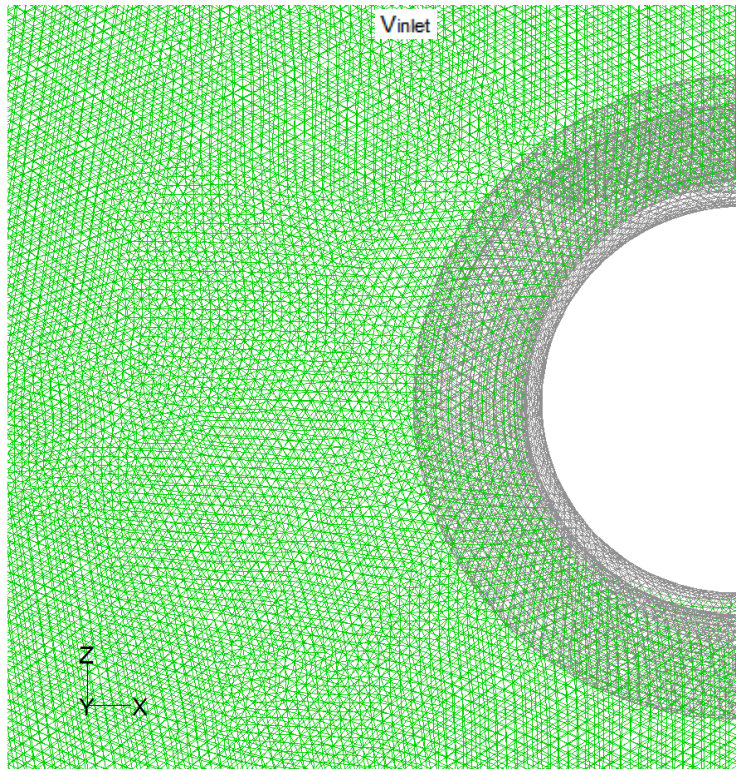
Figure 76 – 30ft-R - Unstructured Grid, Zoom

Again, as seen in the 25ft-R case, the elevation detail shows the δ between each of the linearly stacked 2D structured mesh elements in the global region of the mesh. The local region shows the tightly packed unstructured elements, which were created independent of any user enforced restrictions.
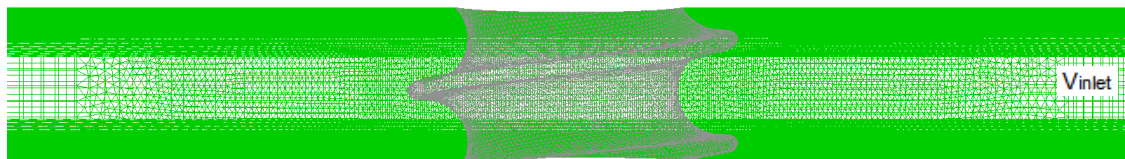
Figure 77 – 30ft-R - Unstructured Grid, Elevation Detail
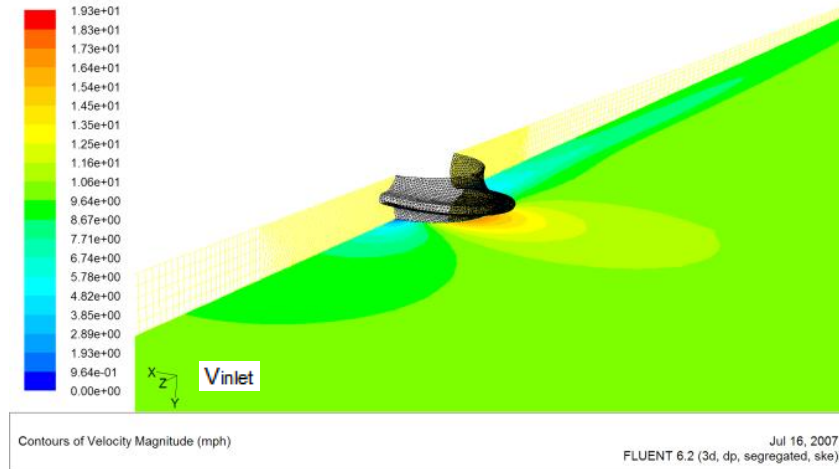
Figure 78 – 30ft-R Spire. – Vel. Magnitude Plane 10 Contours (k-ε turbulence model)

Figure 78 shows the velocity distribution over *plane 10* of the 30ft-R spiral tower. The velocity magnitude is computed based on all of the node points that exist within the *default interior* of the domain. The maximum velocity, which is displayed by the legend in red, is shown to have a value around 19.3mph. This is slightly larger than the maximum velocity reported in the 25ft-R spiral structure analysis because of the additional velocity vectors that are a result of the spiral flanges and larger structure diameter.
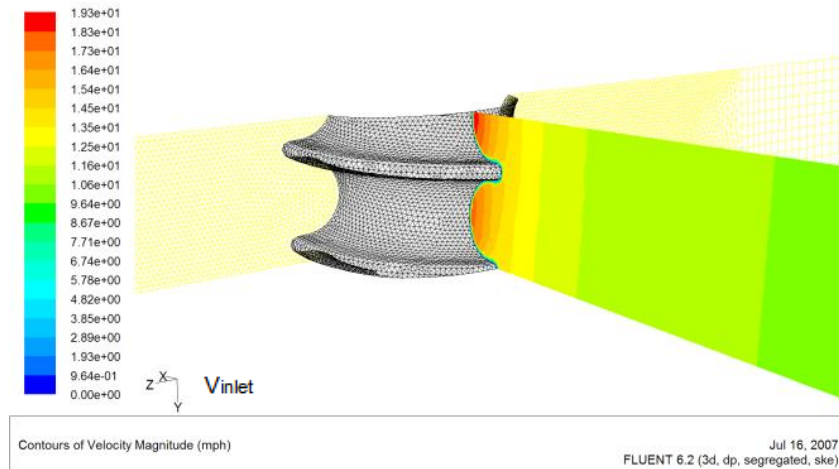
Figure 79 – 30ft-R Spire. – Vel. Magnitude Plane 11a Contours (k-ε turbulence model)

Plane 11b was created at the center of the spiral structure to display the velocity distribution over the plane that the turbines will be operating on. It is evident that the region near the spiral tower is where the points of maximum velocity occur. As all other cases have displayed thus far, the velocity distribution is uniform. This confirms that the boundary conditions were correctly defined for this problem set.
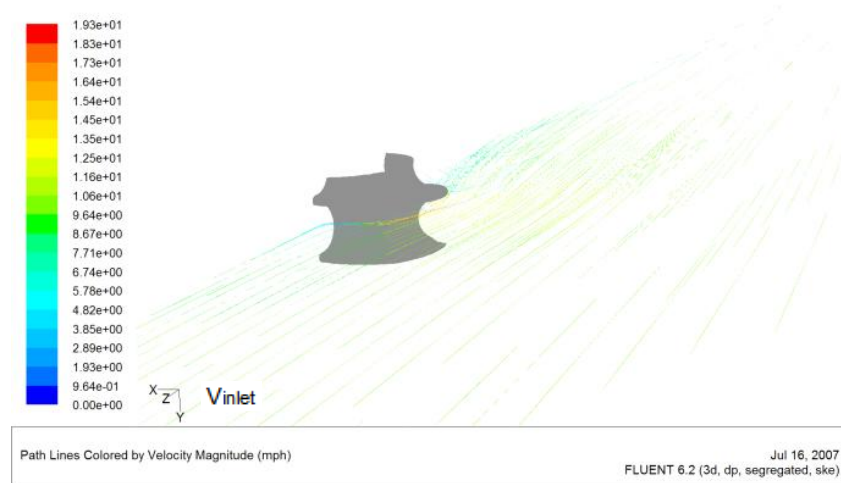
Figure 80 – 30ft-R Spire. – Vel. Magnitude Plane 10 Pathlines (k-ε turbulence model)

The velocity magnitude pathlines display the fluid flows path, direction, and speed around the spiral tower structure.

3.6 FINAL CFD RESULTS

The analysis that was previously presented provides the user with a visual understanding of the various regions that encase the objects. This can be taken one step further by extracting and analyzing specific data points. Figure 81 & Figure 82 graphically show node points that will be studied.
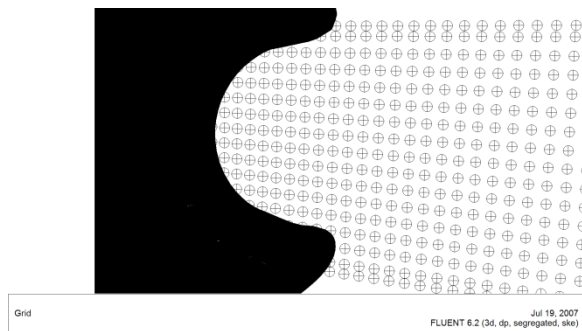
Figure 81 - Fluent Line/Rake Data Points (1)
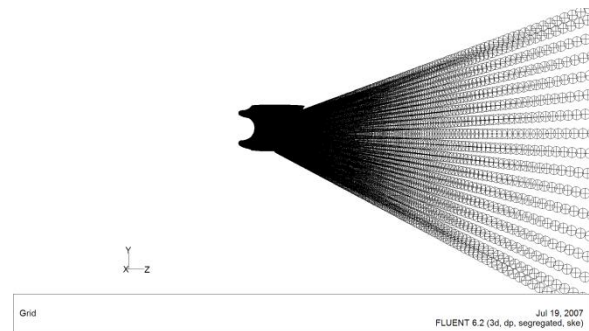
Figure 82 - Fluent Line/Rake Data Points (2)

3.6.1 25ft Radius Wind Shell

3.6.1.1 Amplification Factor (Min & Max Values)

For the 25ft-R spiral structure case, the maximum velocity occurs at the intersection of plane 11a, plane 9, and the intersection of the spiral structure. At this point the maximum value was calculated to have a velocity of 18.5mph. The region of where the minimum velocity is located is at the rear of the structure where plane 8 intersects with plane 9. This value was calculated to be as low as zero mph.

The amplification factor can be simply calculated by dividing the velocity of interest by the free stream velocity.[18] Thus, the maximum velocity of 18.5mph would be divided by the free stream velocity of 10mph and would result in an amplification factor of 1.85. The minimum amplification would be zero.

3.6.1.2   Amplification Factor (15ft Wind Turbine Cross-Section)

The average velocity distribution over the 15ft tip-to-tip wind turbines surface area was derived by averaging each node point displayed in Figure 83.
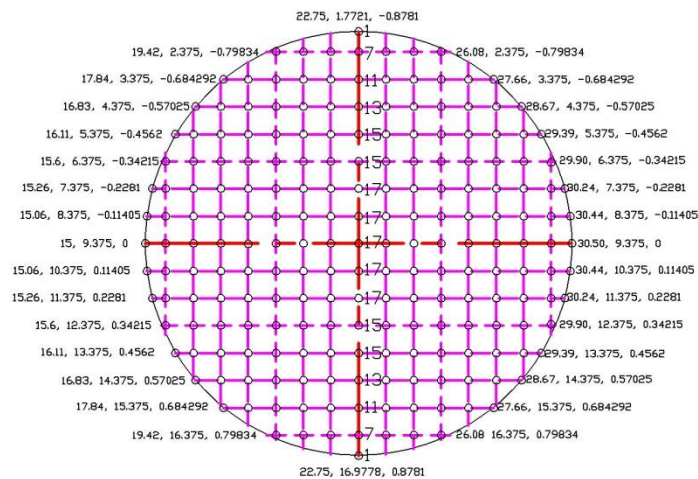
Figure 83 – 25ft-R Spire - Avg. Vel. Distribution Coordinates

---
[18] See Glossary

The coordinates that define this region where determined specific to the tested model. The numbers that are displayed along the vertical axis represent the quantity of node points that were used from each row. These node points were exported one line at a time into Microsoft Excel where they were they were averaged to a final value of 15.246mph.

The average amplification factor over the 15ft tip-to-tip wind turbine cross-section was calculated to be 1.5246. The data points that were used to determine this factor can be viewed in Table 10.

3.6.2   30ft Radius Wind Shell

3.6.2.1   Amplification Factor (Min & Max Values)

For the 30ft-R spiral structure case, the maximum velocity occurs at the intersection of plane 11b, plane 9, and the intersection of the spiral structure. At this point the maximum value was calculated to have a velocity of 19.3mph. The region of where the minimum velocity is located is at the rear of the structure where plane 8 intersects with plane 9. This value was calculated to be as low as zero mph.

The amplification factor can be simply calculated by dividing the velocity magnitude by the free stream velocity. Thus, the maximum velocity of 19.3mph would be divided by the free stream velocity of 10mph and would result in an amplification factor of 1.93. The minimum amplification would be zero.

3.6.2.2 Amplification Factor (15ft Wind Turbine Cross-Section)

The average velocity distribution over the wind turbines surface area was derived by averaging each node point displayed in Figure 84.
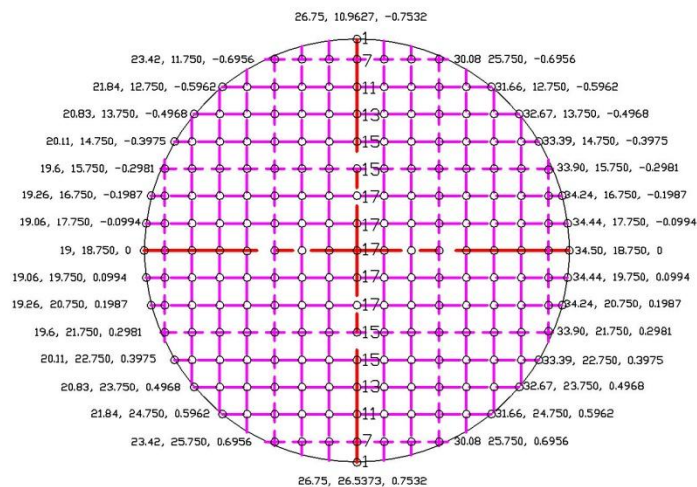
Figure 84 – 30ft-R Spire - Avg. Vel. Distribution Coordinates

The coordinates that define this region where determined specific to the tested model. The numbers that are displayed along the vertical axis represent the quantity of node points that were used from each row. These node points were exported one line at a time into Microsoft Excel where they were they were averaged to a final value of 15.396mph.

The average amplification factor over the 15ft tip-to-tip wind turbine cross-section was calculated to be 1.5396. The data points that were used to determine this factor can be viewed in **Table 11**.

3.6.3   Result Comparison (25ft-R vs. 30ft-R)

The width of the 25ft-R structure is roughly 83.33% the size of the 30ft-R structure. The average velocity of the 25ft-R spiral tower is 99.02% of the 30ft-R spiral tower. In order to justify whether the 16% increase in size is worth the 1% gain in energy, additional information needs to be known such as the cost of material, turbine lifespan, and tower lifespan. If the parameters work to the favor of supporting the larger structure based on a unit analysis, this could result in a very large cost savings when multitudes of turbines are applied.

3.7 CFD WIND SHELL CONCLUSIONS

Final CFD results show that when comparing the amplification factors of 25ft-R and 30ft-R spiral structures, the delta in average velocity over the surface area of the 15ft diameter turbine is 0.15mph. To determine if this amplification is justifiable, the additional power generated must be compared against a number of dynamic parameters. To begin, the lifespan of operation for one tower must be determined. A lifespan of operation of 100 years versus a number of 15 years will have a substantial affect in the final cost/benefit analysis. For each year of additional operation the larger tower will gain added value. The next item that is required to complete an accurate analysis would be today's equivalent cost/unit energy as well as the equivalent projected cost/unit through the towers last years of operation. The additional power that is generated as a result of tower amplification may have larger value in 100 years in comparison to present prices (energy could in fact cost 10 times as much as it costs today if some of the world's most prominent energy sources continue to diminish). A similar analysis would have to be performed on the additional material costs due to the increased tower size. It must be realized that although the 0.15mph seems minute if one turbine was to be used for a short period of time, but it is important to realize that the larger number of turbines a tower is comprised of the more effective this means of power amplification.

It is not the purpose of this thesis to make the determination of "the best spiral shell size", but rather the intent was to provide meaningful information from which experts can make informed decisions from. It is important to note that even experts will need to use a number of projections of the future, none of which are guaranteed to be exact. It is for this reason that I believe that additional studies should be pursued, in addition to this work, with the sole intent of

complimenting prior studies. It is my opinion that power generation by way of clean energy technologies is the way of the future and is here to stay. With the proper funding for research and development, I am sure that this will be a promising technology of the future.

3.8   FUTURE CONSIDERATIONS

The information provided within this thesis details a series of test cases that were administered to achieve the amplification factor of two spiral towers of varying radii. The results of these analyses have been verified to be valid based on theoretical calculations as well as a number of independent grid types. Although this information may be adequate to determine several production parameters, there are a number of alternative analyses that can be performed to compliment these results. For example, if the proper computational resources were readily available, the same analysis presented in this thesis could be run as *unsteady (time dependent)*. This analysis should produce results similar to that of the *steady* solver, but with the added versatility to create artistic renderings of the flow phenomenon. This allows for a much more detailed analysis by providing the user with a tool to study turbulent flow, vortices, and flow behavior over time. The continuity of the flow can also be analyzed as a function of time. This can be taken a step further by manipulating an additional parameter known as the Strouhal number (which in this cases presented within this document would be between 0.19-0.20). The Strouhal number, often used in the study of unsteady flow conditions, could be used to mimic actual flow conditions relative to a specific condition or region. By definition the Strouhal number is used for analyzing oscillating flows in unsteady fluid flow dynamics problems. [19]

---

[19] "The Strouhal number represents a measure of the inertial forces due to the unsteadiness of flow or local acceleration to the inertial forces due to changes in velocity from one point to another in a flow field." (The Engineering Tool Box, 2007)

In order to minimize research costs, future analyses would be run using Fluent's parallel processing capabilities on OSC's supercomputer farm. This was not implemented in this thesis due to the learning curve that is required to understand the Linux kernel and v-editor program (a text editor used to write batch scripts, which is required to submit jobs to the OSC Supercomputer system). A comprehensive understanding of these two items would make testing of the large quantities of models of varying parameters (shapes, sizes, etc) a feasible task. Initial discussions between Cleveland State University and OSC Supercomputer have resulted in an allotment of 4000 units (or 4000 computational hours). Future correspondence should resolve any issues with the *putty* and v-editor issues pertaining to the submission of batch jobs.

Additional efforts to maximize power generation can be allocated to the optimization of the wind turbines blades weight, curvature, and usable surface area. The goal would be to not only improve wind capture by way of structural modifications but also to improve the reliability of the mechanical components and efficiency of the turbines.

REFERENCES

1. Abbott, J., & Dohenhoff, V. (1959). *A.E. Theory of Wing Sections.* New York: Dover Publications.

2. American Wind Energy Association. (2006). *Wind Web Facts Sheets*. Retrieved October 27, 2006, from American Wind Energy Association: http://www.awea.org/pubs/factsheets.html

3. Betz, A. (1966). *Introduction to the Theory of Flow Machines.* Oxford: Pergamon Press.

4. Carcangiu, M., & Cambuli, F. (2005). *The Economy of Large Scale Wind Turbines*. Retrieved October 1, 2006, from Fluent: http://www.fluent.com/about/news/newsletters/05v14i2/a10.htm

5. Dutton, A. G., Halliday, J. A., & Blanch, M. J. (2005). *The Feasiblility of Building-Mounted/Integrated Wind Turbines (BUWT's): Achieving their potential for carbon emissions reductions.* London & Rutherford: Energy Research Unit, CCLRC.

6. Energy Information Administration, Official Energy Statistics From the U.S. Government. (2007, May). *International Energy Outlook 2007*. Retrieved September

2, 2007, from Energy Information Administration, Official Energy Statistics From the U.S. Government: http://www.eia.doe.gov/oiaf/ieo/world.html

7. ESI Group. (2007). *About Turbulent Length Scale*. Retrieved May 10, 2007, from ESI Group Customer Portal: http://www.esi-cfd.com/content/view/499/192/

8. Fluent Inc. (2007, January). *CFD Flow Modeling Software & Solutions, Online Technical Support Portal*. Retrieved January 26, 2007, from Fluent: http://www.fluent.com/services/technical_support/index.htm

9. Fluent Inc. (2001, December). Gambit 2 Tutorial Guide. Lebanon, NH, United States of America.

10. GET. (2006, September 11). *Green Energy Technologies*. Retrieved October 9, 2006, from Green Energy Technologies: http://www.getsmartenergy.com/index.htm

11. Greenwood, D. T. (1965). *Principles of Dynamics.* Prentice Hall Inc.

12. Hahm, T., & Kroning, J. (2002). *In the Wake of a Wind Turbine*. Retrieved October 16, 2006, from Fluent: http://www.fluent.com/about/news/newsletters/02v11i1/a1.htm

13. Hamrock, B. J. (1994). *Fundamentals of Fluid Film Lubrication.* McGraw-Hill.

14. Hanlon, P. (2001). *Compressor Handbook.* New York: McGraw-Hill.

15. Hansen, M. (2000). *Aerodynamics of Wind Turbines: Rotors, Loads and Structures.* London: James & James.

16. Hoffman, J. D. (2001). *Numerical Methods for Engineers and Scientists, Second Edition.* Marcel Dekker Inc.

17. Inman, D. J. (2001). *Engineering Vibration, Second Edition.* Prentice Hall Inc.

18. Kelecy, F. (2002). *Wind Turbine Blade Aerodynamics*. Retrieved October 2, 2006, from Fluent: http://www.fluent.com/about/news/newsletters/02v11i1/a2.htm

19. Kirby Mountain. (2005, November 3). *The Gearbox: Wind Powers Achilles Heal*. Retrieved February 9, 2007, from Wind Power Monthly: http://www.kirbymtn.blogspot.com/2005/11/gearbox-wind-powers-achilles-heel.html

20. Kulkarni, A., & Moeykens, S. (2005, January 6). *Flow Over a Cylinder*. Retrieved October 17, 2006, from Fluent [FlowLab 1.2]: http://flowlab.fluent.com/exercise/pdfs/cylinder.pdf

21. Lam, J. (2002). *Mapping a Wind Farm*. Retrieved October 1, 2006, from Fluent: http://www.fluent.com/about/news/newsletters/02v11i1/a3.htm

22. McMaster-Carr. (2006). *McMaster-Carr Product Database*. Retrieved October 9, 2006, from McMaster-Carr: http://www.McMaster.com

23. Ohio Alternative Power. (2005). *Ohio Alternative Power*. Retrieved September 7, 2006, from Ohio Alternative Power: http://www.ohioalternativepower.com

24. Rao, S. S. (2004). *Mechanical Vibrations, Fourth Edition.* New Jersey: Pearson Prentice Hall.

25. Rashidi, M., & Cironi, M. (2006, September 1). *SmartEnergy Spire, A Wind System Using the Bernoulli Principle*. Retrieved October 4, 2006, from WindTech International: http://www.windtech-international.com/content/view/751/62/

26. Rashidi, M., & Cironi, M. (2006, September). WindTech International, Vol. 2, No. 6. *SmartEnergy Spire* .

27. Renewable Energy Systems. (2006). *Frequently Asked Questions*. Retrieved October 23, 2006, from Renewable Energy Systems: http://www.res-ltd.com/wind-power/faqs.htm

28. Rubb Building Systems. (2005). *Rubb Building Systems*. Retrieved July 11, 2006, from Rubb Building Systems: http://www.rubb.com

29. Ruith, M., Shashidhar, S., Vishak, T., & Kumar, R. (2004). *A Power of Wind Change*. Retrieved October 12, 2006, from Fluent: http://www.fluent.com/about/news/newsletters/04v13i2/s3.htm

30. Seaman Corporation. (2005). *Seaman Corporation*. Retrieved August 4, 2006, from Seaman Corporation: http://www.seamancorp.com

31. Senall, J. (2007). *Rochester / Finger Lakes Smart Energy Initiative Market Opportunity*. Retrieved August 11, 2007, from Distributed Energy, The Journal For Onsite Power Solutions: http://www.gradingandexcavation.com/de_news_081707_rochester.html

32. Sheridan, C. (2006, October 1). A Spire Built to Inspire. *Cleveland Plain Dealer* , p. 2.

33. Tannehill, J. C., Anderson, D. A., & Pletcher, R. H. (1997). *Computational Fluid Mechanics and Heat Transfer, Second Edition.* Taylor and Francis.

34. Thake, J. (2000). *The Micro-Hydro Pelton Turbine Manual.* Colchester, Essex, UK: Intermediate Technology Pub.

35. The Engineering Tool Box. (2007, 10 22). *Strouhal Number*. Retrieved 10 23, 2007, from The Engineering Tool Box: http://www.engineeringtoolbox.com/strouhal-number-d_582.html

36. WCPN News. (2007, February 22). *Clarification on Wind Turbine Report*. Retrieved August 28, 2007, from WCPN News: http://www.wcpn.org/news/2007/01-03/0226wind.html

37. WCPN News. (2007, February 22). *New Wind Turbine for Urban Environments*. Retrieved August 28, 2007, from WCPN News: http://www.wcpn.org/news/2007/01-03/0222windspire.html

38. White, F. M. (2003). *Fluid Mechanics, Fifth Edition.* New York: McGraw-Hill.

39. Wikipedia. (2007). *Burj Dubai*. Retrieved January 27, 2007, from Wikipedia: http://en.wikipedia.org/wiki/Burj_Dubai

40. Wikipedia. (2007). *Chicago Spire*. Retrieved January 26, 2007, from Wikipedia: http://en.wikipedia.org/wiki/Chicago_Spire

APPENDICES

1 NOMENCLATURE

v_{avg} = average velocity

v_1 = speed of fluid in front of the rotor

v_2 = speed of fluid downstream of the rotor

$\dot{m}$ = mass flow rate

ρ = density

S = area of a disc

$\dot{E}$ = delivered power

P_{max} = maximum power

C_p = coefficient of performance

E_x = elastic modulus

$DENS$ = mass density

psi = pounds per square inch

$ESTRN$ = strain (dimensionless quantity)

R = radius

r = radius

$Ma(M)$ = Mach Number

a = speed of sound

u = velocity

D = diameter

μ = dynamic viscosity

ν = kinematic viscosity

$\dfrac{D}{Dt}$ = derivative with respect to time (t)

f = function

$\nabla \mathbf{p}$ = pressure gradient

∂ = partial derivative

δ = delta (change in)

L = characteristic length

l = size of the eddy

β = dimensionless parameter

ψ = stream function for 2D flow

Λ = U*a²

θ = angle (degrees)

ϕ = angle (degrees)

e_x = unit vector denotation

p = pressure

g = gravity

z = height/elevation

V = velocity

y^+ = boundary layer parameter (used to determine initial spacing)

Re = Reynolds number (dimensionless)

$k - e$ = turbulent flow model

St = Strouhal number

f = frequency of vortex shedding

cu = computational unit

2 GLOSSARY

<u>Algebraic Equations</u> – Equations that need to be solved simultaneously throughout a problem domain in order to find the numerical representations of the problem. (Wikipedia, 2007)

<u>Amplification Factor</u> – This is dimensionless quantity that is used to describe the increase or decrease in flow speed at a given point or over a given region. The amplification factor is defined as the (velocity of interest)/(free-stream velocity).

<u>Attribute</u> – a property that is inherent in a database entity that is often used to characterize a specific element or variable. (Wikipedia, 2007)

<u>B.L.</u> – Boundary Layer (Originated by Ludwig Prandtl in 1904. For a sufficiently large Reynolds number a thin region existed near a solid boundary where viscous effects were at least as important as inertia effects no matter how small the viscosity of the fluid might be.). (Tannehill, Anderson, & Pletcher, 1997)

<u>Boundary Types</u> – unknowns that are often determined in direct correlation with the physical model. Examples of boundary types could include wall, velocity inlet/outlet, pressure inlet/outlet, or even planes of symmetry. (Fluent Inc., 2007)

<u>Case</u> – An engineering representation of a physical model that is used to accurately represent and simulate real life engineering situations. Cases are often assigned a series of attributes

106

that are specific to the given problem, which is then stored as the variable called "data". (Fluent Inc., 2007)

CFD – Computational Fluid Dynamics (A methodology that is used to solve complex problems in the field of computational fluid dynamics and heat transfer. This computational approach has gained extensive popularity due to the rise wide stream availability of the digital computer). (Wikipedia, 2007)

Computational Domain – Often a rectangle but can be of any size or shape. Often through the study of computational fluid dynamics you will need to convert between physical coordinates and transformed coordinates. (Tannehill, Anderson, & Pletcher, 1997)

Consistency – Relates to the accuracy to which a FDE approximates a PDE. The FDE can be tested by setting variables such as Δt and Δx to zero. (Tannehill, Anderson, & Pletcher, 1997)

Continuum Types – continuous matter, including both solids/fluids and liquids/gases. (Fluent Inc., 2007)

Contours – a curve connecting points where the function has a same particular value. In the instance of wind direction the contour would be classified as an isogon and the wind speed would be classified as an isotach. (Fluent Inc., 2007)

Convergence – Generally if a scheme is consistent and stable it is convergent. The solution to the finite-difference equation approaches the true solution to the PDE having the same initial and boundary conditions as the mesh is refined. (Tannehill, Anderson, & Pletcher, 1997)

Coordinate System – A system for assigning a tuple of numbers to each point in an n-dimensional space.

Coupled – An approach to solving algebraic equations and all dependent variables simultaneously. This is often more complex method in comparison to the segregated approach. (Fluent Inc., 2007)

Decompose – to break down or simplify into smaller parts. Often required in pre-meshing programs in order for a mesh to be satisfied. (Fluent Inc., 2007)

Discretization – Concerns the process of transferring continuous models and equations into discrete counterparts. This process is usually carried out as a first step toward making them suitable for numerical evaluation and implementation on digital computers. (Wikipedia, 2007)

Explicit – Is a scheme for which only one unknown appears in the difference equation in a manner that permits evaluation in terms of unknown quantities. (Tannehill, Anderson, & Pletcher, 1997)

External Flow – Flow that does not penetrate the into the inside of a part or component. Takes place on the external faces of the given body. (Fluent Inc., 2007)

FDE – Finite Difference Equation (FDE's are equations that have been developed through testing and are commonly used to represent PDE. These equations can then be numerically modeled via computer simulation. In more complex problems a common result of this action leads to multiple algebraic equations). (Tannehill, Anderson, & Pletcher, 1997)

FOS – Factor of Safety, a criterion that is specifically defined to determine the redundancies within a given design. (Wikipedia, 2007)

Gradient – often a physical quantity that describes in which direction and a what rate the given variable changes most rapidly around a particular location. Often a dimensional quantity that is expressed in some form of physical units. (Fluent Inc., 2007)

Grid Independence – an approach that is used to verify CFD results by comparing the convergence of multiple sets of results, which directly correlate with the coarseness and quality of the grid. (Fluent Inc., 2007)

Grid/Mesh – Preliminary step to performing the CFD analysis. Discretizes the model and spatial domain into small cells (preferably rectangles of minimum skew, but can consist of pyramidal solids in 3D). (Fluent Inc., 2007)

Implicit – Often needed when a third unknown (usually time) appears in the difference equation, which forces the algebraic formulation of several equations to be solved simultaneously. (Tannehill, Anderson, & Pletcher, 1997)

Initialize – the process of specifying initial conditions to a given problem. (Fluent Inc., 2007)

Intermittent – subject to interruption or periodic stopping. (Wikipedia, 2007)

Internal Flow – Flow that occurs within a given body or shape. Can be affected by an outside flow source, but does not need to be. (Fluent Inc., 2007)

Iterate – a classification of a procedure that repeats itself often within a computer program until the specified criterion is achieved. (Fluent Inc., 2007)

Laminar – Also known as streamline flow, occurs when a fluid flows in parallel layers, with no disruption between layers. In fluid dynamics, laminar flow is a flow regimen characterized by high momentum diffusion, low momentum convection, and pressure and velocity independence of time. (Wikipedia, 2007)

Map – regular structured meshes. (Fluent Inc., 2007)

Monitors – categorization of predefined functions that are used to determine when the iterative calculations meet the specified criterion. (Fluent Inc., 2007)

Navier Stokes Equation – Time dependent equations that represent the most complex time dependent turbulent flows. (Tannehill, Anderson, & Pletcher, 1997)

ODE – Ordinary Difference Equation (Is a relation that contains functions of only one independent variable, and one or more of its derivatives with respect to that variable. (Tannehill, Anderson, & Pletcher, 1997)

Pathlines – 1) Are the trajectory that an infinitesimally small point would make if it followed the flow of the fluid in which it was imbedded. "2) Is the actual path traversed by a given fluid particle. Note: Streamlines, pathlines, and streaklines are identical in steady flow." (Fluid Mechanics, Fifth Edition pg[39])

Pave – unstructured meshes. (Fluent Inc., 2007)

PDE – Partial Difference Equation (Equations that are used to model important physical processes that often take place in nature). (Tannehill, Anderson, & Pletcher, 1997)

Periodic – an interval of time that an event, chain of events, instance or happening, takes place within. It is measured generally between a start point and an end point and it generally repeats, or progresses in a cycle with the end point of one period being the start point of the next. (Fluent Inc., 2007)

Profile (aerodynamics) – cross section of an object that is undergoing testing that shows the curvature of the upper and lower surfaces. (Fluent Inc., 2007)

Residual – Residuals are related to the concept of truncation error and are used to determine the proper time to terminate an iterative set of calculations. (Fluent Inc., 2007)

Round Off and Discretization Error – Error that is a result of the finite number of digits that a computational machine can hold. This error is proportional to the number of grid points in the computational domain. (Tannehill, Anderson, & Pletcher, 1997)

Segregated – An approach to solving algebraic equations independent of one another. (Fluent Inc., 2007)

Stability – A stable scheme is one for which errors from any source (round-off, truncation, mistakes) are not permitted to grow in sequence of numerical procedures as the calculation proceeds from one marching step to the next. (Tannehill, Anderson, & Pletcher, 1997)

T.E. - Truncation Error (The error that is a result of the truncation or removal of terms in the Taylor Series formulation. It can also be represented and the FDE - PDE). (Tannehill, Anderson, & Pletcher, 1997)

Turbulent – Turbulence or turbulent flow is a flow regimen characterized by chaotic, stochastic property changes. This includes low momentum diffusion, high momentum convection, and rapid variation of pressure and velocity in space and time. (Wikipedia, 2007)

Scheme – an important concept connecting the fields of algebraic geometry, commutative algebra and number theory. (Tannehill, Anderson, & Pletcher, 1997)

Steady – A state that is not affected or influenced by time. (Tannehill, Anderson, & Pletcher, 1997)

Streakline – "is the locus of particles that have earlier passed through a prescribed point. Note: Streamlines, pathlines, and streaklines are identical in steady flow." (Fluid Mechanics, Fifth Edition pg[39]).

Streamlines – 1) A family of curves that are instantaneously tangent to the velocity vector of the flow. "2) A line everywhere tangent to the velocity vector at a given instant. Note: Streamlines, pathlines, and streaklines are identical in steady flow." (Fluid Mechanics, Fifth Edition pg[39])

Submap – divides an unmappable face into mappable regions and then creates a structures mesh in these new regions. (Fluent Inc., 2007)

Timeline – is a set of fluid particles that form a line at a given instant. (Fluid Mechanics, Fifth Edition pg[39])

Tri Primitive – divides a three sided face into three quadrilateral regions and creates a mapped mesh in each region. (Fluent Inc., 2007)

UDF – User Defined Functions (A popular option for users wanting to customize a software program. Often used to develop specialized models for a broad range of applications). (Fluent Inc., 2007)

Unsteady – Differs from steady through the appearance of the term $\rho*(du/dt)$ in the momentum equation and $d\rho/dt$ in the continuity equation. These equations are also parabolic but with time as the marching parameter. (Tannehill, Anderson, & Pletcher, 1997)

Vectors – a concept that is characterized by a magnitude and a direction. Can be one of many attributes such as velocity, pressure, temperature, etc. (Wikipedia, 2007)

Wedge Primitive – for a wedge shaped region, creates a triangular mesh at the tip and radial quadrilateral meshes outward. (Fluent Inc., 2007)

WVAF – Wind Velocity Amplification Factor (The factor that the initial velocity or average velocity gets amplified. Formula can be calculated simply by $V_{tower}/V_o = G$ (amplification factor)

3 ABBREVIATIONS

OAP – Ohio Alternative Power (R&D organization that provided general requirements and restraints for the first Spire Smart Energy Tower System designed in 2005).

GET – Green Energy Technologies (R&D organization that provided general requirements and restraints for the redesigned Spire Smart Energy Tower System designed in 2006).

OECD - The Organization for Economic Co-operation and Development was established in 1961 building on the OEEC. It is a Paris-based club for industrialized countries and the best of the rest.

OEEC - Organization for European Economic Co-operation was established under the Marshall Plan

4   ENERGY TRENDS/PROJECTIONS

Figure 85 - World Marketed Energy Consumption 1980-2030

Figure 86 - World Marketed Energy Use: OECD and Non-OECD, 2004-2030

Figure 87 - Marketed Energy Use in Non-OECD Economies by Region, 1990-2030

Figure 88 - World Marketed Energy Use by Fuel Type, 1980-2030

Figure 89 - World Marketed Energy Use by Fuel Type, 1980-2030

Figure 90 - World Coal Consumption by Region, 2004-2030

Figure 13. World Electric Power Generation by Region, 1980-2030

Billion Kilowatthours

History | Projections

OECD

Non-OECD
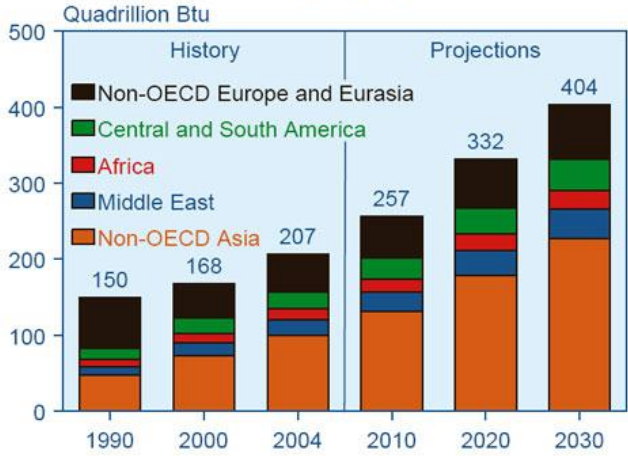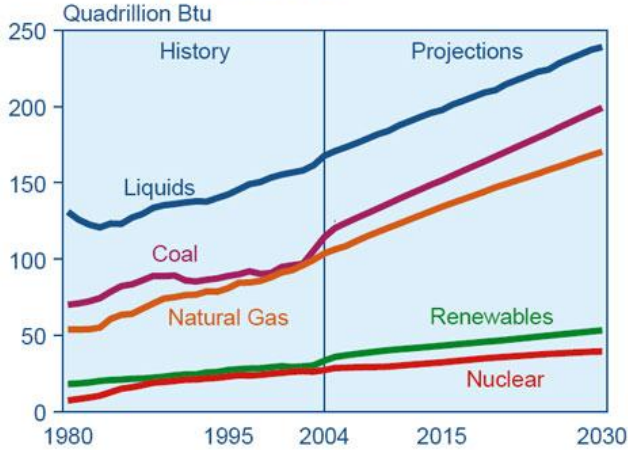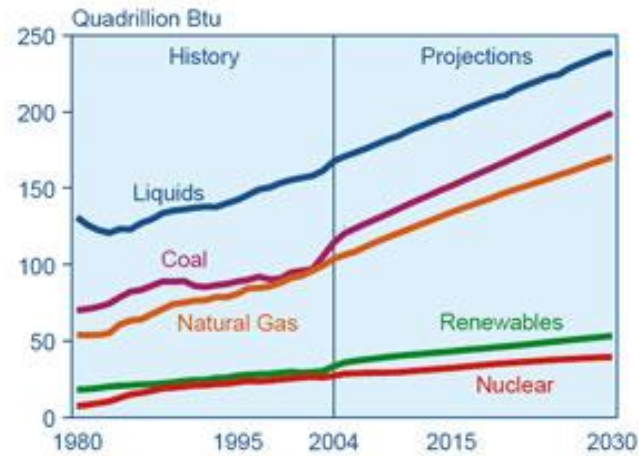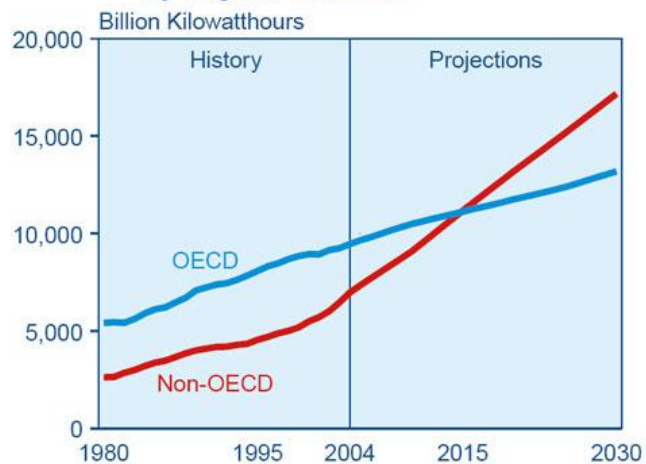
Sources: **History:** Energy Information Administration (EIA), *International Energy Annual 2004* (May-July 2006), web site www.eia.doe.gov/iea. **Projections:** EIA, System for the Analysis of Global Energy Markets (2007).

Figure 91 - World Electric Power Generation by Region, 1980-2030

Figure 14. World Nuclear Generating Capacity by Region, 2004 and 2030

OECD North America — 112 / 131
OECD Europe — 134 / 114
OECD Asia — 61 / 92
Non-OECD Asia — 15 / 72
Non-OECD Europe and Eurasia — 42 / 65
Other Non-OECD — 5 / 8

2004
2030

Gigawatts
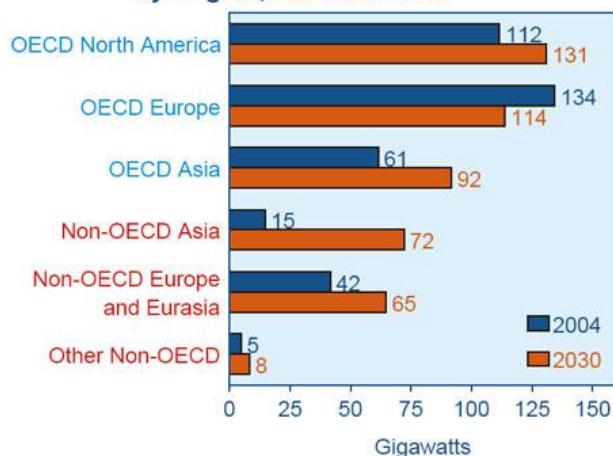
Sources: **2004:** Energy Information Administration (EIA), *International Energy Annual 2004* (May-July 2006), web site www.eia.doe.gov/iea. **Projections:** EIA, System for the Analysis of Global Energy Markets (2007).

Figure 92 - World Nuclear Generating Capacity by Region, 2004 and 2030

5   THESIS SCHEDULE

The magnitude of the project would have been unorganized without the implementation of a Management Schedule. This schedule was a collaborative effort to effectively communicate ideas, concepts, and finished products in a minimal amount of time. The team members from various disciplines were able to visually see and understand all activities detailed in research and design project. Another benefit of the schedule was the ability to implement logic into the process to optimize all time restraints. This not only increased productivity, but also the quality of the final design. By understanding the breakdown of the specific mechanical systems, engineers were able to minimize the number of design iterations when integrating the systems together.

All charts and diagrams were created professionally and were able to be transmitted electronically to each member of the team. The schedule can be viewed in Appendix under the category *Schedule*.

Proposal

David J. Kerze

ID	Description	Dur		%	Start	Finish
D0000	Start	0	0	100	13MAY05A	
D1000	Proceed With Proposal	30	0	100	13MAY05A	25MAY05A
D1030	Present to Green Energy	5	0	100	13MAY05A	17MAY05A
D1040	System Breakdown & Discipline Allocation	10	0	100	13MAY05A	22MAY05A
D1010	Prepare Project/Thesis Strategy	20	0	100	25MAY05A	13JUN05A
D1020	Prepare Project/Thesis Brief	15	0	100	13JUN05A	29JUN05A

Conceptual Design

David J. Kerze

ID	Description	Dur		%	Start	Finish
D2000	Prepare Design Alternatives	90	0	100	13MAY05A	10AUG05A
D2010	Proceed With Conceptual Design	60	0	100	18MAY05A	16JUL05A
D2030	Coordinate Mechanical Systems	30	0	100	18MAY05A	16JUN05A
D2040	Development-Schedule/Activity/Resource	30	0	100	17JUN05A	16JUL05A
D2020	Proceed With 3D Model, Z-Corporation	5	0	100	17JUL05A	21JUL05A

Prototype

Green Energy

ID	Description	Dur		%	Start	Finish
D3000	Proceed With Prototype	3	0	100	13MAY05A	15MAY05A
D3010	Design and Fabricate Tooling - Prototype	30	0	100	16MAY05A	14JUN05A
D3020	Fabricate Prototype Components	90	0	100	15JUN05A	12SEP05A
D3030	Prototype Approved	10	0	100	13SEP05A	22SEP05A

Schematic Design

David J. Kerze

ID	Description	Dur		%	Start	Finish
D4010	Shell Aerodynamics-Design/Testing/Analysis Schem	7	0	100	13MAY05A	19MAY05A
D4030	Internal Support Cage Structure Design-Schem	2	0	100	13MAY05A	14MAY05A
D4040	Cable Support (Safety Factor)-Schem	2	0	100	13MAY05A	14MAY05A
D4090	Preliminary Cost Estimate	5	0	100	13MAY05A	17MAY05A
D4060	Maintenance Accessibility System-Schem	2	0	100	15MAY05A	16MAY05A
D4080	Outline BOM	4	0	100	22MAY05A	25MAY05A
D4110	Re-Do Schematic Design	5	0	100	27MAY05A	31MAY05A
D4000	Proceed With Schematic Design	7	0	100	23SEP05A	29SEP05A

Green Energy

ID	Description	Dur		%	Start	Finish
D4020	Internal Tower Structure-Schem	2	0	100	13MAY05A	14MAY05A

Dr. Majid Rashidi

ID	Description	Dur		%	Start	Finish
D4050	Hydrostatic Bearing (Rot.&Stab.)-Schem	2	0	100	20MAY05A	21MAY05A
D4070	Pulley Driven Positioning System-Schem	2	0	100	22MAY05A	23MAY05A
D4100	Review/Approve Schematic Design	3	0	100	24MAY05A	26MAY05A

Table 8 - Schedule Breakdown Table (Part 1)

121

Design Development

David J. Kerze

ID	Task				Start	End
D5000	Proceed With Design Development	1	0	100	01JUN05A	01JUN05A
D5010	Shell Aerodynamics-Design/Testing/Analysis	270	694	0	02JUN05A	06APR07
D5030	Internal Support Cage Structure-Design	20	20	0	13MAY05	01JUN05
D5040	Cable Support (Safety Factor)-Design	20	20	0	13MAY05	01JUN05
D5060	Maintenance Accessibility System-Design	20	20	0	07APR07	26APR07
D5070	Pulley Driven Positioning System-Design	10	10	0	07APR07	16APR07
D5100	Review/Approve Design Development	7	7	0	28APR07	04MAY07
D5080	Detailed BOM	7	7	0	28APR07	04MAY07
D5090	Estimating	3	3	0	05MAY07	07MAY07
D6020	Final Specs for Internal Tower Structure	7	7	0	26MAY07	01JUN07

Green Energy

ID	Task				Start	End
D5020	Internal Tower Structure-Design	14	14	0	13MAY05	26MAY05
D6090	Proceed With Final Design	1	1	0	08JUN07	08JUN07

Dr. Majid Rashidi

ID	Task				Start	End
D5050	Hydrostatic Bearing (Rot.&Stab.)-Design	21	21	0	07APR07	27APR07

Final Design

David J. Kerze

ID	Task				Start	End
D6000	Mechanical Release Final Specs	21	21	0	05MAY07	25MAY07
D6030	Final Specs for Internal Support Cage Structure	10	10	0	26MAY07	04JUN07
D6040	Final Specs for Cable Support (Safety Factor)	10	10	0	26MAY07	04JUN07
D6060	Final Specs for Maintenance Accessibility System	10	10	0	26MAY07	04JUN07
D6070	Final Specs for Pulley Driven Positioning System	10	10	0	26MAY07	04JUN07
D6010	Final Specs for Outer Shell	15	15	0	26MAY07	09JUN07
D6080	Final BOM	3	3	0	05JUN07	07JUN07

Green Energy

ID	Task				Start	End
D6120	Review Final Specs	3	3	0	10JUN07	12JUN07
D6130	Final Fix-up Specs	3	3	0	13JUN07	15JUN07
D6110	Cost Estimate Documents	3	3	0	16JUN07	18JUN07

Dr. Majid Rashidi

ID	Task				Start	End
D6050	Final Specs for Hydrostatic Bearing (Rot.&Stab.)	7	7	0	26MAY07	01JUN07

Pre-Production

David J. Kerze

ID	Task				Start	End
D9000	Finish	0	0	100		20JUL07A

Green Energy

ID	Task				Start	End
D6100	Production Schedule	7	7	0	09JUN07	15JUN07

Table 9 - Schedule Breakdown Table (Part 2)
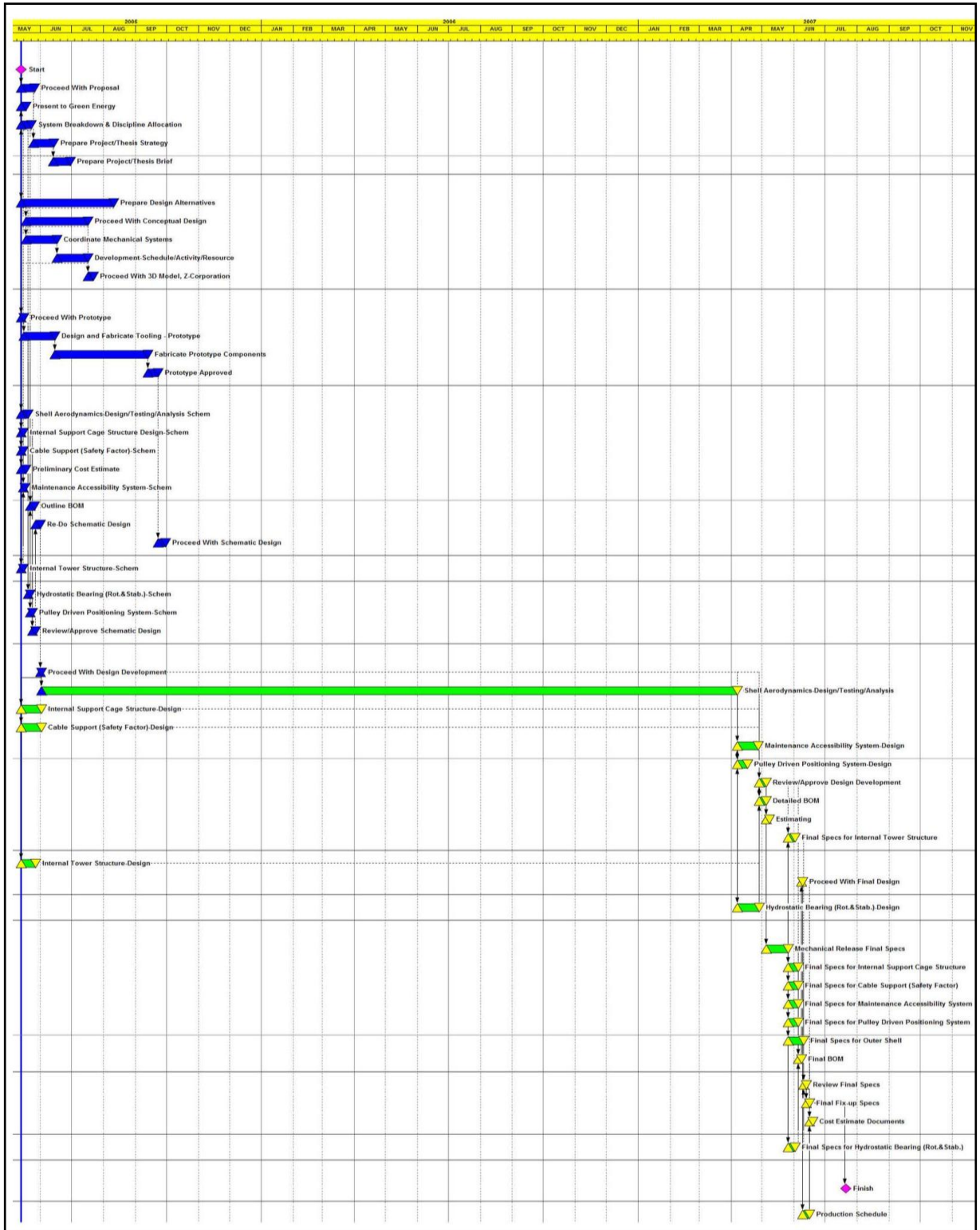
Figure 93 - Schedule Breakdown Ghant Diagram

123

6 SUPPORTING DOCUMENTATION

Plane 8		
x	0	0	0
y	28.125	0	0
z	-1200	-1200	450

Plane 8

Plane 9		
x	0	-450	-450
y	28.125	28.125	0
z	0	0	0

Plane 9

Plane 10		
x	0	-450	-450
y	14.0625	14.0625	14.0625
z	-1200	-1200	450

Plane 10
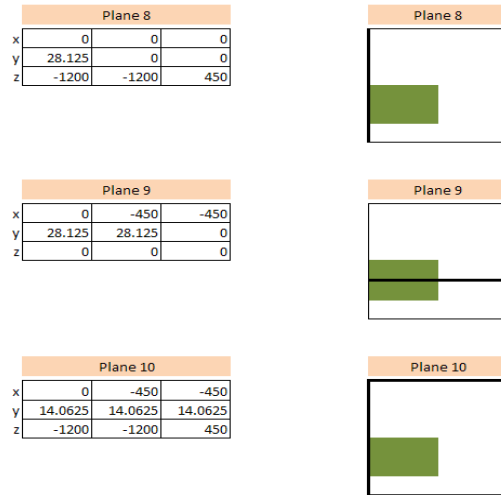
Figure 94 - 3D Cyl. – Defined Planes

Plane 10		
x	0	-450	-450
y	14.0625	14.0625	14.0625
z	-1200	-1200	450

Plane 10

Plane 11a (25ft spire)		
x	0	-450	-450
y	28.125	28.125	0
z	1.5936	1.5936	-1.5936

Plane 11a
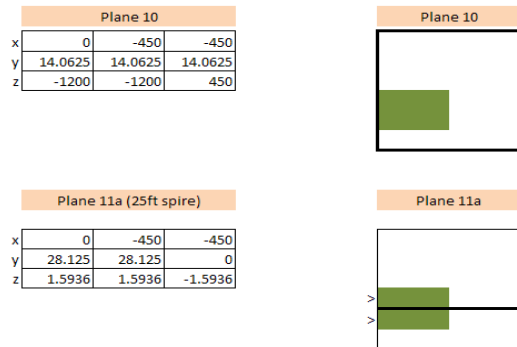
Figure 95 – 25ft Spire – Defined Planes

Plane 10		
x	0	-450	-450
y	14.0625	14.0625	14.0625
z	-1200	-1200	450

Plane 10

Plane 11b (30ft spire)		
x	0	-450	-450
y	28.125	28.125	0
z	1.385	1.385	-1.385

Plane 11b
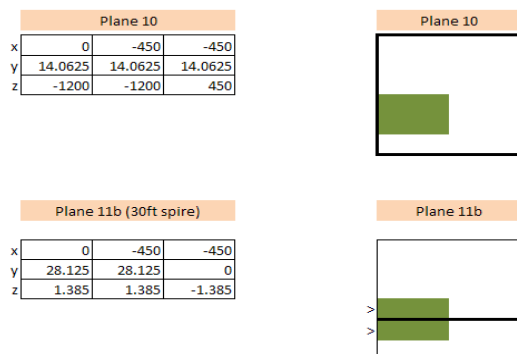
Figure 96 – 30ft Spire – Defined Planes

124

25FT SPIRE - AVERAGE VELOCITY OVER SURFACE AREA OF TURBINE

15.24677346

[Large data table with Pos./Vel. column pairs — numeric spreadsheet data]

Table 10 – 25ft Spire - Avg. Vel. Over Surface Area of Turbine

30FT SPIRE - AVERAGE VELOCITY OVER SURFACE AREA OF TURBINE

15.39677952

[Large data table with Pos./Vel. column pairs — numeric spreadsheet data]

Table 11 – 30ft Spire - Avg. Vel. Over Surface Area of Turbine

STRUCTURED GRID - TURBULENT FLOW REGIME

PARAMETERS:

$Re = \dfrac{U*L}{V}$ $v = \dfrac{u}{p}$;

D(Diameter)
= L = 60ft = 18.288 m;

U(velocity)
= 10mph = 4.4704 $\frac{m}{s}$;

u(kinematic viscosity)
= 1.7894e-5 $\frac{kg}{m*s}$;

p(density) = 1.225 $\frac{kg}{m^3}$;

Obj. Scale Factor ($) = 1;
(factor used to test
various flow regimes)

Vel. Scale Factor (#) = 1;
(factor used to test
various flow regimes)

Re=$\dfrac{((U*\#)*(L*\$))}{V}$= 5,596,820
== Turbulent (Standard
Wall Treatment)

CRITERION:

Re < 1000 Laminar

1000 <= Re <= 20,000
Turbulent (Enhanced Wall
Treatment)

Re > 20,000 Turbulent
(Standard Wall Function)

Figure 97 - Structured Grid - Turbulent Flow Mesh Parameters

Figure 98 - Unstructured Grid - Turbulent Flow Mesh Parameters
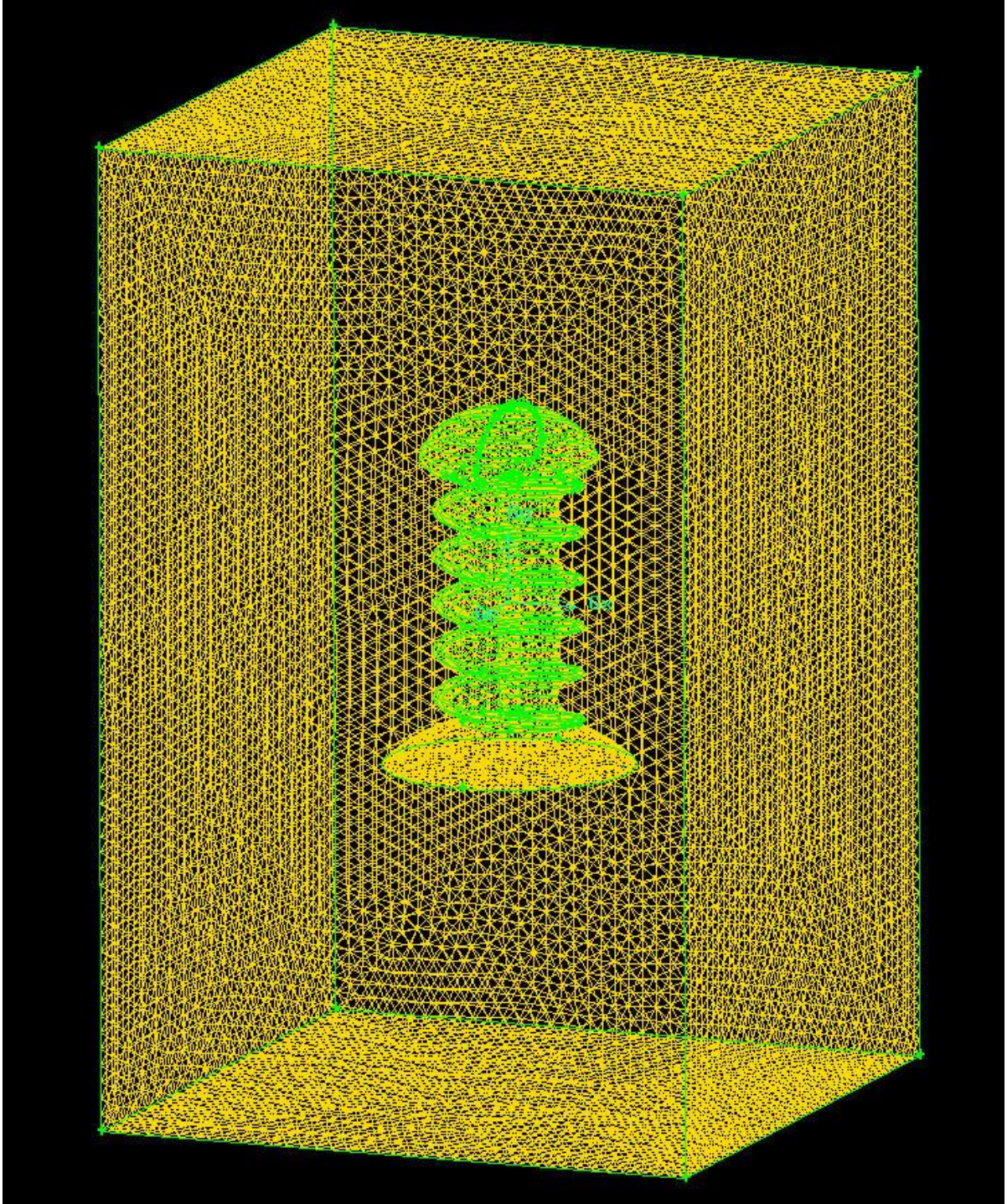
Figure 99 - Full Tower – Original Gambit Mesh (Inaccurate)
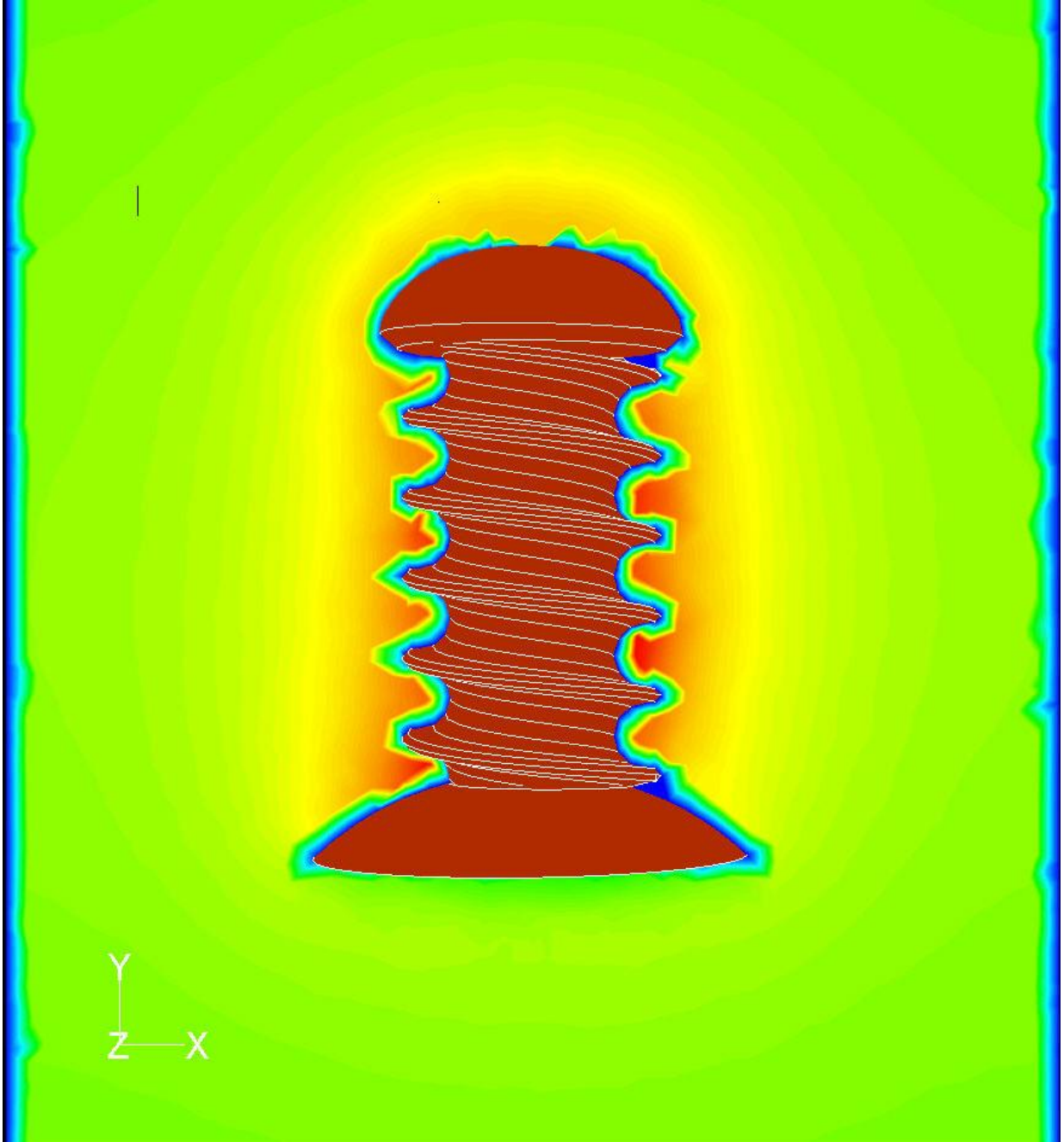
Figure 100 - Full Tower - Velocity Magnitude Distribution (Inaccurate)

7   PUBLICATIONS & RECOGNITION

7.1   *Wind-Tech International*

Figure 101 - Windtech Internation (Magazine Cover Page)

7.2 Cleveland Plain Dealer

7.2.1 Article I

"PD: "A spire built to inspire - Is this the future breezing into town?"
Start: 2006-10-01 14:05
Timezone: Etc/GMT+4
Saw this in today's PD:
A spire built to inspire
Is this the future breezing into town?
Sunday, October 01, 2006
Chris Sheridan
Plain Dealer Columnist
It seems only fitting that the man who agreed to lead a struggling urban university at age 64 would now want to put a windmill on its campus.
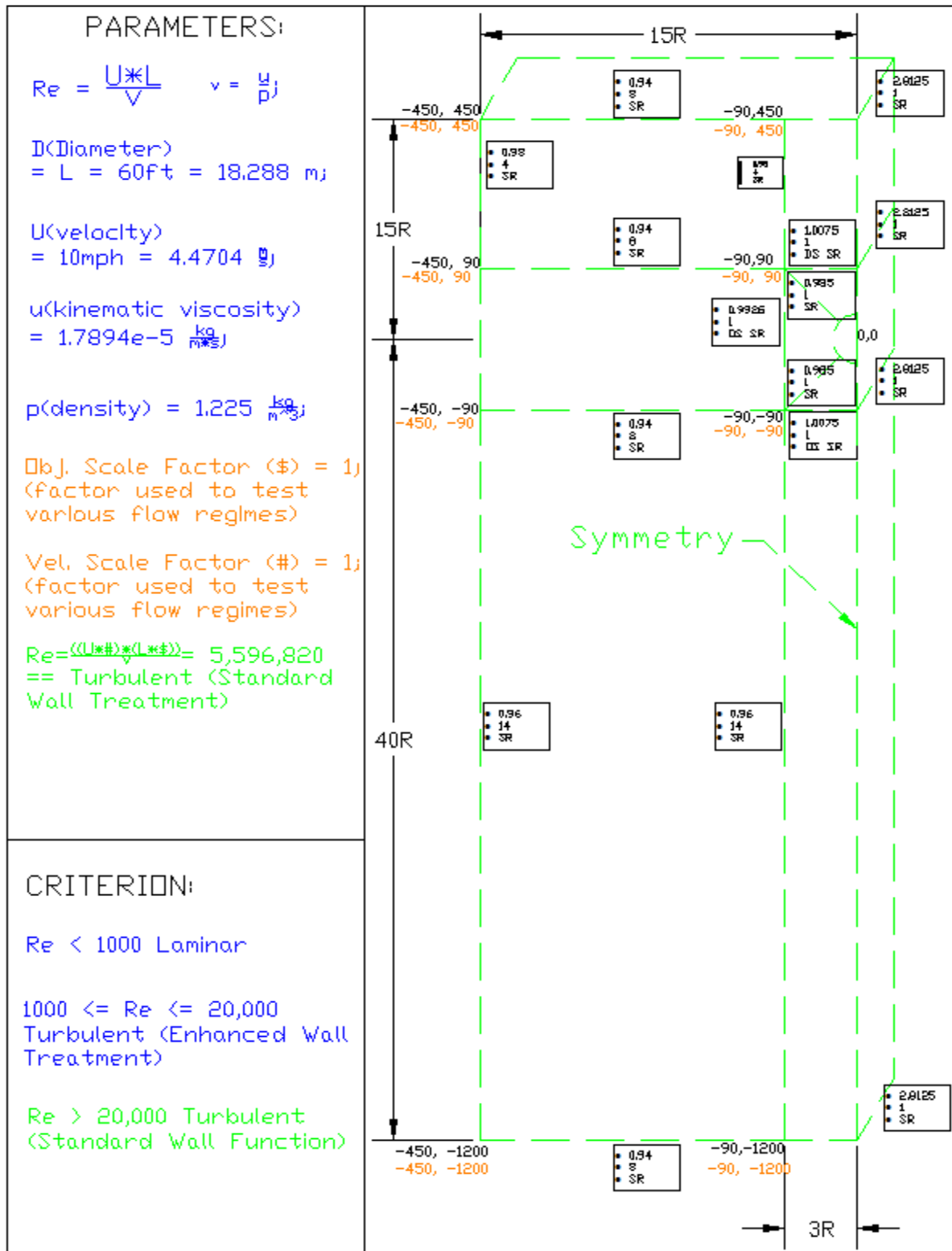*But when the man is Michael Schwartz and the institution Cleveland State University, Don Quixote analogies quickly crumble.*

For one thing, CSU's president isn't talking about a typical three-blade structure like the one that now stands by the Great Lakes Science Center. For another, he expects it to carry far more than symbolic value; ideally, this SmartEnergy Spire eventually will blow lots of dollars directly toward CSU's bottom line.

"It's a terrific idea," he says, beaming at a desk- sized model of the device that he's kept in his office since learning about the technology.

It's also terrifically well-timed. Spiraling energy prices have spurred unprecedented interest in alternative energy options in areas across the country, and specifically in Northeast Ohio. President Bush directed millions in new money toward solar and wind power in the 2007 budget, and federal applications for wind turbines have more than doubled over the last two years. Meanwhile, Cuyahoga County's commissioners appointed a task force this summer to consider alter native energy strategies, starting with an examination of wind power.

But with only about 6 percent of the United States' land mass appropriate for construction of traditional wind turbines - typically as tall as a downtown skyscraper - opportunities are huge for those who can turn innovative designs into reliable and efficient machines. A San Diego company, for example, is plugging a model that has four spinning rotors floating roughly 15,000 feet in the air, while scholars at the Massachusetts Institute of Technology and Johns Hopkins University each offer unique designs to allow wind turbines to stand far out at sea.

Into this heated competition comes CSU engineering professor Majid Rashidi, a man whose passion for product design yielded three patents in just six years. When Akron-area entrepreneur Mark Cironi was looking for someone to make a vague idea reality, Cleveland experts paired him with Rashidi. The professor, whose past inventions have been on a far smaller scale - for example a device to test for leaks in a catheter - soon was hooked by the challenge of creating an entirely new way to capture the wind.

Traditional wind turbines require huge open space. They also are costly to maintain because of the height of the gearbox and massive strain placed on it by translating the energy of giant, turning blades into significant electrical power.

Replacing one big rotor with bunches of smaller ones addressed key maintenance concerns. Still unanswered, however, was the larger question: how to persuade the wind to travel in such a way as to increase its speed?

As on the TV game show "Jeopardy," Rashidi's answer ultimately came in the form of a question: "What if I made it like a screw?"

Because the device is round, it doesn't have to turn to "chase" the wind, like a traditional windmill. Because it can be built in perfectly similar segments, transport is not nearly as complex as it is when ferrying blades that can stretch longer than a football field. Finally, because rotors sit inside the curves, blades are not as susceptible to rain and snow.

CSU has a provisional patent for Rashidi's design, and Cironi and the professor have touted it to nearly anyone who will listen - politicians, business people and, of course, university leaders. Academic institutions have been among the nation's leaders in pursuing alternative energy sources; the University of Pennsylvania, for example, gets nearly a third of its power from wind, while several Minnesota colleges have erected traditional wind turbines on their campuses. Officials at the University of Akron have explored placing multiple spires on its campus, although they'll need substantial funding to make the idea happen.

131

Richard Stuebi, the Cleveland Foundation's BP Fellow for Energy and Environmental Advancement, says the spire targets a new market, the urban niche. But as promising as the spire sounds in theory, the performance of an actual structure over time is what matters most to potential investors.

"It's hard to know if it's going to be a winner," Stuebi said, "but it could be a winner."

Cironi says he has sold five of the structures to a Pennsylvania customer already, but CSU will get the very first spire produced. Schwartz is confident of securing funding and already plans for the model to sport the university's green-and-white colors.

"It makes the statement," the president says, "that this technology was created at CSU.""

(Sheridan, 2006)

7.2.2   Article II

Accessible with subscription.

7.3   WCPN News

7.3.1   Article I

"New Wind Turbine for Urban Environments

Aired February 22, 2007

Later this morning, officials at Cleveland State University will meet to move ahead with plans to build a new type of wind turbine designed specifically for dense urban environments. ideastream's Lisa Ann Pinkerton has more.

The "Smart Energy Spire," as it's called, looks like a giant corkscrew, with two small wind turbines nestled on each side of its grooves. In principle, it's spiral shape is expected to increase the velocity of low speed winds that encounter the grooves, creating a wind tunnel effect. Dr. Majid Rashidi, a Mechanical Engineering Professor at Cleveland State University who helped to engineer the design, says this wind tunnel effect works whether the spire is a stand alone tower or mounted on top of a building.

Majid Rashidi: So when the wind stream hits it it's going to go around the structure. And as it goes around it speeds up and we are exposing the wind turbines to a higher wind velocity than what Mother Nature gives us.
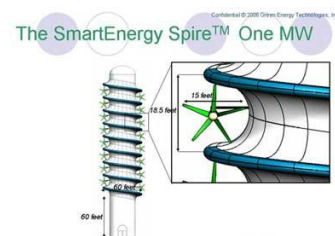

Image courtesy of Green Energy Technologies

Rashidi says CSU has funding to build a prototype of the "Smart Energy Spire" on top of one of its academic buildings. The plan is to construct a two groove spire what will test the accuracy of computer models. Rashidi says even on this small scale, the spire should generate between 100 and 500 kilowatts of power, depending on the wind.

Majid Rashidi: *With this two turn system we can supply four houses full blast with all the appliances and electrical systems on.*

The Akron Company Green Energy Technologies approached CSU to assist with the spire design, and hopes to mass market it in the future.

Dr. Rashidi presented the design plans to a room full of staff members at the Cleveland Natural History Museum on Wednesday, where concerns were raised about the spire's potential to harm flying wildlife. Past wind turbine projects, which didn't undergo proper environmental impact studies have been known to kill large numbers of animals that flew too close. David Krista, coordinator of biodiversity at the museum, says the small 20 foot diameter of the Spire's turbine blades means they could spin very fast, up to 200 rotations per minute.

David Krista: *While the big turbines, like were talking about on Lake Erie, those turbines have a 300 foot diameter they don't spin at fast maybe 20 rpms. He quoted 200 rpms. So the concern is how fast those guys are spinning. Those essentially could be blenders. So I'm concerned about the energy efficiency but I'm also concerned about the wild life impacts.*

Dr. Rashidi says the spire prototype will go through studies to satisfy public concerns over wildlife impacts and sight selection. Contracts with fabricators and parts suppliers will also need to be negotiated making it a year or more before the first Wind spire can be built. Lisa Ann Pinkerton, 90.3."

(WCPN News, 2007)

7.3.2   Article II

"Clarification on Wind Turbine Report:

On February 22, 90.3 aired a report about Cleveland State University's efforts to develop a new type of wind turbine - one that would utilize a spire in place of big rotor blades. It's called a wind spire, and it shows promise for making wind power generators safe for wildlife and practical for densely populated urban environments like Cleveland.

Our report did not mention that CSU and Green Energy Technologies, an Akron-based company, are in a dispute over the patent of the device. Dr. Majid Rashidi, a Mechanical Engineering Professor at CSU, is party to the dispute and was a primary source for our story. However, after the report aired he contacted WCPN to clarify statements attributed to him.

While we reported that Green Energy Technologies approached CSU to "assist with the spire design," Dr. Rashidi says the more accurate way to describe it would be to say that Green Energy asked CSU to "assist with designing and developing a wind energy system." The distinction is important, Rashidi says, because he claims he alone "invented, designed and engineered" the new wind spire device.

Dr. Rashidi also clarified that the prototype wind spire he demonstrated before the press would not generate the 100 to 500 kilowatts referenced by him during the demonstration. He now says that it is the finished full scale design that would eventually generate that level of electrical energy.

This week Green Energy Technologies decided not to file a lawsuit over the patent dispute at this time."

(WCPN News, 2007)